Theoretical Studies on the Optical Properties of Surface Frenkel Excitons

Kensei EHARA

1983

Abstract

Optical properties of surface Frenkel excitons have been studied theoretically in terms of a simple model. Special attention is paid to the influence of the geometrical anisotropy caused by the presence of the surface upon the oscillator strengths of the surface excitons. The dipole-dipole interactions are partitioned into intralayer interactions, short-range interlayer ones, and long-range interlayer ones. The effect of the difference in excitation energies between the surface atoms and the bulk ones is included in the model. An interplay between the dipole-dipole interactions and the surface geometrical anisotropy is one of interesting features of the model. The properties of the surface excitons are analyzed by solving Dyson's equation for the resolvent. Depending on the parameter values, the surface excitons can show two kinds of giant oscillator strengths; one is due to the short-range interlayer interactions and the other is due to the long-range ones. The strong polarization dependence of these effects are pointed out. In addition to the usual surface excitons, the model predicts a somewhat 'anomalous' surface localized mode. Its relation to the familiar surface polariton is also discussed.

Acknowledgements

The author would like to express his sincere thanks to Professor A. Yoshimori for a number of discussions essential to this study, encouragement throughout the work, and critical reading of the manuscript. He also wishes to express his particular gratitude to Professor K. Cho for suggesting this problem and helping him to simplify the model, as well as for many valuable discussions. Thanks are due to Dr. H. Nagayoshi, Dr. H. Kasai, and Professor M. Nakayama in Kyushu University for useful discussions. Mrs. N. Fukuda is gratefully acknowledged for typewriting the manuscript. He is indebted to Mr. Yamane, Mr. Inaoka, Mr. Kawai, and other members of his laboratory for various kinds of helps in preparing the manuscript.

CONTENTS

§1 Introduction

1-1 Surface Elementary Excitations in Solids — Classification

If there is a certain kind of bulk elementary excitation in solids, then there usually exists a corresponding surface version, which is localized at or near the surface and is propagating in the directions parallel to the surface. As such a surface elementary excitation, we know for example, electronic surface states, surface phonons, surface excitons, surface plasmons, surface exciton (or phonon)-polaritons, surface polarons, and so on.*) They have two dimensional crystal momentum $\vec{K}_{//}$ as a good quantum number, and their energies are in the

---

*) There is some confusion in the nomenclature of these surface modes. Some authors[1] refer to surface exciton-polaritons simply as surface excitons and surface phonon-polaritons as surface (optical) phonons. In this paper, we use the term 'surface excitons' and 'surface phonons' as eigenstates of the Hamiltonian of a material in Coulomb gange which has no transverse electromagnetic fields, in order to discriminate them from 'surface polaritons' that are solutions of the Maxwell equations. On the other hand, 'surface plasmons' are universally used to mean the solutions of the Maxwell equations; namely they are the eigenstates of the Hamiltonian of material plus electromagnetic field.

gap of the bulk band (for a given $\vec{K}_{//}$). In addition to these truely localized states, there may sometimes arise a so called surface resonance within the bulk band, the amplitude of which, though it is an extended mode, is large in the surface region.

In a conceptual experiment, we can create a surface, starting with an infinite crystal, in successive two steps; first we divide the infinite crystal into two parts by cutting the bonds through some plane, and thus obtain two semi-infinite crystals with ideal surfaces. Constituent atoms (or ions) in the surface region now see different local environment from that seen by bulk atoms, and the position of an atom is not an equilibrium position any more. Therefore, next, atoms in the surface region should move to new equilibrium positions (relaxation and/or reconstruction). From a theoretical point of view, the effect of this second step may be described by some appropriate potential localized at a few atomic layers from the surface seen by the elementary excitation in consideration. Thus it comes that surface can be created from an infinite crystal by [I] ideal cleavage and then [II] adding a surface potential. Each surface elementary excitation comes into existence either in step [I] or in [II]. This fact leads us to an idea that surface elementary excitations can be classified according to whether their existence is attributed merely to cleavage (type [I]) or to the surface potential (type [II]). For example, since

the dispersion relations of surface plasmons are calculated by the use of a bulk dielectric function, they clearly belong to the type [I]. On the other hand, (electronic) surface states are, as is well-known, highly sensitive to surface atomic structures, so they are members of the type [II] surface modes. According to this rule, we can classify main surface elementary excitations as in Table I.*) There exists an important difference between the properties of the type [I] modes and of the type [II] modes that the former are essentially describable within a classical theory of continuous media, although their details may rely on quantum treatment, and their wave functions have extension in a range of a few hundreds or thousands of atomic distance from the surface, whereas the nature of the latter depends on the atomic surface structure and they usually localize in a range of a few atomic distances from the surface.

Generally speaking, the investigations of surface elementary excitations have been less numerous in comparison with those of corresponding bulk counterparts. Experimentally, the detection of these surface modes usually requires careful preparation of a specimen with a well-controlled surface as well as spectroscopic techniques of high surface sensitivity. In some cases, special geometry to detect surface modes is required additionally.**) Also theoretical difficulties arise chiefly

---

*) It is also possible to discriminate the two types of surface modes simply by spatial extention of their wave functions. In any case, there may be intermediate ones difficult to discriminate.

**) For example, since surface plasmons and surface polaritons

Table I: Classification of surface elementary excitations in solids. The type [I] modes are insensitive to the microscopic surface structures and come into existence merely on cleavage, while the type [II] modes are highly sensitive to them, though they may exist at the stage of cleavage.

[I]	surface plasmon surface exciton-polariton surface phonon-polariton surface polaron Rayleigh wave
[II]	one-electronic surface state surface exciton surface optical phonon

do not couple directly to the vacuum electromagnetic fields, ATR (attenuated total reflection) geometry is frequently employed to detect them.[2)]

---

because the Bloch theorem does not hold in the direction perpendicular to the surface.

1-2 Surface Excitons

The above general statement, in fact, directly applies to the case of surface excitons. In contrast to bulk excitons in various solids that have a long history of both theoretical and experimental investigations,[3)] study of surface excitons started only a decade ago or so. Since then, existence of surface excitons has been verified experimentally in several semiconductors and insulators. Theories have been also developed to give explanations of some of the features observed. It seems, however, that as a whole, we are in an early stage of development, and that much is yet to be studied in both theory and experiment on this subject.

The necessity for studying surface excitons is as follows besides interest in itself. Firstly, the nature of the transport phenomena along surface may be influenced by the existence of surface excitons. Secondly, it is pointed out[4)] that when the energy level of a surface exciton lies below that of a bulk exciton, then it may provide a main source of the damping of

a bulk exciton. Thirdly, since the unique determination of atomic cofigurations on reconstructed (and/or relaxed) surfaces in semiconductors are, in the present state of the art, usually difficult both theoretically and experimentally, the informations at hand relevant to surface atomic structure would be useful in order to determine it correctly. As discussed already, surface excitons are among the type [II] modes, which are sensitive to the surface atomic structure, and a detailed investigation on them must provide useful informations about it.

1-3 Wannier vs. Frenkel Pictures of Surface Excitons

As it is well-known,[5] bulk excitions can be classified into two extreme types; the Wannier exciton and the Frenkel exciton. In the Wannier case, an electron and a hole are bound loosely each other, and their relative motion is decribed by a hydrogenic wave function which extends over many unit cells. In the Frenkel case, an electron and a hole are tightly bound and stay in the same atomic site. For most semiconductors, and for at least the excited states of exciton of alkali halides, the Wannier model gives a good description, while the Frenkel model works quite well for organic molecular crystals. Excitons in rare gas solids seem to be difficult to interpret with either one of these two models, and belong to the intermediate case.

The above classification is useful also for surface excitons. A surface Wannier exciton was recently discussed by Del Sole and Tosatti.[6] They constructed a Wannier exciton of essentially two dimensional character from a pair of surface state bands and calculated the binding energy as a function of surface state penetration depths. Experimentally, however, no evidence has been obtained to indicate the existence of such a surface Wannier exciton state so far. Influences of the presence of surface on Wannier excitons constructed from bulk bands have been discussed by many authors[7-11] in the context of so called ABC (additional boundary condition) problem, that has attracted much attention in the recent polariton physics. According to these theories, the presence of surface distorts the wave function of the relative motion of an electron and a hole, and thus the surface, in effect, acts as a repelling potential, resulting in "surface dead layer"; namely, surface Wannier excitions cannot exist in this case. On the other hand, surface excitons found in organic molecular crystals are definitely those of the Frenkel type.[12] In fact, they can be thought of as the same as bulk excitons, slightly perturbed by the difference in local environment of the bulk and the surface. In the case of rare gas solids, this may also be true for at least the ground state of surface excitons. Surface core excitons observed in MgO are known to be described fairly well by a localized excitation model,[13] which suggests that these surface excitons are also of

the Frenkel type. In addition to these crystals, there is the evidence[14] which shows that surface core excitons found on GaAs should be thought of as the Frenkel excitons rather than the Wannier excitons, although, in this case, these surface excitons cannot be regarded simply as perturbed bulk excitons (see the footnote on Page 24 in the next section). Therefore most surface excitons so far observed on molecular crystals, ionic crystals, and even semiconductors seem to be described fairly well by the Frenkel model, although detailed understanding of the structures of these surface excitons require further accumulation of experimental results.

1-4 Purpose of This Thesis

The above mentioned GaAs's experiment is conspicuous among the others performed on cubic crystals.*) It is the only case where the polarization dependence of optical excitations of surface excitons is investigated. The fact that the surface exciton transition is strongly dependent on the polarization of incident radiation was thus discovered. As it will be discussed in some detail in the next section, at present, we have no theory to account for this observation. It is well-known that the dipole-dipole interaction causes L-T (longitudinal--

---

*) Turlet and Philpott[15] measured polarized reflection spectra on crystalline anthracene, a highly anisotropic crystal.

transverse) splittings of dipole-active (bulk) excitons. In cubic crystals triply degenerate exciton states split into two T (transverse)-modes that have transition dipole moments perpendicular to $\vec{K}$ (the three demensional wave vector) and one L (longitudinal)-mode that has a dipole moment parallel to $\vec{K}$.*) Thus the dipole-dipole interaction brings about the anisotropy of excitons with respect to $\vec{K}$ in cubic systems. The L-mode, however, cannot couple with photons that are transverse in character, and is not detectable in optical measurements. Therefore the optical spectrum is always isotropic independent of the polarization of incident radiation, unless some anisotropic perturbation is applied externally.

The presence of surface alters this situation. It is, in itself, a strong anisotropic perturbation. In the similar way of thinking as the classification of surface elementary excitations made in 1-1, it may be possible to classify the anisotropic properties caused by surfaces into two types;

[I] the geometrical anisotropy — this makes $K_{\perp}$ (the normal component of the wave vector) no more a good quantum number, and thus causes the classification into T- and L-modes to

---

*) Here and after, we consider $\vec{K}$ to be finite, but vanishingly small (optical selection rule). Otherwise, if $\vec{K}$ is large enough, all three modes become L-T mixed modes for the general direction of $\vec{K}$, and if $\vec{K}$ is exactly zero, the shape of the specimen comes into discussion.[5]

be less meaningful, and

[II] the crystal-field anisotropy —— due to reconstruction and/or relaxation as well as the lack of half-space material, surface atoms feel the crystal field whose symmetry is lower than the original cubic symmetry;

i.e. this is the anisotropy of microscopic origin.

The second anisotropy mentioned above may cause not only energy level splittings but also some anisotropy of surface exciton oscillator strengths, but the changes in oscillator strengths thus caused are probably expected to be of order unity. It is hard to expect that it, or at least it alone, is the main origin of the observed 'giant anisotropy' of the surface excitons. In the first step, we may put the type [II] anisotropy out of our analysis. On the other hand, as concerns the type [I] anisotropy, we, of course, cannot drop it, which is caused merely by the presence of surface. The purpose of this thesis is to study how the interplay between the dipole-dipole interaction and the surface geometrical anisotropy influences the surface optical properties, above all, those of surface excitons on the basis of a simple model, and to find a possible explanation of the observed 'giant anisotropy' of the surface excitons.

In the next section, we give a brief survey of the studies of surface excitons so far made including the study on GaAs, with an emphasis on experimental aspects. Uncertainties in assignments and unsettled ploblems in interpreting experimental

results will be pointed out. We set up our model, and derive the Hamiltonian in §3. There, starting with the Frenkel excitons on a slab-like lattice geometry, we rewrite the dipole-dipole interaction in a layerwise form, and thus obtain three kinds of interactions; intralayer, short-range interlayer, and long-range interlayer interactions. Assuming small but finite $K_{//}$ with optical excitations in mind, we introduce some parameters to describe them. The long-range interaction is shown to have an exponential dependence on the interlayer distance, while the short range one is approximated by a nearest-layer interaction. If we list up the elementary features contained in our model, we have

(i) presence of surface,

(ii) surface potential, which is localized at the outermost layer and is necessary to permit the existence of surface excitons,

(iii) nearest-layer coupling,

(iv) exponential coupling,

and finally

(v) vectorial character of excitations.

The features (i) and (v) provide the geometrical anisotropy, whereas neglect of the crystal-field anisotropy means that the surface potential in (ii) is assumed isotropic. Models containing two, or at most three features mentioned above have ever been treated in the past, either in the theory of the

surface Frenkel excitons[16-18] or in the context of 'ABC' problem.[19-21] Inclusion of all the five features, however, inhibits an application of the methods developed so far to the present problem, and a different approach should be employed. This is done in §4, where the Dyson equation for the resolvent is solved. Our approach consists of (a) the integral equation method, and (b) $K_{//}$-expansion. In (a), the eigenmodes for the bulk system with periodic boundary condition are utilized to represent the Dyson equation and thus the kernel of the integral equation is shown to become a sum of separable forms (or degenerate kernels, in analytical languages), with which, in principle, the integral equation can be solved. To suppress the explosion of computational complexities, the $K_{//}$-expansion is proposed, since $K_{//}$ is a small parameter in our theory. As will be shown explicitly, the $K_{//}$-expansion is not a simple one. A solution for exactly vanishing value of $K_{//}$ is different from that for small but finite values of $K_{//}$. Namely, our solution is non-analytic near the point $K_{//}=0$, which reminds us of the non-analiticity of bulk exciton energy, i.e. L-T splitting. Of course, they stem from the same origin — the long range nature of the dipole-dipole interaction. Therefore we should pay much attention to the behavior of the solution near $K_{//}\sim 0$; otherwise the $K_{//}$-expansion is similar to the usual perturbation expansion. Using the solution for the resolvent, we calculate the density of states and the absorption

spectrum in §5. From the density of states we can clearly identify at most three surface localized states. Two of them are surface excitons in the usual sense; they owe their existence to the surface potential and belong to type [II] surface modes. The other one is, in a sense, 'anomalous'; it owes its existence merely to the cleavage, hence belongs to type [I] modes. The absorption spectrum is calculated as a function of the polarization direction of the incident radiation. How the exchange of the oscillator strengths takes place between the surface excitons and the bulk excitons as well as among bulk excitons themselves is investigated and shown. A remarkable feature is that the surface excitons can show giant oscillater strengths depending on the parameter values. There are two origins of them; one is the short range interaction and the other is the long range one. Moreover, the condition for the giant oscillator strengths of the latter origin is examined in some detail with respect to a polarization dependence. Section 6 is devoted to discussions. Firstly, we study the behavior of the 'anomalous' surface mode in detail, and its relationship to surface polariton is pointed out. Then we try to interpret the observed giant anisotropy of GaAs surface core excitons on the basis of our results. Usefulness of polarization dependent spectroscopies in the investigations of the surface excitons on solids other than GaAs is also suggested. Limitations and possible extensions of our model are discussed. Finally, we summarize the results in §7.

§2 Survey of Surface Exciton Studies

In this section, we give a brief review of the investigations so far made on surface excitons.

2-1 Organic Crystals

There had been some controversy[22] concerning the origins of the fine structures seen in the reflection spectrum of the b-polarized 0-0 transition of the first singlet of the crystalline anthracene. Turlet and Philpott[15] have performed careful measurements of the spectra, and from the surface treatment sensitivities of the fine structures they concluded that the two sharp dips observed at low temperatures are due to the surface and subsurface exciton transitions. They also proposed a model that explains the differences in energy between the surface and the bulk excitons in terms of the site shift energy.[12] Structures probably due to the surface excitons have been observed in transmission spectra,[23] too, and there is an evidence that these surface excitons are also involved in the fluorescence emissions first observed by Glockner and Wolf.[24] To date, reflection minima attributed to surface excitons have been observed not only in anthracene, but also in tetracene[25] and naphthalene.[26]

Theories of surface excitons in molecular crystals have been developed independently by Hoshen and Kopelman,[16] and by

Schipper.[17] In both of their theories, the Koster-Slater approach[27] was employed and the surface was represented by two kinds of localized perturbations (one is the cleavage and the other is the surface relaxation, such as discussed in 1-1) introduced into infinite (or periodic) crystal with a tight-binding type model of exciton. They discussed the condition for the existence of surface excitons in terms of the exciton transfer energy and the site shift energy. Later, Ueba and Ichimura[18] extended the theory of Hoshen and Kopelman to the case where there are two translationally nonequivalent molecules per unit cell and showed that the Davydov splitting of surface excitons can be smaller than that of bulk excitons. They pointed out the possibility of interpreting the two sharp reflectivity dips observed on crystalline anthracene as due to the Davydov pair of the surface excitons. Though there is little doubt about the existence of surface excitons in these organic molecular crystals now, understanding of the details of these states will require further theoretical and experimental efforts.

2-2 Rare Gas Solids

The first experimental evidence for the existence of surface excitons in solid Ar, Kr, and Xe was given by Saile and co-workers[4] in 1976. In their experiments, optical transmission and reflection spectra were measured on thin rare gas films by

means of synchrotron radiation. They found structures due to surface excitons at energies slightly below the well-known bulk exciton absoption bands. For these structures of surface origin, a splitting into two or three components is observed. For example, in the case of Ar, two prominent peaks at 11.71 eV and 11.81 eV and a weak shoulder at about 11.93 eV below the bulk n=1 (j=3/2) and n=1' (j=1/2) excitons*) that have the energy location of 12.06 eV and 12.23 eV, respectively, and two peaks at 12.99 eV and 13.07 eV below the bulk n=2 (13.57 eV) and n=2' (13.75 eV) excitons are observed (Fig. 2-1). On the basis that the observed surface exciton splitting is too small in

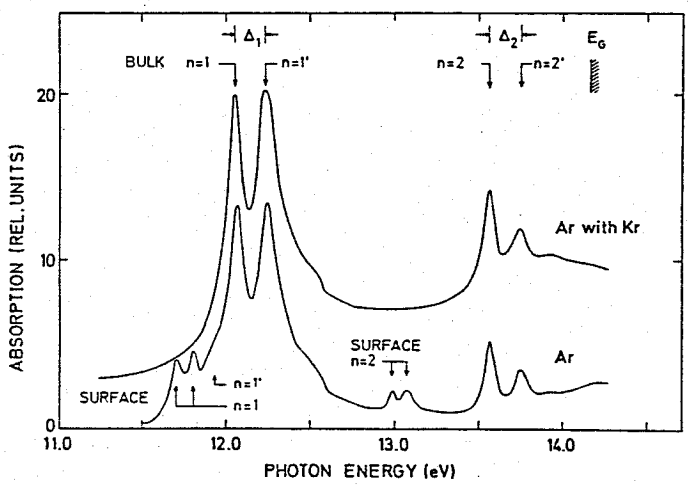

Fig. 2-1. Absorption spectrum of a clean Ar film and of the same Ar film with a Kr overcoating. Those peaks which are sensitive to the surface treatment was identified as the surface exciton peaks (after Saile et al.[4]).

*) Notations of the hydrogenic series are used; i.e., n is the principal quantum number. In the parenthesis, j is the total angular momentum of a hole in the p-like valence band.

comparison with the spin-orbit splitting of the corresponding bulk excitons, they proposed, as a possible model, that it might not be the spin-orbit splitting but be a surface-crystal-field splitting of the j=3/2 excitons. Even if we admit this conjecture, the question of why then the n=1' surface exciton is hard to see and why the n=2' surface exciton cannot be observed at all still remains to be answered.

On the contrary, Ueba[28] argued that the observed splitting of the surface exciton peaks could be explained in terms of the spin-orbit splitting, pointing out that the spin-orbit splitting of surface excitons can be smaller than that of the corresponding bulk excitons. This argument, however, also have an apparent shortcoming that it cannot explain why three surface excitons appear from two (n=1 and n=1') bulk excitons. At present, we have no convincing assignments that account for all the observed features of the surface related transitions as a whole.

2-3 Si

Among a lot of semiconductor reconstructed surfaces, Si (111) 7×7 surface has been the most controversial one with respect to its surface atomic geometry. Various models of reconstruction have been proposed,[29] but none have attained a general agreement.

In 1977, Margaritondo and Rowe[30] studied the $L_{2,3}$ absorption edge on Si (111) 7×7 surface with electron energy loss spectro-

scopy (EELS) and found a large excitonic effect for the Si 2p core level to empty surface state transitions. EELS was taken in the second derivative mode, and two peaks in the difference between the spectra with and without gallium overlayer were identified as surface transitions. From a careful comparison of the two peak energies with X-ray photoemission spectroscopy (XPS) data, they concluded that the excitonic shifts for Si (2p) to empty surface state transitions are at least about 0.9 eV for the one peak and 2.1 eV for the other peak, in comparison with about 0.9 eV for the bulk $L_{2,3}$ absorption edge.

In determining the atomic structure of reconstructed surface, one way is to calculate the surface electronic energy band by assuming a certain reconstruction geometry and compare it with experimental data (absorption, photoemission, electron energy loss, etc.). The observation of rather large excitonic shifts indicates the danger of interpreting experimental data in a simple one-electron scheme. Therefore detailed investigations of the nature of surface excitons seem to be required before a sound comparison of band calculations with experiments can be made.

In order to qualitatively explain the observed large excitonic effects in surface core excitons, Altarelli et al.[31] performed a model calculation based on the Koster-Slater method, where two parameters were introduced to represent the core hole potential and the surface reconstruction, respectively, into a

tight-binding model. They found that, depending on the values of the parameters and on the positon of the core hole, in some situations a large enhancement of the binding energy near the surface results, and in other cases excitons are not allowed to be in the first few layers. Though their result is very suggestive in elucidating the nature of the binding of an electron and a hole in the surface region, their model is too naïve to be applied to a real solid. In this connection, it may be pointed out that the most important, though most difficult, question to be answered urgently on semiconductor surface optical properties is how the bulk dielectric screening mechanism is modified near surface. Up to now, we have neither a first principle theory such as developed by Sham and Rice[32] for bulk excitons, nor even a qualitative theory on this problem.

2-4 GaAs

Recent development of synchrotron radiation sources has made photoemission spectroscopy one of the most useful techniques in the field of surface physics. In addition to measuring the conventional energy distribution curves (EDC), this source of variable frequency of light has made possible new modes of experiments such as constant initial energy spectroscopy (CIS) and constant final energy spectroscopy (CFS). So called partial yield spectroscopy is a kind of CFS that counts mainly secondary electrons as a function of photon energy by setting the kinetic

energy window of the analyzer at relatively low energy.

Electrons that are excited deep in the bulk suffer repeated scatterings from the rest of the solid and, in effect, they cannot reach the surface. Only those electrons excited within the "escape depth"[33] from the surface are detectable. That is why photoemission spectroscopy is extremely suitable for the study of electronic surface properties.

By the use of these thechniques, numerous experiments have been made on GaAs, a material of recent industrial importance. In the light of these experiments, as well as several theoretical efforts,[34-37] the overall features of the atomic geometry of GaAs (110) surface are now well-established: there is general agreement that it is 1×1 relaxed surface and that surface As atoms move outwards and surface Ga atoms move inwards, with about 25° bond-angle rotation and a charge transfer from Ga to As surface atoms.

Using partial yield technics, Eastman and Freeouf[38] detected, for the first time, the existence of unoccupied surface states just below the bottom of the bulk conduction band on both Ge (111) and GaAs (110). Soon later, Lapeyre and Anderson[14] performed more extensive measurements on GaAs, using CIS techniques, and showed that the excitations observed by Eastman and Freeouf are not one-electron transitions from core levels to unoccupied surface states, but should be thought of as surface core excitons. Their CIS data are shown in Fig. 2-2, where

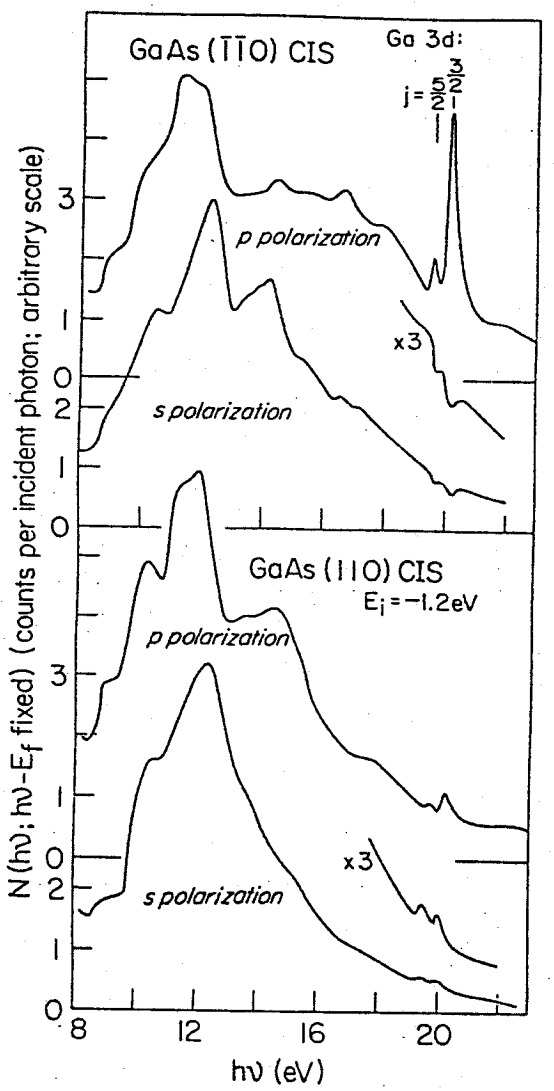

Fig.2-2. Constant initial-energy spectra (CIS's) of GaAs(110) surface for four different geometries. The uppermost curve is for the case where the photon electric field vector E is nearly parallel to the Ga dangling bond, while the other three curves are for E perpendicular (or nearly so) to the Ga dangling bond (after Lapeyre and Anderson [14]).

the CIS's for four different angles of polarization of incident radiation are given. At relatively low photon energy, only a direct excitation of valence electrons to the conduction bands above the vacuum level is possible and the CIS's reflect the features of the conduction bands. When photon energy reaches or exceeds Ga 3d core level threshold, a new channel to excite valence electrons opens ; first a core electron is excited to form a surface exciton, and subsequently it decays via direct recombination or Auger process with the energy supply to excite valence electrons above the vacuum level. The narrow pair of peaks near 20 eV in their CIS's is believed to be due to the enhancement caused by this second process. Many evidences have been reported showing that these structures are not due to simple one-electron trasitions but due to excitons, but here we mention only the following four points:

(i) The exciton enhancement strongly depends on the polarization of incident radiation ; it is dramatically larger for the case where the photon E (electric field)-vector has its largest component parallel to the Ga dangling bond (the uppermost curve in Fig. 2-2) than the other three geometries where the E-vector is nearly perpendicular to the Ga dangling bond.

(ii) The exciton enhancement appears as a doublet originated from spin-orbit splitting of Ga 3d level; the lower structure corresponds to the $d_{5/2}$ orbital and the upper one to the $d_{3/2}$ orbital. A remarkable feature is that the intensities of the j=5/2 and 3/2 components are reversed from the 6:4 statis-

tical weight for the core states.

(iii) The doublet structures in the second curve of the CIS's are minimums instead of peaks.

(iv) The positions of the doublet also depends on the polarization. They shift as large as 0.5 ev.

The second point cited above can be explained by Onodera--Toyozawa theory,[39] which shows that the oscillator strength of spin-orbit split excitons is strongly dependent on the electron--hole exchange interaction. The third and the fourth points may be explained in terms of the Fano effect;[40] the valence excitation continuum overlaps in energy with the surface excitons, and the interference effect among them can account for the appearance of such minimum structures as well as their shifts, although a question remains as to whether the Fano effect alone can explain such large shifts, twice as large as the widths of the structures. On the other hand, we have no theory to explain such a strong polarization dependence as mentioned in (i). In fact, the Ga dangling bond has p_z-like character and a simple calculation with use of Clebsch-Gordan coefficient yields that the oscillator strength ratio of the transition from d to p_z orbital when the E-vector is parallel and perpendicular to the p_z orbital is 4:3. Thus we can expect these surface exciton transitions to be almost isotropic, which is in sharp contradiction to the observation.

In contrast to the case of Ga 3d excitation, Zurcher et al.[41] obtained no evidence that the transition from As 3d core to

empty surface states is excitonic in nature in the same manner of experiments. This is to be expected; it is well established that the surface relaxation causes charge transfer from surface Ga to As atoms, leaving Ga dangling bond states empty and those of As occupied.[34-37] Thus the only available final state in the transition is the Ga dangling bond state. Therefore the transition out of Ga 3d is intra-atomic in character, resulting in a strong binding of an electron and a hole, while the transition out of As 3d is inter-atomic, resulting in a weak binding. In fact, this picture was recently verified quantitatively by Swarts et al.*)[42] in their model cluster calculations and by Daw et al.[43] in their tight-binding calculations. Their results also suggest that the Frenkel model gives a good description for these surface excitons.

---

*) Since dangling bond states are brought about by the presence of surface, surface excitons of the type presently considered have no bulk counterpart. In order to emphasize this character, Swartz et al. called them core surfastons. This nomenclature is, however, not prevalent yet.

§3 Model

3-1 Hamiltonian

We consider a Bravais lattice of slab geometry composed of N lattice planes (see Fig. 3-1). The lattice structure is assumed cubic. Following Heller and Marcus,[44] we arrange an identical atom on each lattice site, which has a s-like occupied orbital and a p-like unoccupied orbital in the ground state. We ignore electron spin and neglect the overlap of the orbitals on different lattice sites (extreme Frenkel limit). Thus we can use the classical oscillator model for excitons. Transfer of atomic excitation occurs only through the dipole-dipole interactions. We assume that the atoms on the first layer have an excitation energy different from that of the atoms on the remaining bulk layers by an amount δ. The origin of δ may be various, but we do not discuss about it here and simply treat it as a parameter. As a basis set, we take Frenkel excitons each of which is localized on one of the layers, say the ℓ-th layer, and propagates along the layer with a wave vector $\vec{K}_{//}$. One more suffix, ν, is necessary to indicate its polarization. Let us define $a^{+}_{\ell\nu(\vec{K}_{//})}$ ($a_{\ell\nu(\vec{K}_{//})}$) as the creation (annihilation) operator of such a state. Since $\vec{K}_{//}$ is a good quautum number, we proceed the calculation with a given $\vec{K}_{//}$ in the following , and drop the index $\vec{K}_{//}$ in these operators. Then the Hamiltonian of our model can be written as

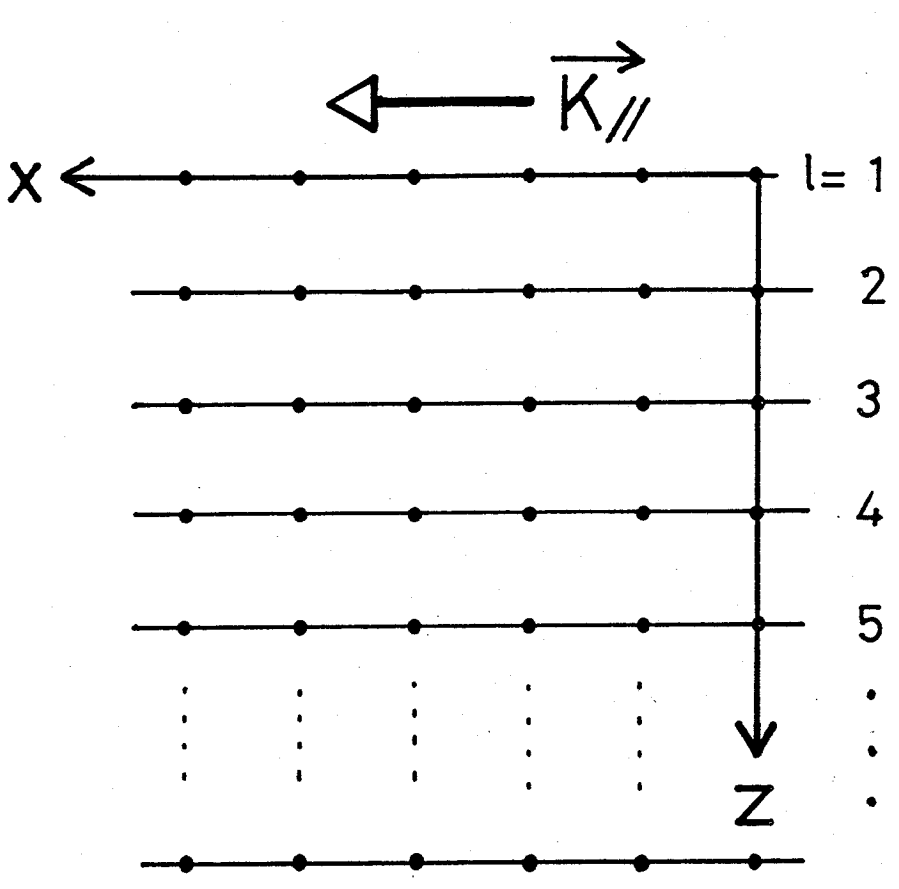

Fig.3-1. Schematic representation of the geometry and the coordinate system. The x-axis is so chosen that its positive direction coinsides with the direction of $\vec{K}_{//}$.

$$H = \varepsilon_b \sum_{\ell=1}^{N} \sum_{\nu} a^{\dagger}_{\ell\nu} a_{\ell\nu} + \delta \sum_{\nu} a^{\dagger}_{1\nu} a_{1\nu}$$

$$+ \sum_{\ell,m=1}^{N} \sum_{\nu,\mu} V_{\nu\mu}(\ell,m)\, a^{\dagger}_{\ell\nu} a_{m\mu} , \qquad (3.1)$$

where ε_b is the atomic excitation energy of the bulk atoms; δ, the surface potential; and $V_{\nu\mu}(\ell,m)$, the dipole-dipole interaction between the ν-polarized exciton localized on the ℓ-th layer and the μ-polarized one on the m-th layer. The expression of $V_{\nu\mu}(\ell,m)$ can be obtained by simple rearrangement of terms in the usual[5] dipole-dipole interactions of the Frenkel excitons in a layerwise form as

$$V_{\nu\mu}(\ell,m) = \frac{1}{N_s} \vec{M}^{*}_{\nu} \cdot \sum_{i,j} \exp[i\vec{K}_{//} \cdot (\vec{R}_{mj} - \vec{R}_{\ell i})] \times$$

$$\times \frac{|\vec{R}_{\ell i} - \vec{R}_{mj}|^2 I - 3(\vec{R}_{\ell i} - \vec{R}_{mj})(\vec{R}_{\ell i} - \vec{R}_{mj})}{|\vec{R}_{\ell i} - \vec{R}_{mj}|^5} \cdot \vec{M}_{\mu} , \qquad (3.2)$$

where N_s is the number of unit meshes in one layer (we assume that we have imposed periodic boundary conditions with respect to the directions parallel to the surface); $\vec{M}_{\nu}(\vec{M}_{\mu})$, the transition dipole moment associated with the $\nu(\mu)$-polarized single-atom excitation; I, the unit dyadic; and $\vec{R}_{\ell i}(\vec{R}_{mi})$, the lattice vector of the i(j)-th site on the ℓ(m)-th layer. In the summation, it is understood that when ℓ=m, the term for i=j should be excluded. The difference $\vec{R}_{\ell i} - \vec{R}_{mj}$ may be rewritten as

$$\vec{R}_{\ell i} - \vec{R}_{mj} = \vec{R}_{\ell m} + \vec{R}_{//} , \qquad (3.3)$$

where $\vec{R}_{\ell m}$ denotes the origin of the ℓ-th layer relative to that of the m-th layer, and $\vec{R}_{//}$ is a two-dimensional lattice vector. Note that $\vec{R}_{\ell m}$ is not necessarily perpendicular to the layers. Then eq. (3.2) becomes

$$V_{\nu\mu}(\ell,m) = \vec{M}_{\nu}^{*}\cdot\sum_{\vec{R}_{//}} \exp(-i\vec{K}_{//}\cdot\vec{R}_{//}) \times \frac{|\vec{R}_{\ell m}+\vec{R}_{//}|^{2}I - 3(\vec{R}_{\ell m}-\vec{R}_{//})(\vec{R}_{\ell m}-\vec{R}_{//})}{|\vec{R}_{\ell m} + \vec{R}_{//}|^{5}}\cdot\vec{M}_{\mu} , \qquad (3.4)$$

where we have dropped the factor $\exp(-i\vec{K}_{//}\cdot\vec{R}_{\ell m})\cong 1$. An exact treatment of the layerwise dipole sum of this kind was given by Mahan and Obermair[20] for the special case of $K_{//}=0$, and also by philpott,[45] who gave the formula with inclusion of the retardation effects. Assuming that $K_{//}$ is small, we analyze the sum in eq. (3.4) and try to find a suitable form with some parameters, in the following subsections, so that our model is general and applicable to any surfaces of lattices (but cubic, of course). The cases of $\ell=m$, and of $\ell\neq m$ will be examined separately in the next two subsections.

3-2 Intralayer Dipole-Dipole Interactions

First, we examine the case when $\ell=m$. Equation (3.4) in this case simply reads

$$V_{\nu\mu}(\ell,\ell) = \vec{M}_{\nu}^{*}\cdot{\sum_{\vec{R}_{//}}}' \exp(-i\vec{K}_{//}\cdot\vec{R}_{//})\frac{R_{//}^{2}I-3\vec{R}_{//}\vec{R}_{//}}{R_{//}^{5}}\cdot\vec{M}_{\mu} , \qquad (3.5)$$

where the prime on the summation means to exclude the term $\vec{R}_{//}=0$. We replace the summation by the 2-D (two dimensional) integral outside the circle of some radius R_0, the value of which is to be determined later. We define the coordinate system such that the (x,y)-plane is in the surface layer with the x-axis parallel to $\vec{K}_{//}$ and the positive direction of the z-axis points inward to the bulk (see Fig. 3-1). Then the summation in eq. (3.5) is replaced by the integral given, in a matrix form, by

$$\frac{1}{\Omega_s} \iint_{R_{//}>R_0} d\vec{R}_{//} \frac{\exp(-i\vec{K}_{//}\cdot\vec{R}_{//})}{R_{//}^5} \begin{pmatrix} -2X^2+Y^2 & -3XY & 0 \\ -3XY & X^2-2Y^2 & 0 \\ 0 & 0 & X^2+Y^2 \end{pmatrix} . \quad (3.6)$$

Here Ω_s is the area of the unit mesh and $(X,Y)=\vec{R}_{//}$. This integral can be evaluated as a power series of $K_{//}R_0$, which will be made in Appendix A. Assuming that $K_{//}R_0<<1$, we retain the terms up to linear in $K_{//}$, and finally we obtain

$$V_{\nu\mu}(\ell,\ell) = \frac{\pi|M|^2 K_{//}}{\Omega_s} \begin{pmatrix} -1/K_{//}R_0+2, & 0, & 0 \\ 0, & -1/K_{//}R_0, & 0 \\ 0, & 0, & 2/K_{//}R_0-2 \end{pmatrix} . \quad (3.7)$$

In the case of 3-D dipole sums, Heller and Marcus showed that the integral approximation gives a correct result when $K\approx 0$, which does not depend on the radius of the exclusion sphere as far as the condition $KR_0<<1$ is fulfilled. In our 2-D case, however, the lowest order terms do depend on R_0, and some means to determine the value of R_0 is necessary. One possible way may be to require that the area of the exclusion circle be equal

to the area of the unit mesh; namely, $\pi R_0^2=\Omega_s$. The intralayer interaction, however, is not a quantity independent of the interlayer interactions, thus it is essential to make our choice of R_0 consistent with the approximations made for the interlayer interactions, which will be done later in subsection 3-3.

On the other hand, the next order terms are independent of R_0. We introduce the interlayer spacing $d_\perp$, and note the following two points; (i) $\Omega_s\, d_\perp$ is equal to the volume of the bulk unit cell Ω, which is valid for arbitrary Bravais lattices, and (ii) the L-T splitting, Δ_{LT}, of the bulk exciton is given by $4\pi|M|^2/\Omega$. Then, we can express the terms next order in $K_{//}$ in terms of the important physical quantity Δ_{LT};

$$\frac{2\pi|M|^2}{\Omega_s} = d_\perp\, \Delta_{LT}/2 \ , \tag{3.8}$$

Now the general form of the intralayer interaction (3.7) may be written, up to linear in $K_{//}$, as

$$V_{\nu\mu}(\ell,\ell) = \Delta_{LT} \begin{pmatrix} -\beta_0+K_{//}d_\perp/2, & 0, & 0, \\ 0, & -\beta_0, & 0, \\ 0. & 0, & 2\beta_0-K_{//}d_\perp/2 \end{pmatrix}, \tag{3.9}$$

where $\beta_0=\pi|M|^2/\Omega_s R_0 \Delta_{LT}$ is a dimensionless parameter.

3-3 Interlayer Dipole-Dipole Interactions

Next we consider the case when $\ell\neq m$. We use the following 2-D Fourier transform of the dipole transfer matrix which is

valid for $z \neq 0$:

$$\frac{r^2 I - 3\vec{r}\vec{r}}{r^5} = \frac{2\pi}{N_s \Omega_s} \sum_{\vec{k}_{//}} \frac{\exp(-k_{//}|z| + i\vec{k}_{//}\cdot\vec{r}_{//})}{k_{//}} \times$$

$$\times \begin{pmatrix} k_x^2, & k_x k_y, & \pm i k_x k_{//} \\ k_y k_x, & k_y^2, & \pm i k_y k_{//} \\ \pm i k_{//} k_x, & \pm i k_{//} k_y, & -K_{//}^2 \end{pmatrix}, \qquad (3.10)$$

where for $\pm$ in the matrix we have the positive sign for $z>0$ and the negative sign for $z<0$, and k_x and k_y are the x- and y-component of the 2-D wave vector $\vec{k}_{//}$, respectively. We could derive this formula most easily from the 2-D Fourier transform of $1/r$:

$$\frac{1}{r} = \frac{2\pi}{N_s \Omega_s} \sum_{\vec{k}_{//}} \frac{\exp(-k_{//}|z| + i\vec{k}_{//}\cdot\vec{r}_{//})}{k_{//}},$$

by operating the differential dyadic operator $\vec{\nabla}\vec{\nabla}$. With the use of eq. (3.10) the sum over $\vec{R}_{//}$ in eq. (3.4) is converted into the one over the 2-D reciprocal lattice vectors $\vec{G}_{//}$,

$$V_{\nu\mu}(\ell,m) = \frac{2\pi |M|^2}{\Omega_s} \sum_{\vec{G}_{//}} \frac{\exp[i\vec{G}_{//}\cdot\vec{R}_{\ell m} - |\vec{K}_{//}+\vec{G}_{//}||Z_{\ell m}|]}{|\vec{K}_{//}+\vec{G}_{//}|} \times$$

$$\times \begin{pmatrix} (K_{//}+G_x)^2, & (K_{//}+G_x)G_y, & \pm i(K_{//}+G_x)|\vec{K}_{//}+\vec{G}_{//}| \\ & G_y^2, & \pm i G_y |\vec{K}_{//}+\vec{G}_{//}| \\ (h.c.) & & -|\vec{K}_{//}+\vec{G}_{//}|^2 \end{pmatrix}, \qquad (3.11)$$

where $Z_{\ell m}$ is the z-component of $\vec{R}_{\ell m}$, $(G_x,G_y)=\vec{G}_{//}$, and (h.c.) means hermitian conjugate. In the above expression we have omitted the factor $\exp(i\vec{K}_{//}\cdot\vec{R}_m)\cong 1$. It is convenient to discuss the $\vec{G}_{//}=0$ term separately from the $\vec{G}_{//}\neq 0$ ones. The $\vec{G}_{//}=0$ term gives

$$V_{\nu\mu}^{long}(\ell,m) = \frac{\Delta_{LT}K_{//}d_{\perp}}{2}\exp(-K_{//}|Z_{\ell m}|)\begin{pmatrix}1 & 0 & \pm i\\ 0 & 0 & 0\\ \pm i & 0 & -1\end{pmatrix}, \qquad (3.12)$$

where we have used eq. (3.8). We see this term depends exponentially on the distance of two layers. Since $K_{//}$ is small compared with the reciprocal of the interlayer spacing, it has a very long interaction range, although each term, in itself, is small, because the small quantity $K_{//}d_{\perp}$ is also contained in the prefactor.

As to the $\vec{G}_{//}\neq 0$ terms in eq. (3.11), we may neglect the small $K_{//}$ effect. In addition, we assume that the symmetry of the 2-D lattice is high enough so that the cancellation of terms for a pair of $\vec{G}_{//}$ occurs. Then we can write the $\vec{G}_{//}\neq 0$ terms as

$$V_{\nu\mu}^{short}(\ell,m) = \frac{2\pi|M|^2}{\Omega_s}\sum_{\vec{G}_{//}\neq 0}\frac{\exp[i\vec{G}_{//}\cdot\vec{R}_{\ell m}-G_{//}|Z_{\ell m}|]}{G_{//}}\times$$

$$\times\begin{pmatrix}G_x^2 & 0 & 0\\ 0 & G_y^2 & 0\\ 0 & 0 & -G_{//}^2\end{pmatrix}. \qquad (3.13)$$

Due to the exponential factor $\exp(-G_{//}|Z_{\ell m}|)$ in the above

expression, this interaction acts between relatively near layers. We may retain only the nearest layer terms and neglect all the other interlayer interactions. One more assumption concerning the 2-D lattice structure that the x-direction be equivalent to the y-direction, as well as the requirement that the trace of the dipole transfer matrix should vanish yields the general form of the nearest layer interaction as

$$V_{\nu\mu}^{\text{short}}(\ell\ ,\ \ell\pm 1) = \Delta_{LT}\begin{pmatrix} -\beta_1 & & \\ & -\beta_1 & \\ & & 2\beta_1 \end{pmatrix}, \qquad (3.14)$$

in terms of a dimensionless parameter β_1.

In passing we note that when $K_{//}$ exactly vanishes, our model dipole-dipole interaction contains only two parameters β_0 and β_1 which describe the intralayer and the nearest layer interactions, respectively. It might also be possible to include in our model the next nearest layer interaction, the third nearest layer one, and so on, with corresponding parameters β_2, β_3 $\cdots$. This kind of layerwise dipole-dipole interactions for the case of $K_{//}=0$ was treated by Mahan and Obermair,[20] who calculated the β's up to β_5 on the (100) plane of cubic lattices. In order to show to what extent the nearest layer approximation is valid, we reproduce a part of their results in Table 3-1. We see β_ℓ falls off very rapidly as ℓ increases, and β_2's are, in fact, negligible on those surfaces. They also pointed out that the whole β_ℓ's are not independent quantities but they

should satisfy

$$\beta_0 + 2\sum_{\ell=1}^{\infty} \beta_\ell = \frac{1}{3} ,$$

where 1/3 comes from the Lorentz-Lorenz local-field factor. In our model, since we have retained only β_0 and β_1, it seems reasonable to require

$$\beta_0 + 2\beta_1 = 1/3 \qquad (3.15)$$

It will be shown in the next subsection that this is indeed a reasonable requirement.

Table 3-1: The layer wise dipole-dipole coupling constant β_ℓ *) for the (100) plane of simple cubic (sc), body-centered cubic (bcc), and face-centered cubic (fcc) lattices (after Mahan and Obermair[20])

	sc	bcc	fcc
β_0	0.35943	0.17972	0.25416
β_1	-0.01303	0.08309	0.04021
β_2	-0.000002208	-0.0006515	-0.00006368

*) $v(\ell)$ in their paper corresponds to our $-\beta_\ell$.

3-4 Eigenmodes of Periodic Bulk Lattice

From eqs. (3.9), (3.12), and (3.14), we see that the y--polarized excitons do not couple with the x- and z-polarized

ones, so we can treat them separately. For simplicity of notation, hereafter we use the parameters r_0, r_1, λ, and K rather than β_0, β_1, Δ_{LT}, and $K_{//}$, that are defined, respectively by

$$\begin{aligned} r_0 &= \beta_0 \, \Delta_{LT} \, , \\ r_1 &= 2\beta_1 \, \Delta_{LT} \, , \\ \lambda &= \Delta_{LT}/6 \, , \end{aligned} \tag{3.16}$$

and

$$K = K_{//} d_{\perp} \, .$$

Then the Hamiltonian for the y-polarized excitons is

$$H_y = (\varepsilon_b - r_0) \sum_{\ell=1}^{N} a_{\ell y}^{\dagger} \, a_{\ell y} - \frac{r_1}{2} \sum_{\ell=1}^{N-1} (a_{\ell y}^{\dagger} \, a_{\ell+1 y} + a_{\ell+1 y}^{\dagger} \, a_{\ell y}) + \delta \, a_{1y}^{\dagger} \, a_{1y} \, . \tag{3.17}$$

If we introduce the vector notations such that

$$\vec{a}_{\ell} = \begin{pmatrix} a_{\ell x} \\ a_{\ell z} \end{pmatrix} \, , \text{ and } \vec{a}_{\ell}^{\dagger} = [a_{\ell x}^{\dagger}, \; a_{\ell z}^{\dagger}] \, ,$$

then the Hamiltonian for the x-z polarized excitons can be written in the matrix form as

$$\begin{aligned} H_{x-z} = & \sum_{\ell=1}^{N} \vec{a}_{\ell}^{\dagger} \cdot \begin{pmatrix} \varepsilon_b - r_0 + 3\lambda K, & 0 \\ 0, & \varepsilon_b + 2r_0 - 3\lambda K \end{pmatrix} \cdot \vec{a}_{\ell} \\ & + \sum_{\ell=1}^{N-1} \left\{ \vec{a}_{\ell}^{\dagger} \cdot \begin{pmatrix} -r_1/2, & 0 \\ 0, & r_1 \end{pmatrix} \cdot \vec{a}_{\ell+1} + (\text{h.c.}) \right\} \\ & + \sum_{\substack{\ell,m=1 \\ (\ell>m)}}^{N} 3\lambda K \, e^{-K|\ell-m|} \, \vec{a}_{\ell}^{\dagger} \cdot \begin{pmatrix} 1 & i \\ i & -1 \end{pmatrix} \cdot \vec{a}_{m} + \end{aligned}$$

$$+ \sum_{\substack{\ell,m=1 \\ (\ell<m)}}^{N} 3\lambda K\, e^{-K|\ell-m|}\, \vec{a}_\ell^{\dagger} \cdot \begin{pmatrix} 1 & -i \\ -i & -1 \end{pmatrix} \cdot \vec{a}_m + \delta \vec{a}_1^{\dagger} \cdot \vec{a}_1 \,. \qquad (3.18)$$

In eq. (3.18) the first term contains the intralayer interactions, the second one represents the interlayer short-range interactions, the third and the fourth ones are the interlayer long-range interactions, and the last one is the surface potential term. We see, at once, that when K is exactly zero, the x- and z--polarized excitons decouple with each other and the Hamiltonian for the x-polarized ones becomes equivalent to H_y. In the following, we concentrate only on H_{x-z} and write it simply as H, with no suffices. The solutions of H_y can be obtained from those of H in the special case of K=0.

The above Hamiltonian is for the slab geometry. The corresponding bulk Hamiltonian, H_b, may be found (i) by dropping the surface potential and then (ii) by imposing the periodic boundary conditions on the N layers such that $\vec{a}_1 = \vec{a}_{N+1}$. Thus we get

$$\begin{aligned} H_b = & \sum_{\ell=1}^{N} \vec{a}_\ell^{\dagger} \cdot \begin{pmatrix} \varepsilon_b - r_0 + 3\lambda K, & 0 \\ 0, & \varepsilon_b + 2r_0 - 3\lambda K \end{pmatrix} \cdot \vec{a}_\ell \\ & + \sum_{\ell=1}^{N} \left\{ \vec{a}_\ell^{\dagger} \cdot \begin{pmatrix} -r_1/2, & 0 \\ 0, & r_1 \end{pmatrix} \cdot \vec{a}_{\ell+1} + (\text{h.c.}) \right\} \qquad (3.19) \\ & + \sum_{\ell=1}^{N} \sum_{\substack{m=-\infty \\ (\ell \neq m)}}^{\infty} 3\lambda K\, e^{-K|\ell-m|}\, \vec{a}_\ell^{\dagger} \cdot \begin{pmatrix} 1, & \pm i \\ \pm i, & -1 \end{pmatrix} \cdot \vec{a}_m \,, \end{aligned}$$

where for ± in the matrix of the last term, we have the positive

sign for $\ell>m$ and the minus sign for $\ell<m$. As concerns the last term, an addittional remark may be worthwhile: We assume here, and in the following also, that N is infinitely large so that, as far as K is finite, NK is also infinitely large. Namely if we want to take the limit $K\to 0$, the limit $N\to\infty$ should be taken before $K\to 0$. This is consistent with the idea of the optical selection rule, and enables the sum over m to extend from $-\infty$ to ∞ for a fixed value of ℓ, or vice versa. On the other hand, it is also possible to consider the case when K is exactly zero. In this case, the long-range term should be simply removed from the Hamiltonian, because the prefactor K in that term vanishes.

We now proceed to calculate the bulk normal modes. We start with the Heisenberg equations of motion for $\vec{a}_\ell$;

$$\begin{pmatrix} \varepsilon_b - r_0 + 3\lambda K - \varepsilon, & 0 \\ 0, & \varepsilon_b + 2r_0 - 3\lambda K - \varepsilon \end{pmatrix} \cdot \vec{a}_\ell + \begin{pmatrix} -r_1/2, & 0 \\ 0, & r_1 \end{pmatrix} (\vec{a}_{\ell-1} + \vec{a}_{\ell+1})$$

$$+ 3\lambda K \sum_{m=-\infty}^{\infty\,\prime} e^{-K|\ell-m|} \begin{pmatrix} 1, & \pm i \\ \pm i, & -1 \end{pmatrix} \vec{a}_m = 0 \,, \qquad (3.20)$$

where ε is the energy eigenvalue, and the prime on the sum is meant to exclude the term $m=\ell$. We assume the form

$$\vec{a}_\ell = \frac{1}{\sqrt{N}} \vec{u}\, e^{ik\ell}, \qquad (3.21)$$

where $k=n\pi/N(n=0, \pm 1, \pm 2, \ldots \pm(N-1), N)$ is the z-component of the wave vector reduced by the reciprocal lattice spacing $1/d_\perp$. The combination of K and k defines the three dimensional wave vector of the bulk exciton, $\vec{Q}=(K,0,k)$. Substituting eq. (3.21)

to eq. (3.20), and performing the summation, we obtain

$$\left\{\begin{pmatrix} \varepsilon_b - r_0 - r_1 \cos k + 3\lambda K - \varepsilon, & 0 \\ 0, & \varepsilon_b + 2r_0 + 2r_1 \cos k - 3\lambda K - \varepsilon \end{pmatrix} + 3\lambda K \left(\alpha(k)V_1 + \alpha(-k)V_2\right)\right\}\vec{u} = 0 \ , \tag{3.22}$$

where

$$\alpha(k) = \frac{1}{e^{K+ik}-1} \ , \tag{3.23}$$

is a function of k containing K as a parameter, and

$$V_1 = \begin{pmatrix} 1 & i \\ i & -1 \end{pmatrix} \ , \qquad V_2 = \begin{pmatrix} 1 & -i \\ -i & -1 \end{pmatrix} \ . \tag{3.24}$$

First we consider the case where K vanishes exactly. The x-polarized exciton is now transverse in character, while the z-polarized one is longitudinal. The energies of them are easily obtained from eq. (3.22);

$$\begin{aligned} \varepsilon_t(k) &= \varepsilon_b - r_0 - r_1 \cos k \\ \varepsilon_\ell(k) &= \varepsilon_b + 2r_0 + 2r_1 \cos k \ , \end{aligned} \tag{3.25-a}$$

with the corresponding eigenvectors,

$$\vec{u}_t(k) = \begin{pmatrix} 1 \\ 0 \end{pmatrix} \ , \quad \vec{u}_\ell(k) = \begin{pmatrix} 0 \\ 1 \end{pmatrix} \ . \tag{3.25-b}$$

Now we impose the requirement that the difference $\varepsilon_\ell(0)-\varepsilon_t(0)$ should be equal to the L-T splitting 6λ, which yields

$$r_0 + r_1 = 2\lambda \ . \qquad (3.26)$$

Noting the relations (3.16), we see the above 'sum-rule' exactly coincides with eq. (3.15). Therefore, if we fix the value of λ, which is itself a measure for the significance of the long-range interaction, our model dipole-dipole interactions contain only one independent parameter which can be a measure for the relative importance of the long-range interaction versus the short-range one.

Now we go back to the case where K is finite (but vanishingly small, of course). The function $\alpha(k)$ plays a significant role here, and it is useful to have its 'asymptotic expansion' in terms of K;

$$\alpha(k) = \frac{1}{K+ik}\,\frac{k}{2}\cot\frac{k}{2} - \frac{1}{2} + O(K) \ , \qquad (3.27)$$

where O(K) means the collection of terms that are of the same order of or higher order than K. Derivation of this formula will be given in Appendix B. Using eq. (3.27) in eq. (3.22), we obtain

$$\left\{\begin{pmatrix} \varepsilon_b - r_0 - r_1\cos k - \varepsilon, & 0 \\ 0, & \varepsilon_b + 2r_0 + 2r_1\cos k - \varepsilon \end{pmatrix} + \frac{6\lambda K}{K^2+k^2}\,\frac{k}{2}\cot\frac{k}{2}\begin{pmatrix} K & k \\ k & -K \end{pmatrix}\right\}\vec{u} = 0 \ . \qquad (3.28)$$

Note that the K-linear terms in the intralayer interactions are

exactly cancelled by those which arise from the long-range interlayer interactions. It is convenient to introduce a wave number k_0 such that (i) k_0 is small enough that it satisfies $k_0^2 \ll 1$, but (ii) k_0 is large enough that the condition $K/k_0 \ll 1$ is fulfilled. If K is small enough, such k_0 will surely exist. The region of k is divided into two, according to whether $|k|$ is smaller or larger than k_0. We solve the eigenvalue eq.(3.28) in these two regions of k, seperately. First we consider the case when $|k| \lesssim k_0$. We note that in this region

$$\frac{k}{2}\cot\frac{k}{2} = 1 - \frac{k^2}{12} + \cdots \simeq 1 \qquad (3.29)$$

Thus eq. (3.28) is rewritten approximately as

$$\left\{\begin{pmatrix} \varepsilon_b - r_0 - r_1 - \varepsilon, & 0 \\ 0, & \varepsilon_b + 2r_0 + 2r_1 - \varepsilon \end{pmatrix} + 6\lambda \cos\theta(k) \begin{pmatrix} \cos\theta(k) & \sin\theta(k) \\ \sin\theta(k) & -\cos\theta(k) \end{pmatrix}\right\} \vec{u} = 0 \ , \qquad (3.30)$$

where $\theta(k)$ is a function of k cotaining K as a parameter that measures the angle between the wave vector $\vec{Q}$ and the x-axis (see Fig. 3-2). In the following, we shall often omit the argument k of $\theta(k)$, where there is no fear of confusion. With the aid of the sum rule (3.26), this equation can be solved easily and we obtain two modes; for the first one, the energy and the eigenvector are given by

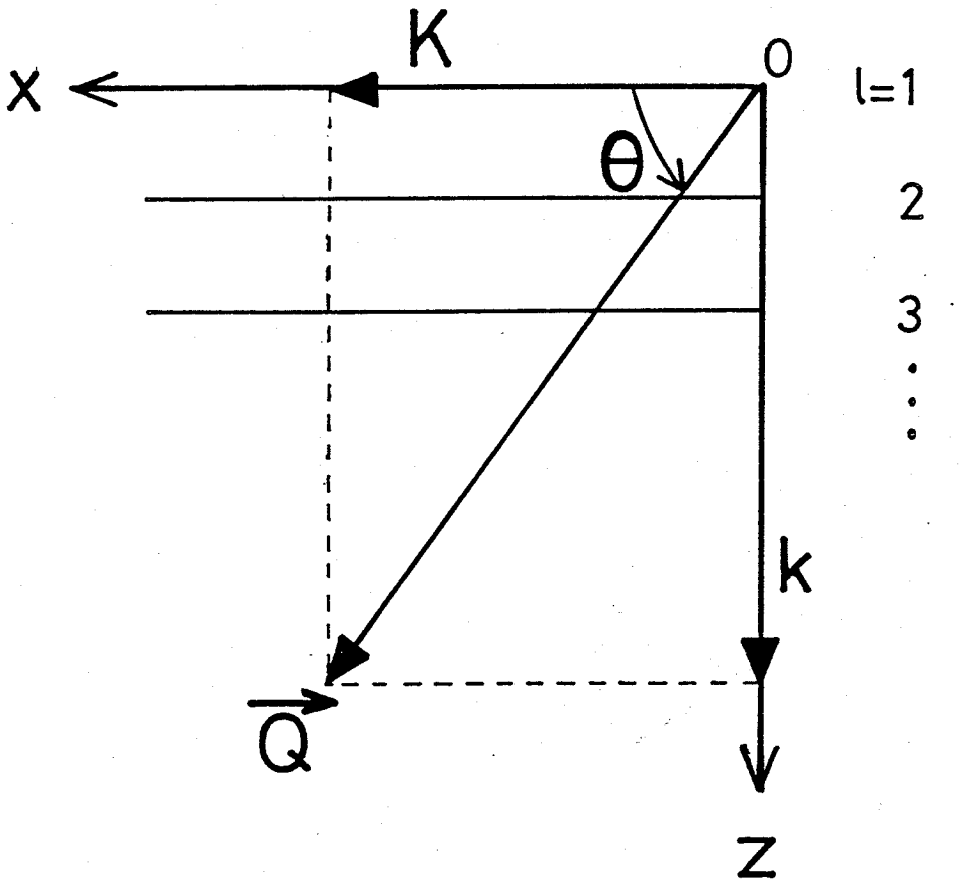

Fig.3-2. Schematic diagram showing the definition of the angle θ.

$$\begin{cases} \varepsilon_t(k) = \varepsilon_b - 2\lambda \\ \vec{u}_t(k) = \begin{pmatrix} \sin\theta \\ -\cos\theta \end{pmatrix} , \end{cases} \tag{3.31}$$

and for the second one,

$$\begin{cases} \varepsilon_\ell(k) = \varepsilon_b + 4\lambda \\ \vec{u}_\ell(k) = \begin{pmatrix} \cos\theta \\ \sin\theta \end{pmatrix} . \end{cases} \tag{3.32}$$

Clearly, these two modes correspond to the T-exciton and the L-exciton, respectively.

In the region where $|k| \gtrsim k_0$, the second term (long-range term) in the curly bracket of eq. (3.28) can be neglected due to the condition (ii) for k_0, and we get simply

$$\begin{cases} \varepsilon_t(k) = \varepsilon_b - r_0 - r_1 \cos k \\ \vec{u}_t(k) = \begin{pmatrix} k/|k| \\ 0 \end{pmatrix}, \end{cases} \tag{3.33}$$

and

$$\begin{cases} \varepsilon_\ell(k) = \varepsilon_b + 2r_0 + 2r_1 \cos k \\ \vec{u}_\ell(k) = \begin{pmatrix} 0 \\ k/|k| \end{pmatrix} . \end{cases} \tag{3.34}$$

Summarizing the results (3.31) to (3.34), we arrive at the unified expressions of the bulk eigenmodes which work for arbitrary values of k;

$$\begin{cases} \varepsilon_t(k) = \varepsilon_b - r_0 - r_1 \cos k \\ \vec{u}_t(k) = \begin{pmatrix} \sin\theta \\ -\cos\theta \end{pmatrix} , \end{cases} \tag{3.35}$$

and

$$\begin{cases} \varepsilon_{\ell}(k) = \varepsilon_b + 2r_0 + 2r_1 \cos k \\ \vec{u}_{\ell}(k) = \begin{pmatrix} \cos\theta \\ \sin\theta \end{pmatrix} . \end{cases} \tag{3.36}$$

The energy band structures of these modes are schematically shown in Fig. 3-3.

At this point, we mention two remarks on the results (3.35) and (3.36). One is on the validity of the approximations made to solve the eigenvalue problem. In the above discussions, the somewhat artificial parameter k_0 has been introduced, which hinders us from seeing to what order in K the above results are valid. To check this is really important especially when we want to try a $K_{//}$-expansion, which we shall explain in the next section. Instead of the above treatment, it is also possible to make a somewhat more mathematical argument, in which all the terms appearing in the Hamiltonian are expanded in the series of K. This will be made in Appendix C. According to the results there, the expressions of energies in eqs. (3.35) and (3.36) are correct up to the linear order in K, i.e., corrections are of order K^2. This is to be expected; the bulk exciton energy cannot have K-linear terms, as far as inversion symmetry exists. On the other hand, the eigenvectors have corrections linear in K. In fact, cos θ in $\vec{u}_t(k)$ and $\vec{u}_{\ell}(k)$ should be replaced by

$$\frac{r_0 + r_1}{r_0 + r_1 \cos k} \frac{k}{2} \cot \frac{k}{2} \times \cos\theta , \tag{3.37}$$

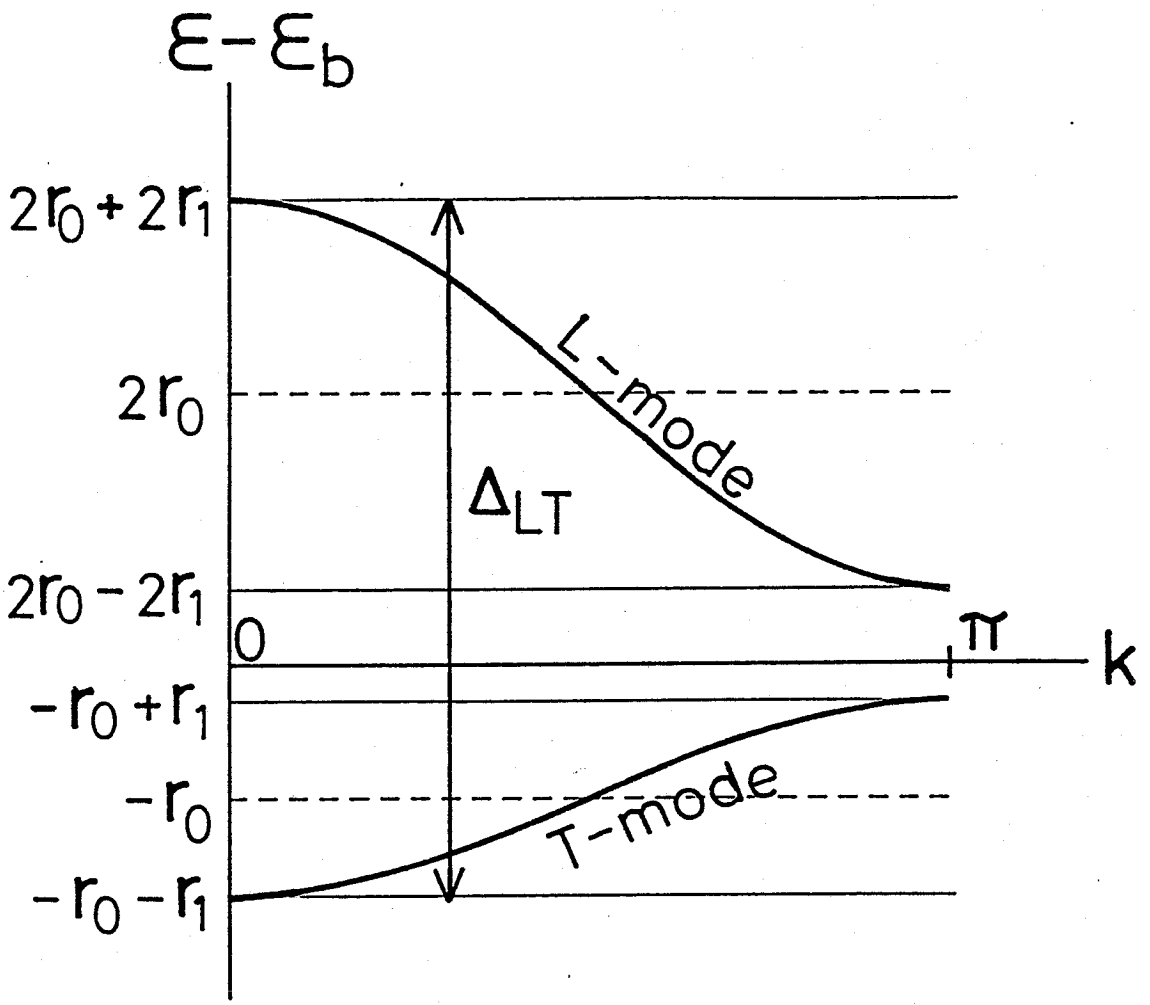

Fig.3-3. Energy band structures of the T- and the L-modes in the periodic lattice.

in order for $u_t(k)$ and $u_\ell(k)$ to be correct up to linear order in K. The Taylor expansion of the prefactor in the expression (3.37) yields

$$\frac{r_0 + r_1}{r_0 + r_1 \cos k} \frac{k}{2} \cot \frac{k}{2} = 1 + \left(\frac{r_1}{4\lambda} - \frac{1}{12}\right) k^2 + \cdots \quad . \quad (3.38)$$

Therefore this correction becomes important only for a relatively larger value of k such that the k^2-term cannot be neglected. This means that the bulk mode deviates from the pure T- or L-mode and becomes rather the L-T mixed mode when k increases, which is also a well-known phenomenon.[5] In this region of k, however, the value of cos θ itself is small (of order K), so the total correction that arises due to the replacement of (3.37) is also small. As it could be checked at each step of the calculations, this correction of order K does not matter in the following arguments at all. Therefore, hereafter we employ the simple expressions of eqs. (3.35) and (3.36) for the eigenvectors rather than the complicated expression (3.37).

The second remark is on the conspicuous nature of the long-range interactions. Noting that the energy eigenvalues in eqs. (3.35) and (3.36) coincide with those in eq. (3.25-a), we see that the long-range interactions apparently play no role in determining the energies (at least in the lowest order in K). As to the eigenvectors, the situation is quite different. This is most clearly understood by taking the k→0 limit. In this limit, $\vec{u}_t(k)$ in eq. (3.35) becomes (0,-1), which coincides

with $\vec{u}_\ell(k)$ in eq. (3.25-b) (except for an unrelevant sign), and $\vec{u}_\ell(k)$ in eq. (3.36) with $\vec{u}_t(k)$ in eq. (3.25-b). Thus the existence of the long-range interactions, or the finiteness of K, drastically alters the nature of the mode belonging to a particular energy band especially where k is small. This demonstrates clearly the 'non-analyticity' of our problem that is brought about by the long-range interactions.

§4 Method of Analysis

We calculate the resolvent Green's functon (in the following, the resolvent Green's function is simply called as the resolvent) from which the density of states and the optical spectra are most easily obtained. We are interested in the surface induced changes of the above quantities. These include (i) the appearance of surface lacalized modes, (ii) the rearrangement of the density of states and the oscillator strengths among the bulk modes, (iii) the exchange of the oscillator strengths between the surface localized modes and the bulk modes, and so on. The advantage of using the resolvent over directly handling the Schrödinger equation is that it elucidates the above points in the easiest possible manner. In this section, we explain the methods to solve Dyson's equation and derive a set of basic equations that determines the resolvent. The actual solution will be given in the subsequent section.

4-1 K-Representation of the Hamiltonian

The eigenmodes of the periodic bulk crystal obtained in the last section serve as a complete basis set to expand the 'spinors' on the N layers in the slab crystal. Thus the operator $\vec{a}_\ell$ can be expanded as

$$\vec{a}_\ell = \frac{1}{\sqrt{N}} \sum_k \sum_\nu e^{ik\ell} \vec{u}_\nu(k)\, b_\nu(k) \quad , \tag{4.1}$$

where ν stands for t or ℓ, and the expansion coefficients $b_\nu(k)$'s have the meaning of the annihilation operators of the bulk normal modes. It is more convenient to use matrix notations and we rewrite eq. (4.1) as

$$\vec{a}_\ell = \frac{1}{\sqrt{N}} \sum_k e^{ik\ell} U(k) \vec{b}_k \quad , \tag{4.2}$$

where the 2×2 matrix U(k) and the vector operator $\vec{b}_k$ are defined, respectively, by

$$U(k) = \begin{pmatrix} \sin\theta, & \cos\theta \\ -\cos\theta, & \sin\theta \end{pmatrix} , \tag{4.3}$$

and

$$\vec{b}_k = \begin{pmatrix} b_t(k) \\ b_\ell(k) \end{pmatrix} . \tag{4.4}$$

Strictly speaking, $\vec{a}_\ell$'s in the original slab model are defined only for the layers from ℓ=1 to ℓ=N, but we may extend this definition periodically to virtual layeres of $\ell \leq 0$ and $\ell \geq N+1$ according to eq. (4.2). This allows us to express the Hamiltonian for the slab geometry (eq. (3.18)) as the sum of the Hmiltonian for the bulk crystal with the periodic boundary condition (eq. (3.19)) and the remaining terms;

$$H = H_b + V_{sr} + V_{\ell r} + V_{sp} \quad , \tag{4.5}$$

where

$$V_{sr} = -\vec{a}_0^\dagger \begin{pmatrix} -r_1/2, & 0 \\ 0, & r_1 \end{pmatrix} \vec{a}_1 - \vec{a}_N^\dagger \begin{pmatrix} -r_1/2, & 0 \\ 0, & r_1 \end{pmatrix} \vec{a}_{N+1} \quad , \tag{4.6}$$

$$V_{\ell r} = - \sum_{\ell=1}^{N} 3\lambda K \, e^{-K|\ell-m|} \, \vec{a}_{\ell}^{\dagger} \left(\sum_{m=-\infty}^{0} V_1 \, \vec{a}_m + \sum_{m=N+1}^{\infty} V_2 \, \vec{a}_m \right) , \qquad (4.7)$$

and

$$V_{sp} = \delta \, \vec{a}_1^{\dagger} \cdot \vec{a}_1 \quad . \qquad (4.8)$$

The surface perturbations V_{sr}, and $V_{\ell r}$ can be viewed as originated from cutting the long-range interactions and the short-range ones, respectively, at the two surfaces of the slab, while V_{sp} is the surface potential, of course. With the use of eq. (4.2), we can express each of the four terms in eq. (4.5) in terms of the operators of the extended basis set, $\vec{b}_k^{\dagger}$ and $\vec{b}_k$. A straightforward calculation yields

$$H_b = \sum_k \vec{b}_k^{\dagger} \begin{pmatrix} \varepsilon_t(k), & 0 \\ 0, & \varepsilon_{\ell}(k) \end{pmatrix} \vec{b}_k \quad , \qquad (4.9)$$

$$V_{sr} = \frac{1}{N} \sum_k \sum_{k'} \frac{r_1}{2} \left(e^{-ik} + e^{ik'} \right) \times \qquad (4.10)$$

$$\times \, \vec{b}_k^{\dagger} \begin{pmatrix} \sin\theta \, \sin\theta' - 2\cos\theta \, \cos\theta', & \sin\theta \, \cos\theta' + 2\cos\theta \, \sin\theta' \\ \cos\theta \, \sin\theta' + 2\sin\theta \, \cos\theta', & \cos\theta \, \cos\theta' - 2\sin\theta \, \sin\theta' \end{pmatrix} \vec{b}_{k'} ,$$

$$V_{\ell r} = \frac{1}{N} \sum_k \sum_{k'} 3\lambda K \left(1 - e^{-KN}\right) \vec{b}_k^{\dagger} \left\{ e^{K+ik'} \, \alpha(k) \, \alpha(k') \, e^{i\theta} \, e^{i\theta'} \, V_1 \right.$$

$$\left. + \, e^{K-ik} \, \alpha(-k) \, \alpha(-k') \, e^{-i\theta} \, e^{-i\theta'} \, V_2 \right\} \vec{b}_{k'} , \qquad (4.11)$$

and

$$V_{sp} = \frac{1}{N} \sum_k \sum_{k'} \delta \, e^{-ik} \, e^{ik'} \times$$

$$\times \vec{b}_k^{\dagger} \begin{pmatrix} \sin\theta \sin\theta' + \cos\theta \cos\theta', & \sin\theta \cos\theta' - \cos\theta \sin\theta' \\ \cos\theta \sin\theta' - \sin\theta \cos\theta', & \cos\theta \cos\theta' + \sin\theta \sin\theta' \end{pmatrix} \vec{b}_{k'}, \quad (4.12)$$

where θ' stands for $\theta(k')$, and the definitions of $\alpha(k)$, V_1, and V_2 are found in eqs. (3.23) and (3.24). In the expression (4.11), the terms containing the factor e^{-KN} clearly represents the interference effect between the surface on one side of the slab and the surface on the opposite side, via the long-range interaction. Since we have assumed that KN is infinitely large, these terms can be neglected. A remarkable feature common to the expressions (4.10), (4.11), and (4.12) is that all the elementary terms contained in the summations are of the form $f(k) \times g(k')$, where $f(k)$ ($g(k')$) is a function only of k (k'); namely, they have a separable form. For a later use, it is advantageous to stress this point, and we rewrite V_{sr} and V_{sp} as

$$V_{sr} = \frac{1}{N} \sum_k \sum_{k'} \frac{n}{2} (e^{-ik} + e^{ik'}) \vec{b}_k^{\dagger} (\sin\theta \sin\theta' T_{ss} + \sin\theta \cos\theta' T_{sc} + \cos\theta \sin\theta' T_{cs} + \cos\theta \cos\theta' T_{cc}) \vec{b}_{k'}, \quad (4.10)'$$

$$V_{sp} = \frac{1}{N} \sum_k \sum_{k'} \delta\, e^{-ik}\, e^{ik'}\, \vec{b}_k^{\dagger} (\sin\theta \sin\theta' S_{ss} + \sin\theta \cos\theta' S_{sc} + \cos\theta \sin\theta' S_{cs} + \cos\theta \cos\theta' S_{cc}) \vec{b}_{k'}, \quad (4.12)'$$

where

$$T_{ss} = \begin{pmatrix} 1, & 0 \\ 0, & -2 \end{pmatrix}, \qquad T_{sc} = \begin{pmatrix} 0, & 1 \\ 2, & 0 \end{pmatrix}$$

$$T_{cs} = \begin{bmatrix} 0, & 2 \\ 1, & 0 \end{bmatrix}, \qquad T_{cc} = \begin{bmatrix} -2, & 0 \\ 0, & 1 \end{bmatrix}, \tag{4.13}$$

$$S_{ss} = \begin{bmatrix} 1, & 0 \\ 0, & 1 \end{bmatrix}, \qquad S_{sc} = \begin{bmatrix} 0, & 1 \\ -1, & 0 \end{bmatrix}$$

$$S_{cs} = \begin{bmatrix} 0, & -1 \\ 1, & 0 \end{bmatrix} \qquad S_{cc} = \begin{bmatrix} 1, & 0 \\ 0, & 1 \end{bmatrix}. \tag{4.14}$$

In order to simplify the notations, we proceed to rewrite the surface perturbations one step further. We introduce a 6×6 matrix [M] each element of which is, again, a 2×2 matrix, and a 6×1 column vector [f(k)] whose elements are functions of k. They are defined by

$$[M] = \left[\begin{array}{c|c|c} \begin{matrix} 0, & 3\lambda KV_1 \\ 3\lambda KV_2, & 0 \end{matrix} & \begin{matrix} 0 \end{matrix} & \begin{matrix} 0 \end{matrix} \\ \hline \begin{matrix} 0 \end{matrix} & \begin{matrix} 0, & r_1T_{ss}/2 \\ r_1T_{ss}/2, & \delta S_{ss} \end{matrix} & \begin{matrix} 0, & r_1T_{sc}/2 \\ r_1T_{sc}/2, & \delta S_{sc} \end{matrix} \\ \hline \begin{matrix} 0 \end{matrix} & \begin{matrix} 0, & r_1Tcs/2 \\ r_1T_{cs}/2, & \delta S_{cs} \end{matrix} & \begin{matrix} 0, & r_1T_{cc}/2 \\ r_1T_{cc}/2, & \delta S_{cc} \end{matrix} \end{array}\right], \tag{4.15}$$

and

$$[f(k)] = {}^t[\alpha(-k)d^{-i\theta}, \ \alpha(k)e^{K+ik}e^{i\theta}, \ \sin\theta, \ e^{ik}\sin\theta, \ \cos\theta, \ e^{ik}\cos\theta]. \tag{4.16}$$

where ${}^t[\ ]$ means transposition of the vector. Now the surface perturbations can be written as

$$V_{\ell r} + V_{sr} + V_{sp} = \frac{1}{N} \sum_{k} \sum_{k'} \vec{b}_k^{\dagger} V_{kk'} \vec{b}_{k'} \quad , \tag{4.17}$$

and, with the aid of the matrix [M] and the vector [f(k)], $V_{kk'}$ in this expression are given compactly as

$$V_{kk'} = {}^{t}[f^{*}(k)][M][f(k')] \ . \tag{4.18}$$

Note that the each element of [M] is a constant with respect to the variables k and k', and that since it is a 2×2 matrix, $V_{kk'}$ is also a 2×2 matrix.

4-2 Dyson's Equation

In the last subsection, we have expressed the Hamiltonian in the k-representation. Now we define the resolvent for the Hamiltonian also in the k-representation as follows,

$$G_{kk'}(z) = \begin{pmatrix} G^{tt}_{kk'}(z), & G^{t\ell}_{kk'}(z) \\ G^{\ell t}_{kk'}(z), & G^{\ell\ell}_{kk'}(z) \end{pmatrix} \ , \tag{4.19}$$

where $G^{\nu\nu'}_{kk'}(z)$ (ν,ν'=t or ℓ) in the right hand side is given by

$$G^{\nu\nu'}_{kk'}(z) = \langle 0 | \ b^{\nu}_{k} \frac{1}{z-H} b^{\nu'\dagger}_{k'} \ | 0 \rangle \ . \tag{4.20}$$

In (4.20) $|0\rangle$ represents the ground state of the crystal and $z=\varepsilon-i0^{+}$. Hereafter, we shall often omit the argument z of $G_{kk'}(z)$. If we take H_b as the unperturbed Hamiltonian, Dyson's equation for the resolvent can be written as

$$G_{kk'} = G_0(k)\,\delta_{kk'} + \frac{1}{N}\sum_{k''} G_0(k)\,V_{kk''}\,G_{k''k'} \,. \qquad (4.21)$$

The unperturbed resolvent $G_0(k)$ is defined similarly as in eqs. (4.19) and (4.20), but with H_b instead of H. Since the operators $\vec{b}_k$ and $\vec{b}_k^{\dagger}$ diagonalize the unperturbed Hamiltonian H_b, the Kronecker δ has been extracted from its difinition. Clearly, the explicit expression of $G_0(k)$ is given by

$$G_0(k) = \begin{pmatrix} \frac{1}{z-\varepsilon_t(k)}, & 0 \\ 0, & \frac{1}{z-\varepsilon_\ell(k)} \end{pmatrix} , \qquad (4.22)$$

where the energy of the bulk T(L)-mode exciton $\varepsilon_t(k)$ ($\varepsilon_\ell(k)$) is given in eq. (3.35) (eq. (3.36)).

The importance of the k-representation lies in the fact that in this representation, the kernel $V_{kk'}$ of the integral eq. (4.21) is of the separable form (see eq. (4.18)). This enables us to solve this equation with no difficulties in principle. We proceed as follows: First let $\Delta G_{kk'}$ denote the second term in eq. (4.21). From eqs. (4.18) and (4.16), we see that the form of the k-dependence of the terms in $\Delta G_{kk'}$ is expected to be one of the six functions $\{\alpha(k)e^{i\theta}$, $\alpha(-k)e^{K-ik}e^{-i\theta}$, $\sin\theta$, $e^{-ik}\sin\theta$, $\cos\theta$, $e^{-ik}\cos\theta\}$ multiplied by $G_0(k)$. Also, the k'-dependence of them is exhausted by $\{\alpha(-k')e^{-i\theta'}$, $\alpha(k')e^{K+ik}e^{i\theta'}$, $\sin\theta'$, $e^{ik'}\sin\theta'$, $\cos\theta'$, $e^{ik'}\cos\theta'\}$ multiplied by $G_0(k')$, which can be easily checked by performing the Born expansion of eq. (4.21) up to the first few orders. Accordingly, $\Delta G_{kk'}$ can be expanded as a sum of the bilinear terms of the

above two groups of functions. Since we have six functions of k and also six functions of k', there arise thirty-six terms in the expansion of $\Delta G_{kk'}$. If we show a first few terms of such an expansion, we have

$$\Delta G_{kk'} = \frac{G_0(k)}{N} \times \Big\{ \alpha(k) e^{i\theta} \alpha(-k') e^{-i\theta'} A_1 + \alpha(k) e^{K+ik_e i\theta} \alpha(-k') e^{-i\theta'} A_2$$

$$+ \alpha(k) e^{i\theta} \alpha(-k') e^{K-ik'_e - i\theta'} A_3$$

$$+ \alpha(k) e^{K+ik_e i\theta} \alpha(-k') e^{K-ik'_e - i\theta'} A_4 + \alpha(k) e^{i\theta} \sin\theta' B_1 + \cdots$$

$$\cdots \Big\} \times G_0(k') \ . \qquad (4.23)$$

Here the expansion coefficients A_1 etc. are 2×2 matrices, each element of which is a function of z, although we have not indicated it explicitly, and is costant with respect to both k and k'. Thirty-six such matrices are necessary in the complete expression of $\Delta G_{kk'}$. If we use the column vector [f(k)] defined in eq.(4.16), this expansion of $G_{kk'}$ of finite number of terms can be written in a more compact form; by adding the unperturbed term to this, the total resolvent becomes

$$G_{kk'} = G_0(k)\, \delta_{kk'} + \frac{G_0(k)}{N}\, {}^t[f^*(k)][N][f(k')]\, G_0(k') \ , \qquad (4.24)$$

Here the matrix [N] is defined as

$$[N] = \left(\begin{array}{cc|cc|cc} A_1 & A_3 & B_1 & B_3 & C_1 & C_3 \\ A_2 & A_4 & B_2 & B_4 & C_2 & C_4 \\ \hline D_1 & D_3 & E_1 & E_3 & F_1 & F_3 \\ D_2 & D_4 & E_2 & E_4 & F_2 & F_4 \\ \hline P_1 & P_3 & Q_1 & Q_3 & R_1 & R_3 \\ P_2 & P_4 & Q_2 & Q_4 & R_2 & R_4 \end{array}\right) , \tag{4.25}$$

and the expansion coefficients $A_1 \sim R_4$ have been introduced. Note that [N] is a 6×6 matrix each element of which is a 2×2 matrix, as is similar to the matrix [M] defined in eq. (4.15). Substituting eqs. (4.18) and (4.24) to the right hand side of Dyson's eq. (4.21), we obtain

$$G_{kk'} = G_0(k)\,\delta_{kk'} + \frac{G_0(k)}{N}\,{}^t[f^*(k)][M][f(k')]\,G_0(k') + \frac{G_0(k)}{N}\,{}^t[f^*(k)][M][I][N][f(k')]\,G_0(k') , \tag{4.26}$$

where [I] is also a 6×6 matrix, with each element being a 2×2 matrix, and defined as

$$[I] = \frac{1}{N}\sum_k G_0(k)\,[f(k)]\,{}^t[f^*(k)] . \tag{4.27}$$

We compare eq. (4.26) with eq (4.24). We notice that the six functions of k in ${}^t[f^*(k)]$ are linearly independent, and that the same is, of course, true for those in [f(k')], so that the coefficient of the each bilinear function in eq. (4.26) should coincide with that in eq. (4.24). This consideration yields

$$[N] = [M] + [M][I][N] . \tag{4.28}$$

This equation can be viewed as Dyson's equation in 'f(k)-representation', where f(k) means the set of functions contained in the vector [f(k)].

4-3 $K_{//}$-Expansion

We have come to the coupled linear equations (4.28), and we are ready to solve the integral equation (4.21). In other words, if we obtain the solution [N] from eq. (4.28), then by substituting it in eq. (4.24) we can obtain the resolvent. There are, however, seventy-eight unknowns*) in [N] and it is a rather complicated task to find out its exact solution. Instead, we seek for an approximate solution, which will be sufficient for our purpose, in the following.

We have a small parameter K (K is equal to $K_{//}d_{\perp}$, as defined before) in our theory, which suggests the perturbation theoretical approach to our problem. The situation is, however, a bit complicated. Behavior of the bulk eigenmodes discussed in §3-4 implies that the solution valid up to first order in K may not be continued smoothly from the zeroth order solution. It also tells us that the finiteness of K is important especically when k is small. Therefore, we have to be careful in the

---

*) Since [N] is a 12×12 matrix, there are 144 unknowns in it. The reciprocity of the resolvent ($G_{kk'}(z) = G^{\dagger}_{k'k}(z^*)$) reduces this number to 78.

expansion with respect to K. For such a $K_{//}$-expansion we have the first requirement to retain the quantity which measures the relative magnitude of k (or k') and K. This quantity is, of cuorse, θ. The angle θ is contained in the six elements in [f(k)]. The first two elements in [f(k)] have a factor $\alpha(k)e^{i\theta}$ (or its complex conjugate) in common. Using eq. (3.27), this can be evaluated as

$$\alpha(k)\, e^{i\theta} = \frac{1}{K} \cos\theta \, \frac{k}{2} \cot\frac{k}{2} - \frac{e^{i\theta}}{2} + O(K) \, . \qquad (4.29)$$

Therefore, except for the trigonometric functions cosθ and sinθ , the first two elements in [f(k)] are of different order in K from the remaining four elements; the formers are of order K^{-1} and the latters K^0. Since the resolvent is expanded in bilinear terms of $[f^*(k)]$ and [f(k')], the coefficients of the bilinear terms composed of the first two elements of $[f^*(k)]$ and [f(k')] should be evaluated at least up to the order of K^2, those composed of the last four terms up to K^0, and those of the cross terms up to K^1. This is the second requirement.

The small parameter K appears also in the matrix [I]. There are twenty-one independent integrals in [I]. Most of which cannot be integrated analytically, but we may evaluate them in the expanded series of K and retain only the first few terms. The second requirement determines up to what order in K each intergral should be evaluated.

We should keep the above two requirements in mind, but

otherwise we can go parallel to the conventional perturbation expansion. The actual evaluation of the integrals to the required order will be given in Appendix D. According to the results there, all the intergrals in [I] can be related to the following 2×2 diagonal matrices;

$$I = \frac{1}{N} \sum_k G_0(k)$$

$$J = \frac{1}{N} \sum_k e^{ik} G_0(k) \tag{4.30}$$

$$\tilde{I} = \frac{1}{N} \sum_k K|\alpha(k)|^2 G_0(k) \ .$$

In order to simplify the notations, we introduce the following matrices;

$$\{A(z)\} = \begin{pmatrix} A_1, & A_3 \\ A_2, & A_4 \end{pmatrix} \ , \tag{4.31(a)}$$

$$\{V\} = \begin{pmatrix} 0, & 3\lambda V_1 \\ 3\lambda V_2, & 0 \end{pmatrix} \ , \tag{4.31(b)}$$

$$\{T_1\} = \begin{pmatrix} 0, & r_1 T_{ss}/2 \\ r_1 T_{ss}/2, & \delta S_{ss} \end{pmatrix} \ , \tag{4.31(c)}$$

$$\{T_2\} = \begin{pmatrix} 0, & r_1 T_{sc}/2 \\ r_1 T_{sc}/2, & \delta S_{sc} \end{pmatrix} \ , \tag{4.31(d)}$$

$$\{T_3\} = \begin{pmatrix} 0, & r_1 T_{cs}/2 \\ r_1 T_{cs}/2, & \delta S_{cs} \end{pmatrix} \ , \tag{4.31(e)}$$

$$\{T_4\} = \begin{pmatrix} 0, & r_1 T_{cc}/2 \\ r_1 T_{cc}/2, & \delta S_{cc} \end{pmatrix} , \qquad (4.31(f))$$

$$\{E_1\} = \begin{pmatrix} 1, & e^K \\ e^K, & e^{2K} \end{pmatrix} , \qquad (4.31(g))$$

$$\{E_2\} = \begin{pmatrix} 1, & -1 \\ 1, & -1 \end{pmatrix} , \qquad (4.31(h))$$

$$\{E_3\} = \begin{pmatrix} 1, & 1 \\ -1, & -1 \end{pmatrix} , \qquad (4.31(i))$$

$$\{I\} = \begin{pmatrix} I, & J \\ J, & I \end{pmatrix} . \qquad (4.31(j))$$

Curly brakets { } are put on these to emphasize that they are 2×2 matrices with each element being a 2×2 matrix, so the scalars in $\{E_1\}$, $\{E_2\}$, and $\{E_3\}$ should be regarded as proportional to the 2×2 unit marix. The unknown matrices $\{B(z)\}$, $\{C(z)\}$, etc. are similarly defined as $\{A(z)\}$ in eq. (4.31(a)) (there are nine such matrices). Now the $K_{//}$-expansion of eq. (4.28) yields the basic set of equations that determine the complete lowest order solution of eq. (4.28) with respect to K. With the aid of the notations introduced above, these equations are given as follows;

$$\{A(z)\} = K\{V\} + \{V\}(\tilde{I}\{E_1\}\{A(z)\} + \frac{iKI}{2}\{E_2\}\{D(z)\} + K\tilde{I}\{E_1\}\{P(z)\}) , \qquad (4.32\text{-}1)$$

$$\{B(z)\} = \{V\} + \{V\}(\overset{\gamma}{I}\{E_1\}\{B(z)\} + \frac{iKI}{2}\{E_2\}\{E(z)\} + K\overset{\gamma}{I}\{E_2\}\{Q(z)\}) \ , \tag{4.32-2}$$

$$\{C(z)\} = \{V\}(\overset{\gamma}{I}\{E_1\}\{C(z)\} + \frac{iKI}{2}\{E_2\}\{F(z)\} + K\overset{\gamma}{I}\{E_1\}\{R(z)\}) \ , \tag{4.32-3}$$

$$\{D(z)\} = \{T_1\}\{I\}\{D(z)\} + (-\frac{i}{2}\{T_1\}\{E_3\}I + \{T_2\}\{E_1\}\overset{\gamma}{I})\{A(z)\}, \tag{4.32-4}$$

$$\{E(z)\} = \{T_1\} + \{T_1\}\{I\}\{E(z)\} \ , \tag{4.32-5}$$

$$\{F(z)\} = \{T_2\} + \{T_1\}\{I\}\{F(z)\} \ , \tag{4.32-6}$$

$$\{P(z)\} = \{T_3\}\{I\}\{D(z)\} + (-\frac{i}{2}\{T_3\}\{E_3\}I + \{T_4\}\{E_1\}\overset{\gamma}{I})\{A(z)\} \ , \tag{4.32-7}$$

$$\{Q(z)\} = \{T_3\} + \{T_3\}\{I\}\{E(z)\} \ , \tag{4.32-8}$$

and

$$\{R(z)\} = \{T_4\} + \{T_3\}\{I\}\{F(z)\} \ . \tag{4.32-9}$$

According to the second requirement in the $K_{//}$-expansion, $\{A(z)\}$ should be calculated up to the order of K^2, $\{B(z)\}$, $\{C(z)\}$, and $\{D(z)\}$ up to K^1, and $\{E(z)\}$, $\{F(z)\}$, $\{P(z)\}$, $\{Q(z)\}$, $\{R(z)\}$ up to K^0. These points will not be repeated when we actually solve the equations.

We now prove some general relations among these unknown matrices, which will be useful in solving the above coupled linear equations. We define a 2×2 matrix U such that

$$U = \begin{pmatrix} 0, & -1 \\ 1, & 0 \end{pmatrix} \ . \tag{4.33}$$

This is a unitary matrix which represents a 90°-rotation in the (x,z)-plane. From the definitions (4.13) and (4.14), we

see, at once, that

$$T_{cs} = U\, T_{ss}, \text{ and } S_{cs} = U\, S_{ss} \ . \tag{4.34}$$

Operating U to the whole equation of (4.32-5) on the left hand side, and comparing it with eq. (4.32-8), we obtain, with the help of eq. (4.34),

$$Q(z) = U\, E(z) \ . \tag{4.35}$$

In a similar way, we can prove the following relations,

$$\begin{aligned} &\{F(z)\} = \{E(z)\}\, {}^{t}U, \quad \{R(z)\} = U\, \{E(z)\}\, {}^{t}U \ , \\ &\{P(z)\} = U\{D(z)\}, \quad \{C(z)\} = \{B(z)\}\, {}^{t}U \ . \end{aligned} \tag{4.36}$$

Other relations come from the reciprocity of the resolvent:

$$G_{kk'}(z) = G^{\dagger}_{k'k}(z^{*}) \ , \tag{4.37}$$

which can be shown from the definitions of $G_{kk'}(z)$. With the help of eqs. (4.37) and (4.24), we obtain

$$\begin{aligned} &\{A(z)\} = \{A(z^{*})\}^{\dagger}, \quad \{E(z)\} = \{E(z^{*})\}^{\dagger}, \quad \{R(z)\} = \{R(z^{*})\}^{\dagger}, \\ &\{B(z)\} = \{D(z^{*})\}^{\dagger}, \quad \{C(z)\} = \{P(z^{*})\}^{\dagger}, \quad \{F(z)\} = \{Q(z^{*})\}^{\dagger}. \end{aligned} \tag{4.38}$$

It can be easily checked that the solution of the basic equations (4.32-1)$\sim$(4.32-9), which is the lowest order approximation with respect to K of the original Dyson's equation (4.28), actually satisfies eq. (4.38). These general relations significantly simplify the calculations. In addition, calculations of the physical quantities such as the density of states and the

absorption spectra do not require the complete solution, which we shall see in the next sections.

§5 Density of States and Absorption Spectrum

5-1 Evaluation of the Density of States

As we have seen in §3, in the crystal with the periodic boundary condition, the energy dispersions of the eigenmodes in our model Hamiltonian are described by the two branches of band of cosine type k-dependence. The density of states (DOS) of such a system is well-known, and it is needless to discuss. Our concern here is in the surface-induced change of the DOS, which we call $D(\varepsilon)$ in the following. This is conveniently obtained from the second term of Dyson's equation (4.21). The connection between the DOS and the resolvent is given by the usual formula;

$$D(\varepsilon) = \frac{1}{\pi} \mathrm{Im}\ (\mathrm{tr} \sum_{k_{//}} \Delta\ G_{kk}) \ , \tag{5.1}$$

where tr means the trace of the 2×2 matrix. Note that this is the DOS with a fixed $K_{//}$. With the help of eqs. (4.24) and (4.27), this equation can be rewritten successively as

$$\begin{aligned} D(\varepsilon) &= \frac{1}{\pi} \mathrm{Im}\ \{\mathrm{tr}\ \frac{1}{N} \sum_{k} (G_0(k))^2\ {}^t[f^*(k)][N][f(k)]\} \\ &= -\frac{1}{\pi} \mathrm{Im}\ \{\mathrm{tr}\ \frac{1}{N} \sum_{k} \frac{\partial G_0(k)}{\partial \varepsilon}\ {}^t[f^*(k)][N][f(k)]\} \qquad (5.2) \\ &= -\frac{1}{\pi} \lim_{\varepsilon' \to \varepsilon} \mathrm{Im}\ \{\mathrm{tr}\ \mathrm{Tr}(\frac{\partial}{\partial \varepsilon'}\ [I(z')])[N(z)] \ , \end{aligned}$$

where the cyclic property of the trace has been used in the

first line. In the last line, Tr means the trace of the 6×6 matrix, and the energy dependence of the matrices [I] and [N] has been made explicit, where z' stands for $\varepsilon'-i0^+$.

We now make the lowest order approximation in the $K_{//}$-expansion. Order estimate of the elements of [N] with respect to K can be easily made with the aid of the set of the basic equations (4.32). That of [I] can be obtained from the results of Appendix D. As a result, we obtain the lowest order approximation to $D(\varepsilon)$ as

$$D(\varepsilon) = -\frac{1}{\pi}\lim_{\varepsilon'\to\varepsilon} \mathrm{Im}\ \mathrm{tr}\ \frac{\partial}{\partial\varepsilon'}\{\hat{\mathcal{I}}(z')\ A(z)/K + I(z')(E_1(z)+E_4(z)) + J(z')(E_2(z)+E_3(z))\}\ , \tag{5.3}$$

where

$$A(z) = \sum_{i=1}^{4} A_i(z)\ . \tag{5.4}$$

Although there are K-linear terms and K-quadratic ones in A(z), as is seen from eq. (4.32-1), we have understood that the lowest order (i.e. K-linear) terms are sufficient in the above formula. Similarly, the lowest order (constant with respect to K) terms of $\hat{\mathcal{I}}(z')$ are sufficient. In I(z'), J(z'), and $E_i(z)$'s, we have only terms constant in K. Consequently, the change of the DOS obtained in eq. (5.3) does not contain K.

We have found that only $E_i(z)$'s and the lowest order A(z) are enough to evaluate $D(\varepsilon)$ in eq. (5.3). In the rest of this

subsection we briefly sketch how to obtain $E_i(z)$'s and $A(z)$.

First we calculate $E_i(z)$'s. Substituting the definitions (4.31(c)) and (4.31(j)) into eq. (4.32-5), we get the following four equations;

$$E_1(z) = \frac{r_1}{2} T_{ss}(J\ E_1(z) + I\ E_2(z)) \ , \tag{5.5}$$

$$E_2(z) = \frac{r_1}{2} T_{ss}(1 + I\ E_1(z) + J\ E_2(z)) + \delta\ S_{ss}(J\ E_1(z)+I\ E_2(z)), \tag{5.6}$$

$$E_3(z) = \frac{r_1}{2} T_{ss}(1 + J\ E_3(z) + I\ E_4(z)) \ , \tag{5.7}$$

$$E_4(z) = \frac{r_1}{2} T_{ss}(I\ E_3(z) + J\ E_4(z)) + \delta\ S_{ss}(1 + J\ E_3(z) + I\ E_4(z)) \ . \tag{5.8}$$

We notice that $E_1(z)$ and $E_2(z)$ are decoupled from $E_3(z)$ and $E_4(z)$. In addition, since all the coefficient matrices (T_{ss}, S_{ss}, I, and J) are diagonal, $E_1(z)$, say, is obtained in the form;

$$E_1(Z) = \begin{pmatrix} E_1^{\,t}(z), & 0 \\ 0, & E_1^{\,\ell}(z) \end{pmatrix} \ . \tag{5.9}$$

Instead of the energy parameters ε and z, we prefer to use

$$x = \varepsilon - \varepsilon_b + r_0 \quad \text{and} \quad y = \varepsilon - \varepsilon_b - 2r_0 \ , \tag{5.10}$$

with the corresponding complex energies

$$v = x - i0^+ \quad \text{and} \quad w = y - i0^+ \ . \tag{5.11}$$

Here x(y) is the energy measured from the center of the bulk T(L)-band. Calculations are straightforward and we only show the final results here;

$$E_1^t(z) = \frac{r_1^2}{8\delta}\cdot\frac{-v+2\delta+{}^c\sqrt{v^2-r_1^2}}{v-x_0}$$

$$E_2^t(z) = E_3^t(z) = \frac{r_1}{8\delta}\cdot\frac{2\delta v-r_1^2+2\delta\,{}^c\sqrt{v^2-r_1^2}}{v-x_0} \qquad (5.12)$$

$$E_4^t(z) = \frac{1}{8\delta}\cdot\frac{4\delta v^2-r_1^2 v-2\delta r_1^2+(-4\delta v+8\delta^2+r_1^2)\,{}^c\sqrt{v^2-r_1^2}}{v-x_0}\ ,$$

Where the complex function ${}^c\sqrt{v^2-r_1^2}$ is defined as

$${}^c\sqrt{v^2-r_1^2} = \begin{cases} -\sqrt{x^2-r_1^2} & \cdots\ x<-|r_1| \\ -i\sqrt{r_1^2-x^2} & \cdots\ |x|<|r_1| \\ \sqrt{x^2-r_1^2} & \cdots\ x>|r_1| \end{cases} \qquad (5.13)$$

and

$$x_0 = \delta + r_1^2/4\delta\ . \qquad (5.14)$$

The expressions of E_i^{ℓ}'s are obtained from the above formulae by simply replacing r_1 and v by $2r_1$ and w, respectively. Note that x_0 is also replaced by

$$y_0 = \delta + r_1^2/\delta\ . \qquad (5.15)$$

Now we go on to the calculation of A(z). We define $\{A^{(1)}(z)\}$

such that it satisfies

$$\{A^{(1)}(z)\} = \{V\} + \{V\}\,\hat{I}\,\{E_1\}\,\{A^{(1)}(z)\} \ . \qquad (5.16)$$

If we multiply this equation by K, and subtract both sides of it from those of eq. (4.32-1), we obtain

$$\{A^{(2)}(z)\} = \frac{1}{K}\{V\}(\{E_2\}\frac{iI}{2} + \{E_1\}\hat{I}\,U)\{D(z)\} + \{V\}\hat{I}\{E_1\}\{A^{(2)}(z)\}, \qquad (5.17)$$

where $\{A^{(2)}(z)\}$ is defined so that it satisfies

$$\{A(z)\} = K\,\{A^{(1)}(z)\} + K^2\,\{A^{(2)}(z)\} \ . \qquad (5.18)$$

In deriving eq. (5.17), we have used one of the relations in (4.36). Since $\{D(z)\}$ is of order K, as can be seen from eq. (4.32-4), $\{A^{(2)}(z)\}$ is of order K^0. The lowest order of $\{A^{(1)}(Z)\}$ is also K^0 but it has K-linear terms, too. For our purpose here, it is enough to evaluate $\{A^{(1)}(z)\}$ in its lowest order. For a moment, however, we examine eq. (5.16) up to the order of K for a later use. In terms of the elements of $\{A^{(1)}(z)\}$, eq. (5.16) is rewritten as

$$A_1^{(1)}(z) = e^K 3\lambda V_1 \hat{I}(z)(A_1^{(1)}(z) + e^K A_2^{(1)}(z)) \ , \qquad (5.19)$$

$$A_2^{(1)}(z) = 3\lambda V_2 + 3\lambda V_2 \hat{I}(z)(A_1^{(1)}(z) + e^K A_2^{(1)}(z)) \ , \qquad (5.20)$$

$$A_3^{(1)}(z) = 3\lambda V_1 + e^K 3\lambda V_1 \hat{I}(z)(A_3^{(1)}(z) + e^K A_4^{(1)}(z)) \ , \qquad (5.21)$$

$$A_4^{(1)}(z) = 3\lambda V_2 \hat{I}(z)(A_3^{(1)}(z) + e^K A_4^{(1)}(z)) \ . \qquad (5.22)$$

We notice that $A_1^{(1)}(z)$ and $A_2^{(1)}(z)$ are decoupled from $A_3^{(1)}(z)$

and $A_4^{(1)}(z)$. Multiplying the both sides of eq. (5.20) by e^K, and subtracting it from eq. (5.19), we get

$$A_1^{(1)}(z) + e^K A_2^{(1)}(z) = e^K 3\lambda V_2 + e^K 6\lambda \bar{V} \hat{I}(z)(A_1^{(1)}(z) + e^K A_2^{(1)}(z)) , \tag{5.23}$$

where

$$\bar{V} = \frac{1}{2}(V_1 + V_2) = \begin{pmatrix} 1, & 0 \\ 0, & -1 \end{pmatrix} . \tag{5.24}$$

This equation can be solved to give

$$A_1^{(1)}(z) + e^K A_2^{(1)}(z) = (1 - e^K 6\lambda \bar{V} \hat{I}(z))^{-1} e^K 3\lambda V_2 . \tag{5.25}$$

Similarly, we have, from eqs. (5.21) and (5.22),

$$A_3^{(1)}(z) + e^K A_4^{(1)}(z) = (1 - e^K 6\lambda \bar{V} \hat{I}(z))^{-1} 3\lambda V_1 . \tag{5.26}$$

These results will be used when we calculate the absorption spectra. As we have already mentioned, it is enough to evaluate $A_i^{(1)}(z)$'s in the lowest order with respect to K for our present purpose. Using the lowest order expression for $\hat{I}(z)$ (see Appendix D) and also taking the limit $e^K \to 1$, finally we get from eqs. (5.25) and (5.26)

$$A^{(1)}(z) = \sum_{i=1}^{4} A_i^{(1)}(z) = \frac{6\lambda}{z-\lambda} G_0^{-1}(0) \bar{V} . \tag{5.27}$$

5-2 Density of States — Results and Discussion

As we have mentioned in §1, from theoretical point of view

the effects of the presence of the surface may be classified into two kinds — [I] the effects of the cleavage and [II] those of the surface potential. As concerns the surface-induced change of the DOS, discrimination between these two effects can be achieved by first letting the surface potential δ vanish and then by taking the difference, namely we devide $D(\varepsilon)$ as

$$D(\varepsilon) = \bar{D}(\varepsilon) + \Delta D(\varepsilon) \ , \tag{5.28}$$

where

$$\bar{D}(\varepsilon) = D(\varepsilon \ ; \ \delta \to 0) \ . \tag{5.29}$$

Both $\bar{D}(\varepsilon)$ and $\Delta D(\varepsilon)$ can be obtained from eqs. (5.3), (5.12) and (5.27). The results are as follows;

$$\begin{aligned} \bar{D}(\varepsilon) = {} & 2\delta(\varepsilon - \varepsilon_b - \lambda) - \delta(\varepsilon - \varepsilon_b + 2\lambda) - \delta(\varepsilon - \varepsilon_b - 4\lambda) \\ & + \frac{\theta(r_1^{\,2}-x^2)}{\pi\sqrt{r_1^{\,2}-x^2}} - \frac{1}{2}\{\delta(x-r_1) + \delta(x+r_1)\} \\ & + \frac{\theta(4r_1^{\,2}-y^2)}{\pi\sqrt{4r_1^{\,2}-y^2}} - \frac{1}{2}\{\delta(y-2r_1) + \delta(y+2r_1)\} \ , \end{aligned} \tag{5.30}$$

$$\begin{aligned} \Delta D(\varepsilon) = {} & \delta(x-x_0) + \frac{2\delta - x}{2\pi(x-x_0)\sqrt{r_1^{\,2}-x^2}}\,\theta(r_1^{\,2}-x^2) \\ & + \delta(y-y_0) + \frac{2\delta - y}{2\pi(y-y_0)\sqrt{4r_1^{\,2}-y^2}}\,\theta(4r_1^{\,2}-y^2) \\ & (|\delta| > |r_1|) \ , \end{aligned} \tag{5.31}$$

where we have used three energy parameters ε, x, and y for convenience, that are all mutually related (see eq. (5.10)), and x_0 and y_0 are defined in eqs. (5.14) and (5.15), respectively. The above expression of $\Delta D(\varepsilon)$ is for the case when $|\delta|>|r_1|$. When $|r_1/2|<|\delta|<|r_1|$, the term $\delta(y-y_0)$ is missing, and when $|\delta|<|r_1/2|$, both $\delta(x-x_0)$ and $\delta(y-y_0)$ are missing. The total number of states must not be changed by introducing the surface into the periodic crystal, which leads to the sum rules;

$$\int_{-\infty}^{\infty} d\varepsilon\ \bar{D}(\varepsilon) = 0\ , \tag{5.32}$$

$$\int_{-\infty}^{\infty} d\varepsilon\ \Delta D(\varepsilon) = 0\ . \tag{5.33}$$

In particular, we can actually show that eq. (5.33) is valid for an arbitrary value of $|\delta|$.

The result for $\bar{D}(\varepsilon)$ is shown in Fig. 5-1, where we have taken $r_1/\lambda=1.0$. This value of r_1 roughly simulates the nearest layer short-range coupling parameter on bcc(100) surface (see Table 3-1 and relations (3.16)). In this figure, as well as in all the following ones, the energy is measured from ε_b and in units of λ. The arrows on the figure stand for δ-functions, the intensities of which are indicated near the points of the arrows. We see that δ-function like decrease in the DOS occurs at the edges of both the bulk T- and L-band, where the bulk DOS diverges, as is well-known. This decrease is partly compensated by the increace in the DOS within the bulk band, which exactly simulates the bulk DOS (1/N of the bulk DOS). A

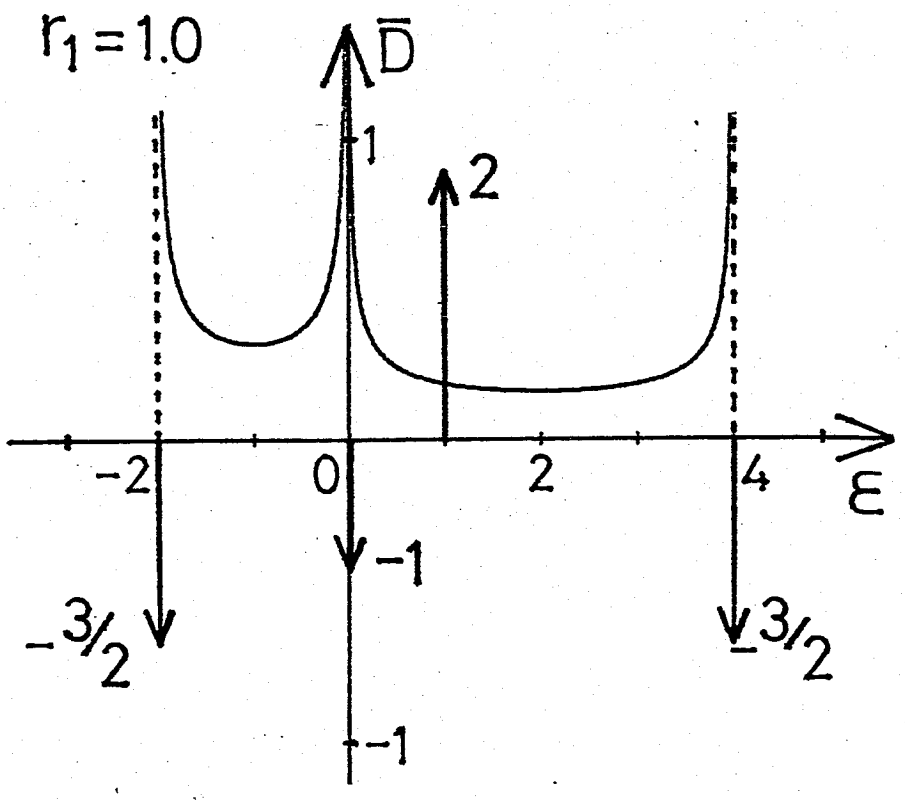

Fig.5-1. Cleavage-induced change $\bar{D}(\varepsilon)$ in the density of states when r_1 in units of λ is 1.0.

remarkable feature is the existence of the δ-function peak within the L-band, which suggests the existence of a surface localized mode. The fact that this peak is infinitely sharp does not necessarily mean that this localized mode has no interaction with the bulk L-modes at all. It means only that the lifetime broadening caused by the interaction with the bulk modes are at most of the order of K, since we have made the lowest order approximation in the $K_{//}$-expansion. In this sence, it should have been called a surface resonance mode, although we keep to call it simply a surface localized mode in the following. The intensity of this peak is 2, which means that there is one such state on each surface of the slab. As r_1 decreases, the bulk band widths decrease, whereas the peak position remains unchanged. Since we have fixed the value of the L-T splitting ($\Delta LT=6\lambda=6$), the position of the top of the L-band remains constant, while the L-band bottom goes upwards. When r_1 becomes smaller than $3\lambda/4$, the L-band bottom goes higher than the location of the peak. In this situation, the mode in consideration becomes a truely localized mode. Anyhow, the behavior of this mode does not depend on the value of the short-range interaction parameter r_1, as far as the lowest order approximation to the DOS in the $K_{//}$-expansion is concerned. An insignificant effect of r_1 on this mode is discernible in its wave function (see the next section).

In §1 we have made the classification of surface elementary

excitations into two types. Surface excitons were classified as type [II] modes, whose behaviors are sensitive to the surface potential. In this sense, the above mentioned localized mode, which owes its existence merely to cleavage, is quite anomalous. We term it 'surface polariton' rather than surface exciton, the reason of which will be discussed in the next section, where we shall analyze the behavior of this mode in some more detail and point out its relation to the usual surface polariton mode.

The results of the δ-induced change in the DOS for five values of δ with $r_1/\lambda=1.0$ are shown in Fig. 5-2 ((a) - (f)). When δ is large enough (see Fig. 5-2 (a)), there are two localized modes whose energies are given in eqs. (5.14) and (5.15). The one at the higher energy is split out of the top of the bulk L-band, and the other at the lower energy is split out of the T-band top. The latter one is located within the L-band (for the present choice of the value of δ; $\delta/\lambda=1.25$) with the infinitely sharp peak, which means, again, that the lifetime broadening of this mode is of higher order than K. Clearly, these two modes belong to the type [II] modes and are the surface excitons in the usual sense. In Appendix E, we shall briefly examine the nature of the wave functions of these modes. In accordance with the results there, the wave function of the surface mode with higher energy is composed mainly of those of the bulk L-excitons with a small T-exciton contributions of order K. On the other hand, the wave function of the lower

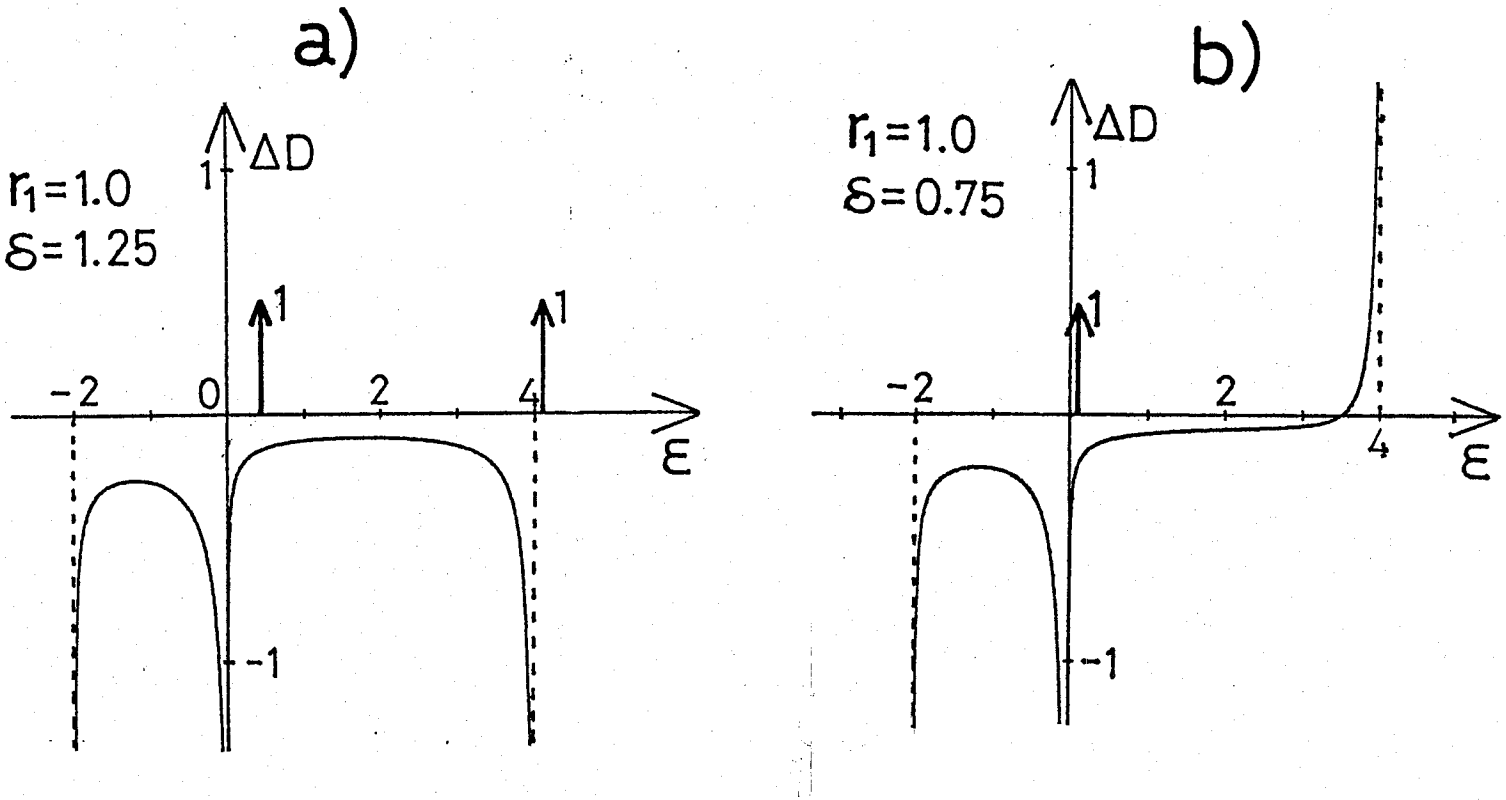

Fig. 5-2 ((a)-(f)). Changes in the DOS induced by the surface potential for various values of δ with r_1=1.0 (δ and r_1 are given in units of λ).

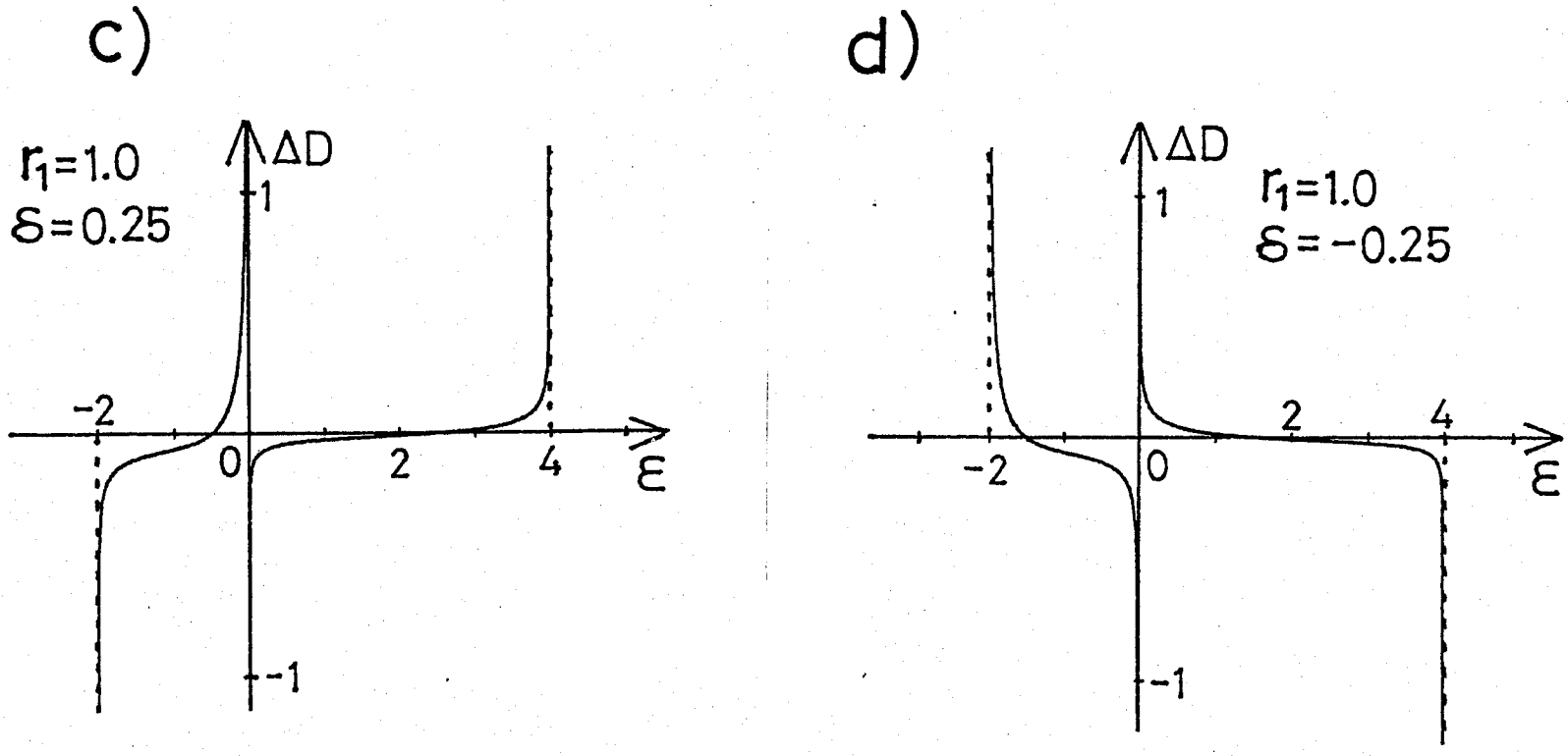

Fig. 5-2 (continued).

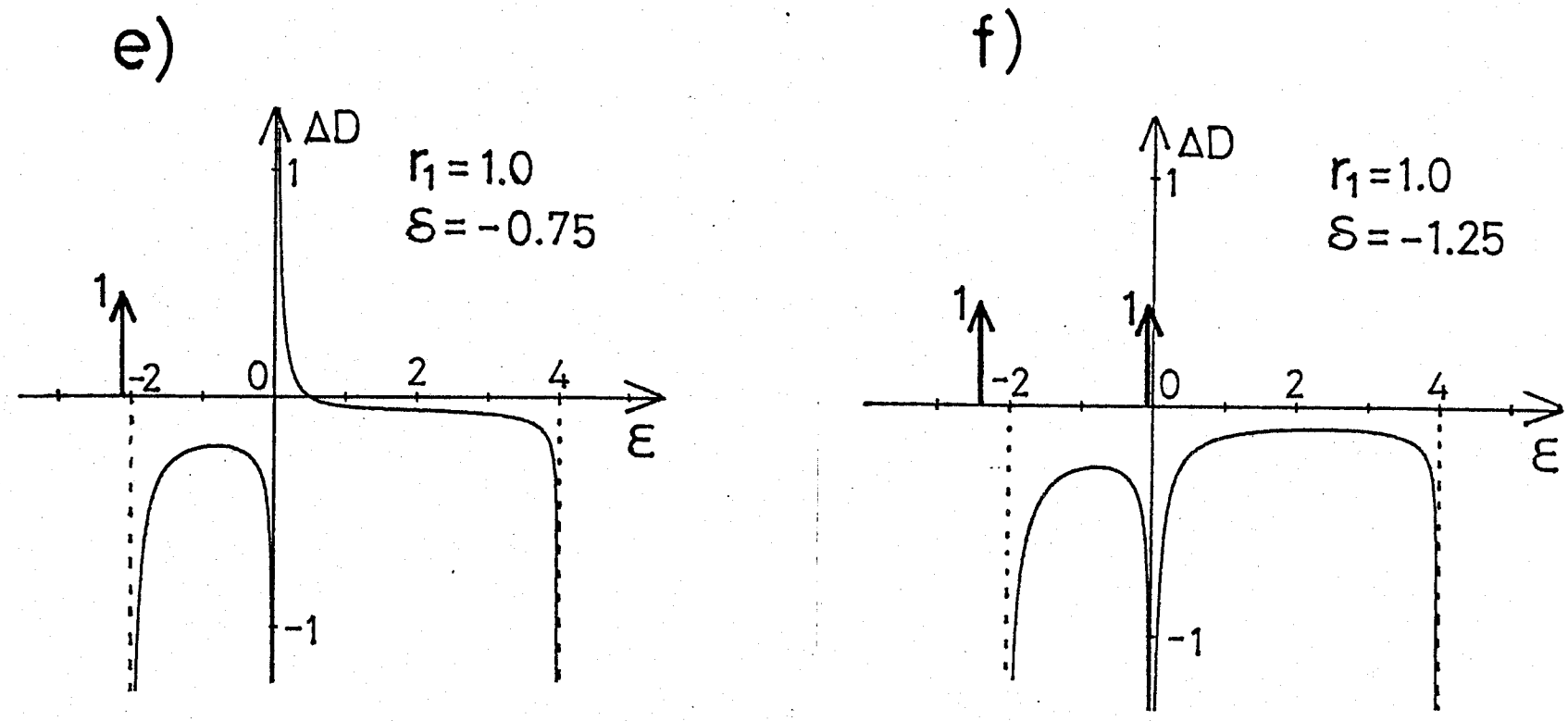

Fig. 5-2 (continued).

one mainly consists of the T-exciton with a small L-exciton contribution. Since it is completely meaningless to call the surface excitons 'L-like' or 'T-like', we rather term the upper surface exciton 'z-polarized' mode and the lower one 'x-polarized' mode. This nomenclature is reasonable because in the most range of the value of k ($k \gtrless k_0$, where k_0 has been introduced in §3-4) the L-mode (T-mode) is almost z-polarized (x-polarized) (see eqs. (3.33) and (3.34)). In the following, we abbreviate them as 'z-pol.' mode and 'x-pol.' mode. The increase in the DOS due to these surface localized modes is compensated by the decrease in that of the extented modes, the spectral feature of which is rather assymmetric with respect to the center of the L- and the T-band. When δ becomes larger, the energy position of the 'x-pol.' surface exciton goes up higher and finally it gets beyond the top of the L-band, resulting in a truely localized mode. Since there arises no qualitative change in the feature of $\Delta D(\varepsilon)$, we do not show the figure corresponding to this case.

When δ becomes smaller, first the 'z-pol.' surface exciton disappears (Fig. 5-2 (b)) and then the 'x-pol.' one disappears (Fig. 5-2 (c)). Corresponding change within the L-band and the T-band also occurs sussessively. When δ is negative and $|\delta|$ bevomes larger, $\Delta D(\varepsilon)$ repeats the above mentioned behaviors in a reverse order (Fig. 5-2 (d)-(f)).

The energies of the 'x-pol.' and 'z-pol.' surface excitons

are shown in Fig. 5-3 (a)(r_1/λ=1.0) and (b)(r_1/λ=0.5) as functions of δ. They are almost proportional to δ when $|\delta|$ is sufficiently large. The excistence of the 'x(z)-pol.' mode is forbidden within the bulk T(L)-band. Just outside the both edges of the band its energy shows a bending, which indicates a strong interaction between the 'x(z)-pol.' surface exciton and the bulk T(L)-band. The criteria for the existences of the surface excitons are shown from the statement after eq. (5.31). We have

$$\begin{aligned} |\delta| &> |r_1/2| \quad \text{for 'x-pol.' mode ,} \\ |\delta| &> |r_1| \quad \text{for 'z-pol.' mode .} \end{aligned} \tag{5.34}$$

Let us compare the above results for the DOS with those when K=0. When K exactly vanishes, the bulk T(L)-mode becomes equivalent to the x(z)-polarized extended mode. The long-range interaction $V_{\ell r}$ is missing in the Hamiltonian (4.5) and since $\sin\theta=1$ and $\cos\theta=0$, all the other interactions become diagonal as can be seen from eqs. (4.10) and (4.12). It is straightforward to show that the terms

$$2\delta(\varepsilon-\varepsilon_b-\lambda)-\delta(\varepsilon-\varepsilon_b+2\lambda)-\delta(\varepsilon-\varepsilon_b-4\lambda) \tag{5.35}$$

are missing from $\bar{D}(\varepsilon)$ in eq. (5.30), with $\Delta D(\varepsilon)$ being unchanged. As far as the δ-induced change $\Delta D(\varepsilon)$ which includes the surface exciton contributions is concerned, the finiteness of K apparently plays no role. In fact, the surface exciton energies given in

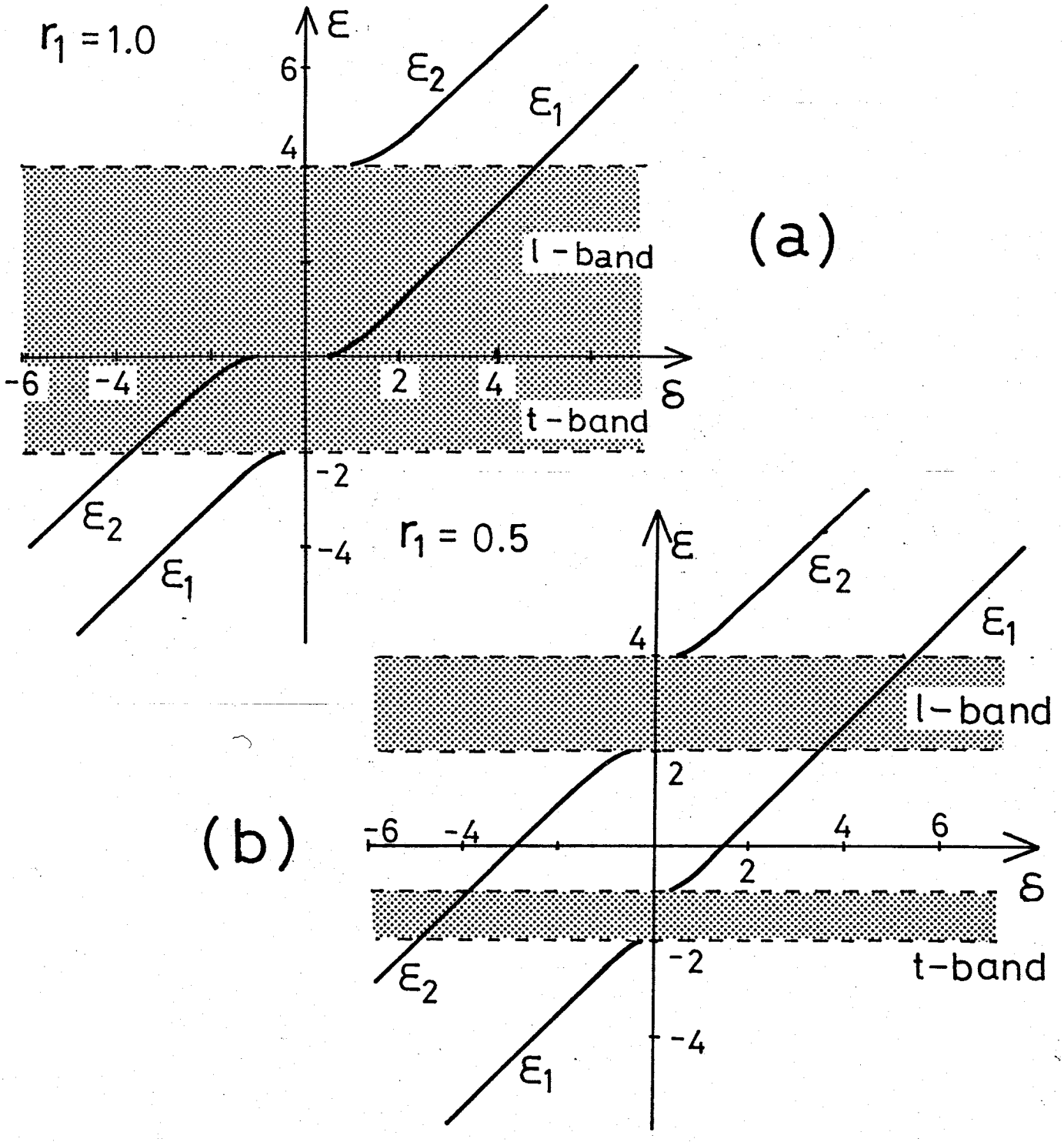

Fig.5-3. Energies of the 'x-pol.' (ε_1) and the 'z-pol.' (ε_2) surface excitons as functions of δ (ε, r_1, and δ are in units of λ and ε is measured from ε_b): (a) r_1=1.0, (b) r_1=0.5.

eqs. (5.14) and (5.15) as well as the criteria for their existences given in eq. (5.34) are equivalent to the results of Schipper[17] and of Hoshen and Kopelman,[16] who have taken no long-range interaction into account. The only difference exists that we have two apparently independent systems, namely x-pol. and z-pol. modes. A qualitative difference from the K=0 results, however, is found in $\bar{D}(\varepsilon)$. The 'surface polariton' mode at the energy $\varepsilon_b+\lambda$ cannot be expected from the K=0 theory. If we notice that $\bar{D}(\varepsilon)$ in eq. (5.30) is of the zeroth order in K, we see that the non-analiticity of our model is explicit in $\bar{D}(\varepsilon)$. The finiteness of K influences more on the behavior of the wave functions or the properties related to them rather than the energies of the modes, which we shall see in the following subsections.

5-3 Evaluation of the Absorption Spectrum

Let us assume that a p-polarized external electromagnetic field with a frequency $\varepsilon/\hbar$ and a wave vector (reduced by the inverse lattice spacing) $\vec{Q}=(K,0,k)$ is applied to the crystal. The perturbation caused by this field may be decribed by

$$\hat{\varepsilon}\cdot\vec{P}\,(-\vec{Q})\,\exp(-i\varepsilon t/\hbar)\ , \tag{5.36}$$

where $\hat{\varepsilon}$ is the unit vector perpendicular to $\vec{Q}$ and

$$\vec{P}(-\vec{Q}) = \frac{1}{\sqrt{N}}\sum_{\ell}\sum_{\nu}\left(\vec{M}_\nu\, a_{\ell\nu}(-\vec{K}_{//}) + \vec{M}^*_\nu\, a^\dagger_{\ell\nu}(\vec{K}_{//})\right) e^{ik\ell}\ , \tag{5.37}$$

is the $(-\vec{Q})$-Fourier component of the polarization operator. Since $\hat{\varepsilon}=(\sin\theta, 0, -\cos\theta)$ (θ is defined similarly as in Fig. 3-2), $\hat{\varepsilon}\cdot\hat{P}(-\vec{Q})$ in eq. (5.36) can be rewritten as

$$\hat{\varepsilon}\cdot\hat{P}(-\vec{Q}) = M\, b_t(-k) + M^*\, b_t^{\dagger}(k) \ , \tag{5.38}$$

where we have used eq. (4.2). Strictly speaking, $b_t(-k)$ in this equation is the operator in the '$(-\vec{K}_{//})$-subspace', but this does not matter in the following argument. The absorption spectrum is given by the familiar golden rule formula

$$\sum_e |\langle e|\ \hat{\varepsilon}\cdot\vec{P}(-\vec{Q})|0\rangle|^2\ \delta(\varepsilon-\varepsilon_e) \ , \tag{5.39}$$

apart from the numerical factors. Here $|e\rangle$ is the excited state of the crystal, and ε_e its excitation energy. This formula can be rewritten successively as

$$\begin{aligned} &\frac{1}{\pi}\,\mathrm{Im}\,\langle 0|\ \hat{\varepsilon}\cdot\vec{P}^{\dagger}(-\vec{Q})\ \frac{1}{\varepsilon-H-i0^+}\ \hat{\varepsilon}\cdot\vec{P}(-\vec{Q})|0\rangle \\ &= \frac{|M|^2}{\pi}\,\mathrm{Im}\,\langle 0|\ b_t(k)\ \frac{1}{\varepsilon-H-i0^+}\ b_t^{\dagger}(k)|0\rangle \ , \\ &= \frac{|M|^2}{\pi}\,\mathrm{Im}\ G^{tt}_{kk}(z) \ . \end{aligned} \tag{5.40}$$

Our interest is in the surface induced change of the absorption spectrum, which is given by

$$I(\varepsilon) = \frac{|M|^2}{\pi}\,\mathrm{Im}\,\Delta\, G^{tt}_{kk}(z) \ . \tag{5.41}$$

Thus the calculation of the absorption spectrum is done by that

of the resolvent, again. We assume $|\vec{Q}|$ is finite but vanishingly small and let K, k→0, with the angle θ being fixed. The formula (5.41) gives the absorption spectrum as a function of θ. Due to the refraction effect, the complementary angle of θ does not usually coincide with the incident angle of radiation, but rather symbolically we shall call θ the incident angle, because the one-to-one correspondence between them may be expected. With this respect, we should point out that the so-called polariton effects are completely neglected in our theory. Questions as to the applicability of our model that arise due to the neglect of the polariton effects will be briefly discussed in the next section. Now from eqs. (4.24) and (5.41) we get

$$I(\varepsilon) = \frac{|M|^2}{\pi} \mathrm{Im}\,(G_0^t(k))^2\,({}^t[f^*(k)][N][f(k)])_{tt}\,, \qquad (5.42)$$

where the subscript tt means the (1,1)-component of the 2×2 matrix and we have omitted the factor 1/N for simplicity. According to the argument given above we consider the k→0 limit. Following expressions are available:

$$\text{(a)}\begin{cases} \beta(-k)\beta(k) \approx \dfrac{e^{-K}}{K^2}\cos^2\theta \\ \gamma(-k)\beta(k),\quad \beta(-k)\gamma(k) \approx \dfrac{1}{K^2}\cos^2\theta \\ \gamma(-k)\gamma(k) \approx \dfrac{e^{K}}{K^2}\cos^2\theta \end{cases} \qquad \begin{bmatrix} K,k\to 0 \\ \theta : \text{fixed} \end{bmatrix}$$

$$
\text{(b)}\begin{cases}\beta(-k)\sin\theta,\ \gamma(-k)\sin\theta,\ \beta(-k)e^{ik}\sin\theta,\ \gamma(-k)e^{ik}\sin\theta \approx \frac{1}{K}\cos\theta\sin\theta, \\ \beta(-k)\cos\theta,\ \gamma(-k)\cos\theta,\ \beta(-k)e^{ik}\cos\theta,\ \gamma(-k)e^{ik}\cos\theta \approx \frac{1}{K}\cos^2\theta, \end{cases}
$$

$$
\text{(c)}\begin{cases}\sin^2\theta\ e^{ik} \approx \sin^2\theta\ , \\ \sin\theta\cos\theta\ e^{ik} \approx \sin\theta\cos\theta\ , \\ \cos^2\theta\ e^{ik} \approx \cos^2\theta\ , \end{cases} \tag{5.43}
$$

where $\beta(k)=\alpha(-k)e^{-i\theta}$ and $\gamma(k)=\alpha(k)e^{K+ik}e^{i\theta}$ are the first two elements of the vector $[f(k)]$. Except for the trigonometric functions, the above expressions (a), (b), and (c) are correct up to the order of K^{-1} ((a) and (b)) and of K^0 ((c)), which can be verified by the use of eq. (4.29) and the theorem proved in Appendix C. With the aid of these relations, eq. (5.42) can be rewritten as follows,

$$
\begin{aligned}
I(\varepsilon) = \frac{|M|^2}{\pi}\,\mathrm{Im}\,\left(\frac{1}{z-\varepsilon_t(0)}\right)^2 \Big\{ & \sin^2\theta\ E(z) \\
& + \sin\theta\cos\theta\ \left(\frac{B(z)+D(z)}{K} + F(z) + Q(z)\right) \\
& + \cos^2\theta\ \left(\frac{e^{-K}A_1(z)+A_2(z)+A_3(z)+e^{K}A_4(z)}{K^2} + \frac{C(z)+P(z)}{K} + R(z)\right)\Big\}_{tt},
\end{aligned} \tag{5.44}
$$

where

$$
E(z) = \sum_{i=1}^{4} E_i(z)\ , \tag{5.45}
$$

and the other quantities $B(z)$, $C(z)$, and so on are defined

similarly.

Now we must solve the set of basic eqs. (4.32-1)∿(4.32-9). We notice that (i) all that is necessary is to obtain the sum of each four matrices such as shown in eq. (5.45) except for $A_i(z)$'s, and that (ii) only the (1,1)-components of these matrices are relevant. These considerations greatly simplify our calculations. The solutions for $E_i(z)$'s and the lowest order approximations to $A_i(z)$'s have been already obtained in eq. (5.12) and eqs. (5.25) and (5.26), respectively. We express the unknown matrices in terms of these known ones. We analyze B(z)+D(z) first. Comparing eq. (4.32-4) with (4.32-5), we obtain

$$\{D(z)\} = K\{E(z)\}\left(-\frac{iI}{2}\{E_3\} + U^{\dagger}\,\hat{\gamma}\,\hat{I}\,\{E_1\}\right)\{A^{(1)}(z)\} . \qquad (5.46)$$

We rewrite this equation in terms of the elements of the matrices and sum up the elements of D(z) . The result is

$$D(z) = K\left\{(E_1(z)+E_2(z)-E_3(z)-E_4(z))\left(-\frac{iI}{2}\right)+E(z)\,U^{\dagger}\,\hat{\gamma}\,\hat{I}\right\}A^{(1)}(z) . \qquad (5.47)$$

Using the relations in eq. (4.38), we get

$$B(z)+D(z) = K\,A^{(1)}(z)\,\hat{\gamma}\,\hat{I}\,U\,E(z) + K\,E(z)\,U^{\dagger}\,\hat{\gamma}\,\hat{I}\,A^{(1)}(z) . \qquad (5.48)$$

Since $A^{(1)}(z)$, $\hat{\gamma}$, $\hat{I}$, and E(z) are diagonal, B(z)+D(z) has only off-diagonal elements, which do not contribute to I(ε). In a similar manner, we can show that F(z)+Q(z) is off-diagonal. Hence we find that there are no terms proportional to sinθcosθ

in $I(\varepsilon)$. Next we examine $A^{(2)}(z)$. Comparing eq. (5.17) with (5.16), we get

$$A^{(2)}(z) = \frac{1}{K} \{A^{(1)}(z)\} \left(\{E_2\} \frac{iI}{2} + \{E_1\} \tilde{I} U\right) \{D(z)\} . \quad (5.49)$$

Substituting eq. (5.46) into (5.49), we can express $A^{(2)}(z)$ in terms of $A^{(1)}(z)$ and $E(z)$. After some manipulations, we obtain

$$A_d^{(2)}(z) = \frac{1}{K}\left\{\left(\frac{I}{2}\right)^2 (E_1(z) - E_2(z) - E_3(z) + E_4(z)) + (\tilde{I})^2 U E U^\dagger\right\} A^{(1)}(z) , \quad (5.50)$$

where the subscript d for $A^{(2)}(z)$ denotes the diagonal part of the matrix. We can obtain $C(z)+P(z)$ using relations in eq. (4.38) and eq. (5.47). The result for the diagonal part is

$$(C(z) + P(z))_d = 2 K U E(z) U^\dagger \tilde{I} A^{(1)}(z) . \quad (5.51)$$

Finally $R(z)$ can be expressed in terms of $E(z)$ by the use of one of the relations in eq. (4.36).

After all, $I(\varepsilon)$ can be written in the form

$$I(\varepsilon) = I_s(\varepsilon) \sin^2\theta + I_c(\varepsilon) \cos^2\theta , \quad (5.52)$$

where the normal incidence spectrum $I_s(\varepsilon)$ and the grazing angle incidence spectrum $I_c(\varepsilon)$ are given respectively by

$$I_s(\varepsilon) = \frac{|M|^2}{\pi} \mathrm{Im} \left(\frac{1}{z-\varepsilon_t(0)}\right)^2 E_t(z) , \quad (5.53)$$

$$I_c(\varepsilon) = \frac{|M|^2}{\pi} \mathrm{Im} \left(\frac{1}{z-\varepsilon_t(0)}\right)^2 \left\{ \frac{e^{-K} A_1^{(1)}(z) + A_2^{(1)}(z) + A_3^{(1)}(z) + e^{K} A_4^{(1)}(z)}{K} \right.$$

$$+\left(\frac{IA^{(1)}(z)}{2}\right)^2\left(E_1(z)-E_2(z)-E_3(z)+E_4(z)\right)+UE(z)U^{\dagger}\left(\frac{1}{2}A^{(1)}(z)+1\right)^2\Big\}_{tt}. \tag{5.54}$$

5-4 Absorption Spectrum — Results and Discussion

Similarly to the DOS, the absorption spectrum can be divided into two contributions;

$$I(\varepsilon) = \bar{I}(\varepsilon) + \Delta I(\varepsilon) , \tag{5.55}$$

where $\bar{I}(\varepsilon)=I(\varepsilon;\delta\to 0)$ is the change in the absoption spectrum due to the cleavage and $\Delta I(\varepsilon)$ is the one due to the surface potential. Both $I_s(\varepsilon)$ and $I_c(\varepsilon)$ can be divided in the same manner. Substituting eqs. (5.12), (5.25) and (5.26) into eqs. (5.53) and (5.54) ($E_i^{\ell}(z)$'s are obtained from $E_i^{t}(z)$'s by the procedure described just below the equation (5.12)), we can get the expressions for $\bar{I}_s(\varepsilon)$, $\bar{I}_c(\varepsilon)$, $\Delta I_s(\varepsilon)$, and $\Delta I_c(\varepsilon)$ that are the lowest order approximations in the $K_{//}$-expansion. Their explicit expressions are rather lengthy and will be given in Appendix F. In experimental measurements surface excitons are often identified by the contamination sensitivity of their peaks (or more moderate structures) in absorption spectra. It is natural that those peaks, which remain in the difference between the spectrum measured on a clean surface and the one on a contaminated surface, are identified as surface exciton peaks. It is $\Delta I(\varepsilon)$ that has a direct correspondence to such

a difference spectrum in the experimental contamination test. Therefore we concentrate on $\Delta I(\varepsilon)$ in the following discussions.

Fig. 5-4 ((a)-(d)) shows the δ-induced change of the normal incidence spectrum $\Delta I_s(\varepsilon)$ for four values of δ and $r_1/\lambda=1.0$. In the case of normal incidence of radiation, only the x-polarized modes (equivalent to the T-modes in this case) can be excited and no changes occur within the L-band region. We should remember that the so-called bulk exciton absorption is located at the edge (the bottom when $r_1>0$ and the top when $r_1<0$) of the T-band with its intensity being proportional to N (if we neglect the spatial damping of radiation). We see in Fig. 5-4(a) that a part of the oscillator strength of this bulk exciton absorption is rearranged within the T-band due to the surface potential δ and that a part of it is given to the x-pol. surface exciton. When $|\delta|$is small enough so that the surface exciton cannot exist (Fig. 5-4 (b) and (c)), the rearrangement of the oscillator strength still takes place, and the feature of which is critically dependent on the sign of δ. Fig. 5-4 (d) is for the case when the surface exciton exists below the bulk band. We see that the osicillator strengths of the extended states are transferred to the surface exciton due to δ. Such a behavior of the oscillator strengths is in fact reported in the recent experiments performed on the surface of solid Kr,[46] although our model seems to be too crude to make a quantitative comparison.

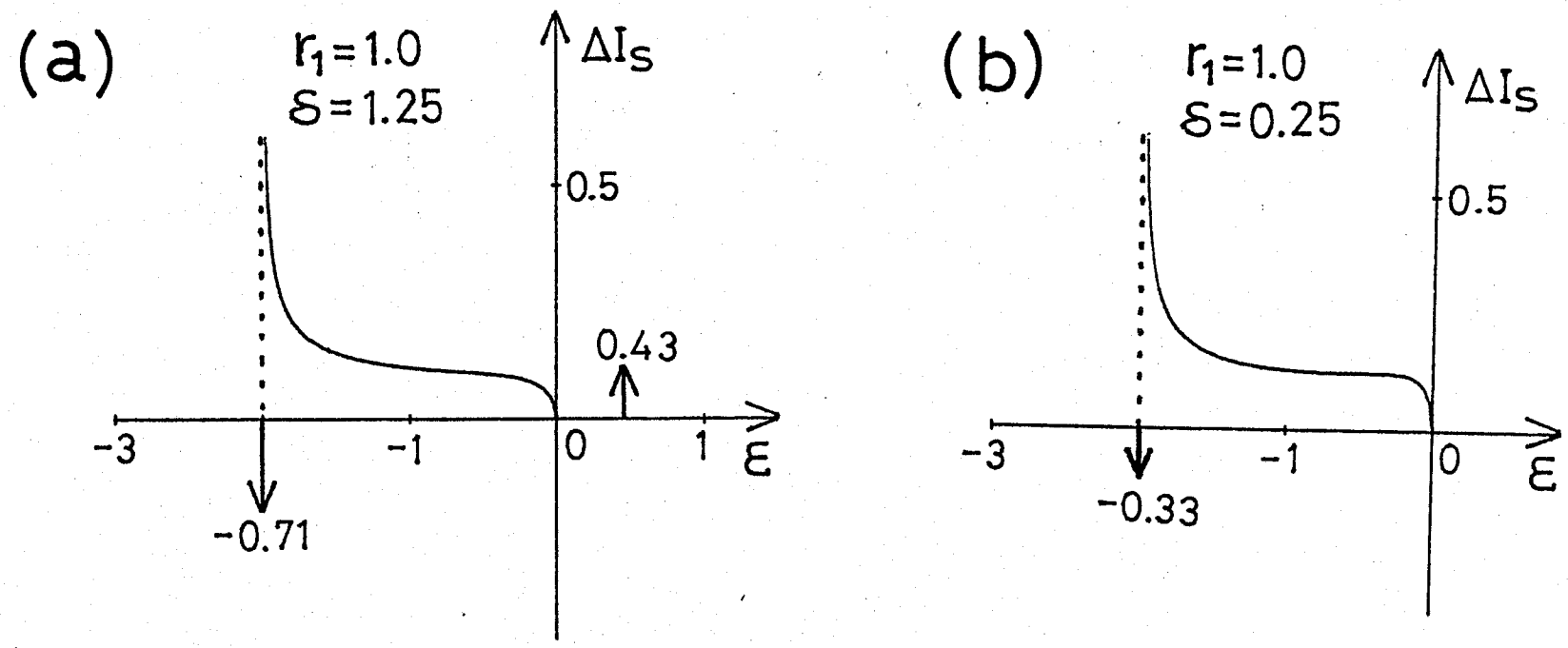

Fig. 5-4 ((a)-(d)). Changes in the normal incidence absorption intensity induced by the surface potential for various values of δ with r_1=1.0 (δ and r_1 are given in units of λ).

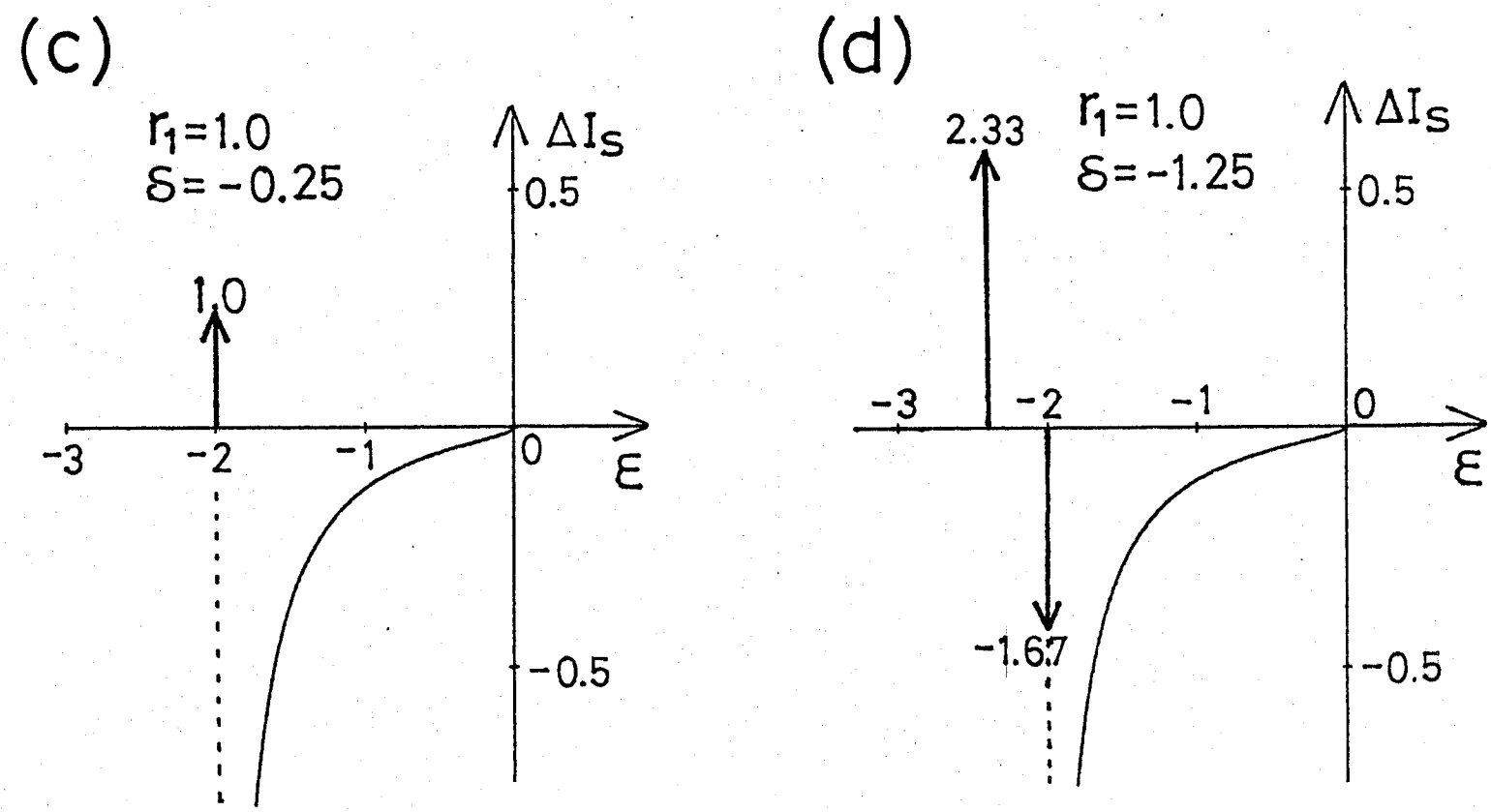

Fig. 5-4 (continued).

We show the δ-induced change of the grazing angle incidence spectrum in Figs. 5-5 and 5-6. In the case of oblique incidence of radiation the bulk L-modes as well as the 'surface polariton' take a part in $\Delta I_c(\varepsilon)$. Fig 5-5 is for the case $r_1/\lambda=1.0$, where the 'surface polariton' is located within the L-band. The δ-function like structure at the energy $(\varepsilon-\varepsilon_b)/\lambda=1.0$ represents the change in the absorption due to the 'surface polariton', which originally has a large oscillator strength of order 1/K (see the expression for $\bar{I}_c(\varepsilon)$ in Appendix F). The other sharp structures are related to the surface exciton absorption. We see that the L-mode absorption is drastically altered especially around the 'surface polariton' energy. Overall features of $\Delta I_c(\varepsilon)$ are determined by the sign of δ, although the oscillator strengths of the surface excitons depend so much on the value of δ. This is also true of the case $r_1/\lambda=0.5$, where the 'surface polariton' energy is in the gap of the bulk band (Fig. 5-6). In this case the absorption spectrum within the L-band region suffers no significant changes.

Our main interest here is the oscillator strengths of the surface excitons. Apart from an insignificant factor, these are given by the absorption intensities of the surface excitons. With the aid of the explicit expressions of $\Delta I(\varepsilon)$, the oscillator strengths of the 'x-pol.' and the 'y-pol.' surface excitons as functions of θ are given, respectively, in the form

$$f_1(\theta)/|M|^2 = f_{s1} \sin^2\theta + f_{c1} \cos^2\theta \ , \qquad (5.56)$$

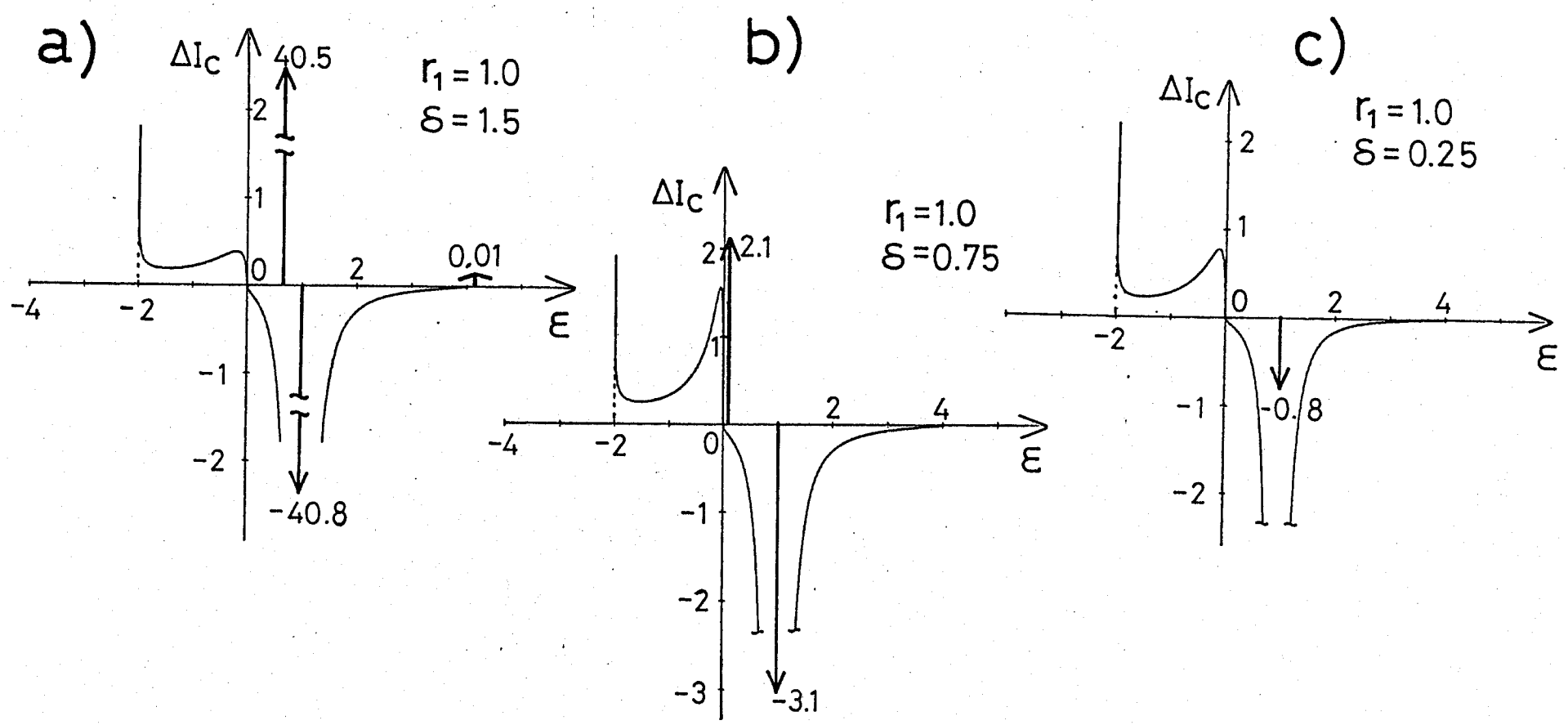

Fig. 5-5 ((a)-(f)). Changes in the grazing angle incidence absorption intensity induced by the surface potential for various values of δ with r_1=1.0. (δ and r_1 are given in units of λ)

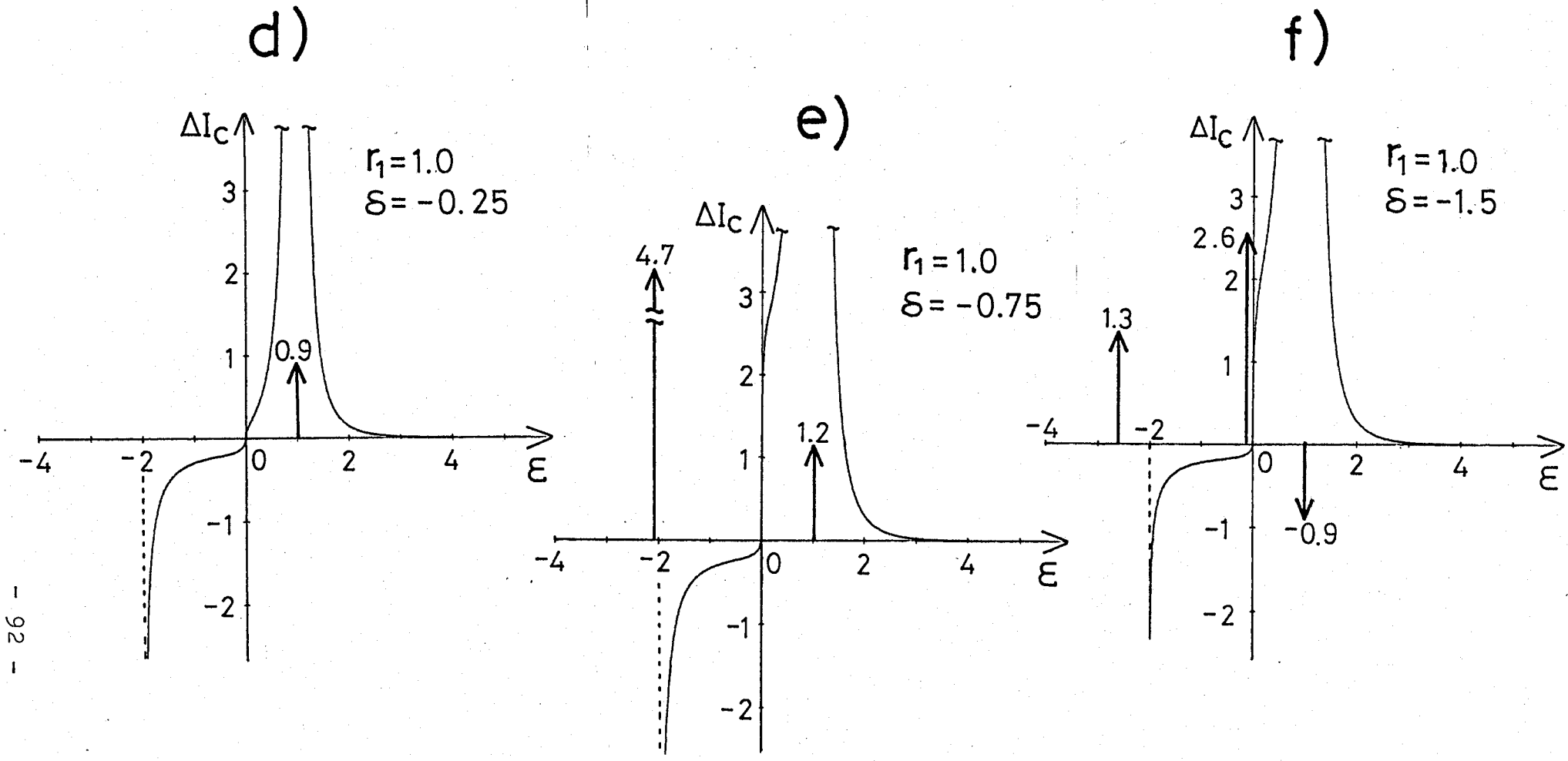

Fig. 5-5 (continued).

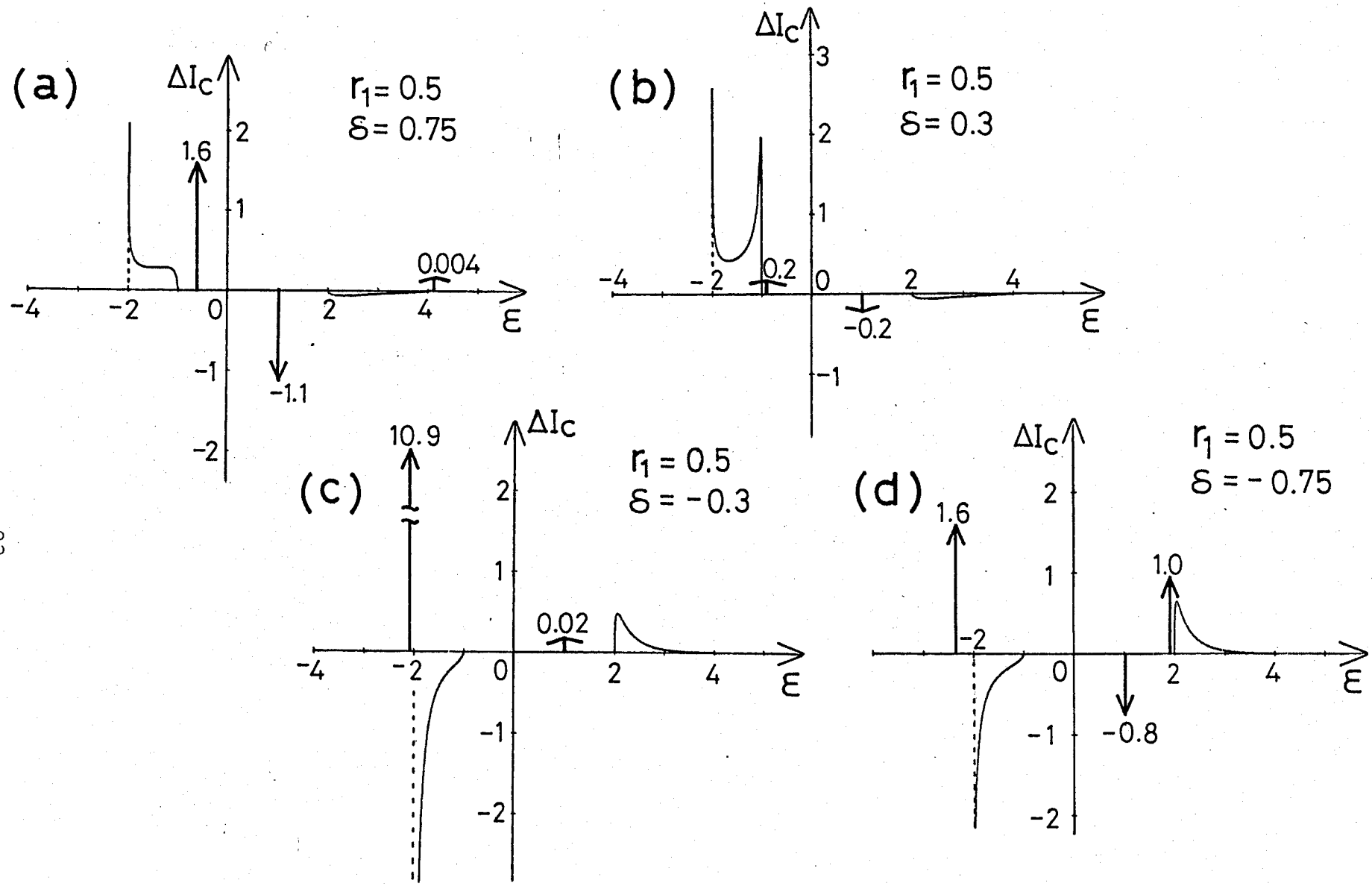

Fig.5-6 ((a)-(d)). The same as Fig.5-5 except that r_1=0.5 .

$$f_2(\theta)/|M|^2 = f_{c2}\cos^2\theta \ , \tag{5.57}$$

where the coefficients f_{s1}, f_{c1}, and f_{c2} are given by

$$f_{s1} = \frac{2\delta - r_1}{2\delta + r_1} \ , \tag{5.58}$$

$$f_{c1} = \frac{a\lambda^2 (2\delta - r_1)}{(3\lambda - r_1 - x_0)^2(2\delta + r_1)} \ , \tag{5.59}$$

$$f_{c2} = \frac{(\delta - r_1)^2(\delta^2 - r_1^2)}{\delta^2(2r_1 - 3\lambda - y_0)^2} \ . \tag{5.60}$$

Figs. 5-7 show these coefficients f_{s1} (panel (a)), and f_{c1} and f_{c2} (panel (b)) as functions of δ for the case $r_1/\lambda=1.0$. When the absolute value of δ becomes sufficiently large, these coefficients approach the isolated single layer values: $f_{s1}=1$, $f_{c1}=0$, and $F_{c2}=1$. In the region $|\delta|<|r_1/2|$ the 'x-pol.' surface exciton cannot exist. At the lower side of this region, the oscillator strength of the 'x-pol.' surface exciton (f_{s1} and f_{c1}) shows the significant enhancement. The region of δ where the values of f_{s1} and f_{c1} deviate considerably from their asymptotic values coinside with the region where the energy of the 'x-pol.' surface exciton as a function of δ shows a marked bending (see Fig. 5-3). In this situation the surface exciton suffers a strong mixing with the bulk excitons via the short range interaction and its wave function extends rather deep into the bulk. It is interesting to note here that the oscillator strength of the surface exciton is strongly correlated

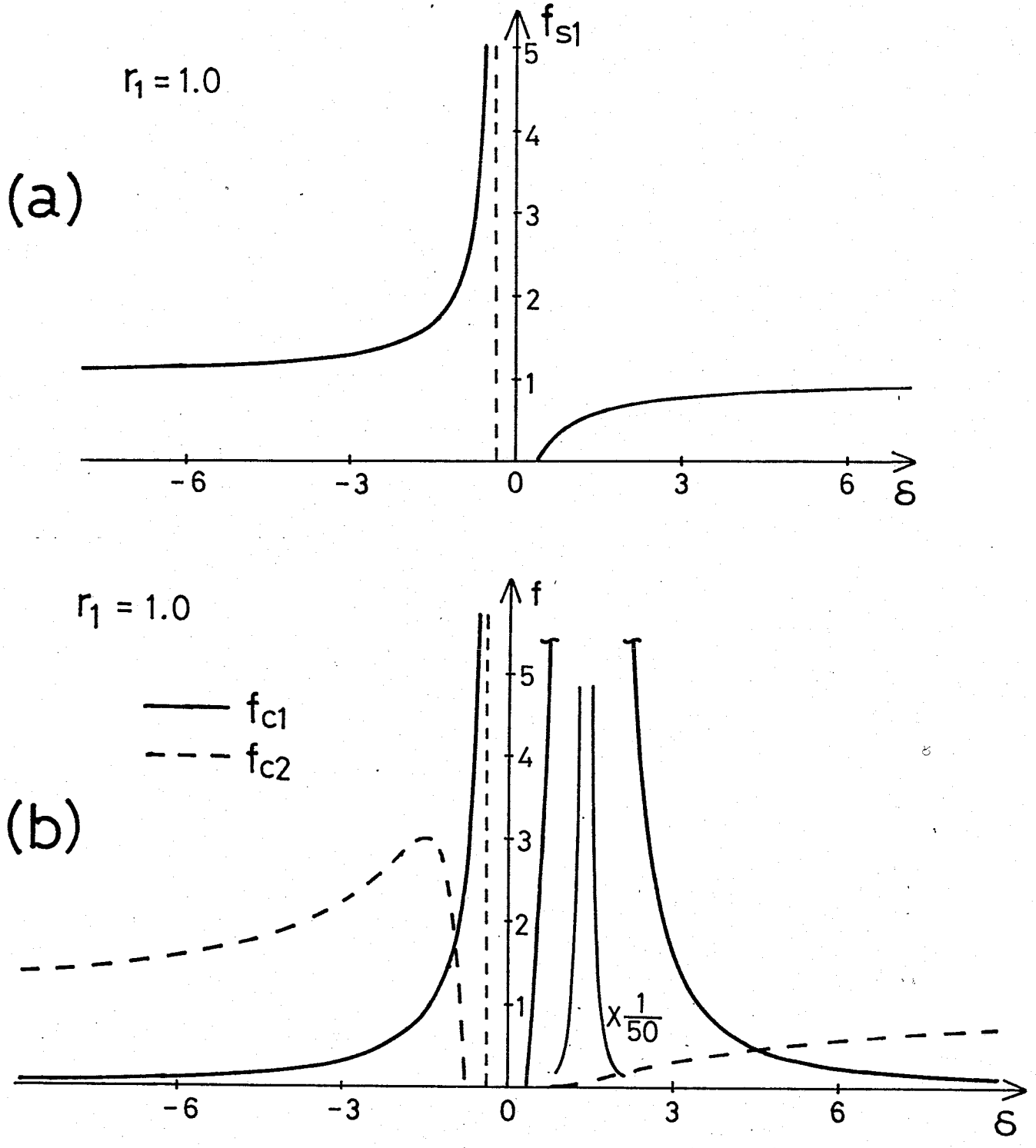

Fig. 5-7. Oscillator strengths of the surface excitons as functions of δ for the case r_1=1.0 (δ and r_1 are given in units of λ): (a) f_{s1}, (b) f_{c1} and f_{c2}.

with the spatial extension of its wave function. In the following we show this in a simplified model where the excitons have transition dipole moments in only one (x, say) direction. We neglect the long-range interaction and assume that the wave function of the surface exciton has the form

$$\psi(\ell) = \sqrt{e^{2\kappa-1}}\, e^{-\kappa\ell} \qquad (\kappa>0) \ , \tag{5.61}$$

where the normalization conditon $\sum_{\ell=1}^{\infty} |\psi(\ell)|^2=1$ has been taken into account. The constant $1/\kappa$ measures the spatial extension. The transition dipole moment M_s is given by

$$M_s = \langle 0| \ (\sum_{\ell} \psi(\ell)\ a_{\ell x})^{\dagger}\ P_x(-\vec{Q})\ |0\rangle \ , \tag{5.62}$$

in which the polarization operator $P_x(-\vec{Q})$ can be obtained from eq. (5.37). If we assume that the wave number Q of the external electromagnetic field is negligibly small compared with κ, then

$$M_s \propto \sqrt{e^{2\kappa}-1} \ / \ (e^{\kappa}-1) \ . \tag{5.63}$$

The oscillator strength f is propotional to $|M_s|^2$. If the surface exciton has a large spatial extension, κ is small compared with 1. Expanding e^{κ} with respect to κ, we get

$$f \propto 1/\kappa \ . \tag{5.64}$$

Therefore the deeper the surface exciton extends into the bulk, the larger the oscillator strength becomes. This corresponds to remarkable enhancement of the oscillator strength of the

'x-pol.' surface exciton just below the inhibited region $|\delta|<|r_1/2|$. The constant κ is determined from the ratio of the short-range interaction r_1 to the energy separation between the 'x-pol.' surface exciton and the T-band edge. This kind of enhancement is similar in nature to the well-known giant oscillator strength of the impurity-trapped excitons in semiconductors and insulators.[47)]

When the energy of the surface exciton is located just above the top of the T-band, its wave function is mainly composed of those of the bulk T-excitons at the Brillouin zone boundary ($k=\pm\pi$). Correspondingly, the wave function may be of the form

$$\psi(\ell) = \sqrt{e^{2\kappa}-1}\, e^{-\kappa\ell}\, e^{\pm i\pi\ell} . \qquad (5.65)$$

A straightforward calculation yields

$$f \propto \kappa , \qquad (5.66)$$

which is valid for small κ. Therefore the reduction of the oscillator strength takes place in this region of δ, which is clearly seen in the figure.

Another enhancement of f_{cl} is also observed (panel (b)). Divergence of f_{cl} occurs for the value of δ with which the energy of the 'x-pol.' surface exciton coincides with that of the 'surface polariton'. Since this enhancement is seen only in the oblique incidence spectra, it is clearly the effect of the long-range interaction. This phenomenon can be qualitatively

explained with the simple model as follows: When the long-range interaction of the form $K\, e^{-K\ell}$ as well as the short-range one exist (as is the case for our model), the wave function of the surface exciton may be expressed as the sum of the rather swiftly damping function $e^{-\kappa\ell}$ and the extended function $K\, e^{-K\ell}$ (we have assumed $\kappa >> K$);

$$\psi(\ell) = \sqrt{e^{2\kappa} - 1}\ (e^{-\kappa\ell} + c\ K\ e^{-K\ell}) \ , \qquad (5.68)$$

where c is some constant, which we assume positive without loss of generality. Note that the normalization factor is determined solely by the first term in the bracket, which is correct as far as $\kappa >> cK$ holds. Therefore, for a value of κ being not so small, c can become very large without affecting the normalization. The oscillator strength is obtained as

$$f \propto \sqrt{2^{2\kappa} - 1}\ \left(\frac{1}{e^{\kappa} - 1} + c\right) \ . \qquad (5.69)$$

We see that the larger the value of c becomes, the larger the oscilltor strength. Now we apply this simple argument to our case. As we shall see explicitly in the next section, the wave functon of the 'surface polariton' is composed mainly of the long-range term $e^{-K\ell}$. When the energy of the 'x-pol.' surface exciton approaches that of the 'surface polariton', the wave function of the surface exciton more resembles that of the 'surface polariton', and correspondingly c becomes large. This is the reason for the enhancement of f_{c1}. In contrast to the 'x-pol.' surface exciton, the energy of the 'z-pol.'

one cannot reach that of the 'surface polariton' for the case $r_1/\lambda=1.0$, and therefore f_{c2} does not show drastic enhancement but only shows a rather moderate maximum structure.

As we have seen above, there are two kinds of mechanisms for the giant oscillator strengths of the surface excitons in our model. One is due to the short-range interaction and the other is due to the long-range one. We can vary the relative magnitude of the short-range interaction vs. the long-range one by varying the value of r_1. Behaviors of the oscillator strengths for the case $r_1/\lambda=0.5$ are shown in Fig. 5-8. This value of r_1 simulates the nearest layer coupling on fcc(100) surface (see Table 3-1). We see that the enhancement of the oscillator strengths due to the short-range interaction is confined to the rather narrower region of δ compared with Fig. 5-7, and that, on the contrary, the region of the enhancement due to the long-range interaction becomes broader. A qualitative difference from the case of Fig. 5-7 is that also f_{c2} shows the giant oscillator strength, which is possible, because in this case the 'z-pol.' surface exciton can approach the 'surface polariton'in energy. For comparison we also show the case where r_1 is negative ($r_1/\lambda=-0.2$) in Fig. 5-9. This value of r_1 roughly corresponds to the nearest layer coupling parameter on scc(100) surface (see Table 3-1). All the behaviors of the oscillator strengths in this figure can be interpreted similarly. A remarkable feature common to the above three cases is the

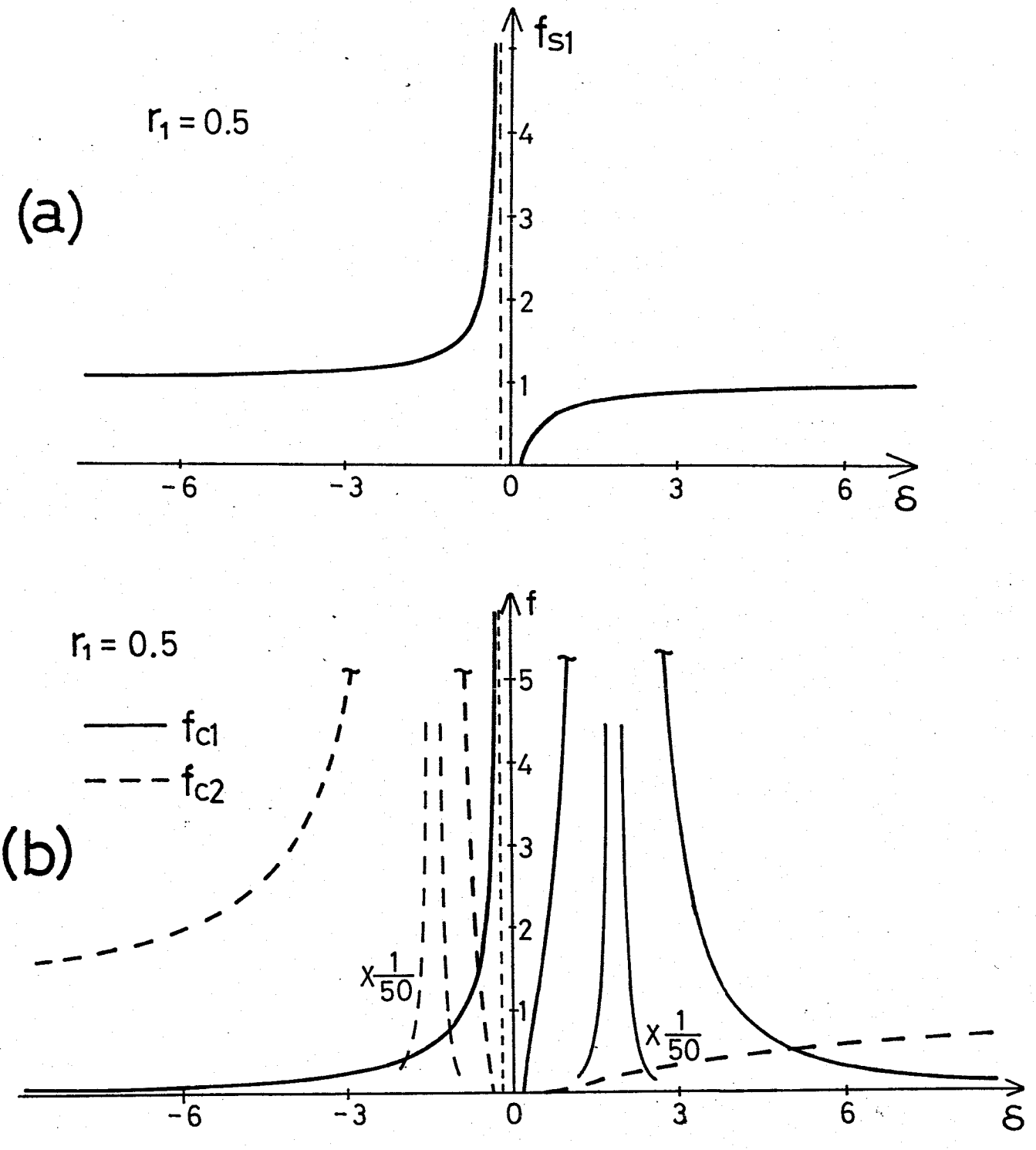

Fig. 5-8. Oscillator strengths of the surface excitons as functions of δ for the case r_1=0.5 (δ and r_1 are given in units of λ): (a) f_{s1}, (b) f_{c1} and f_{c2}.

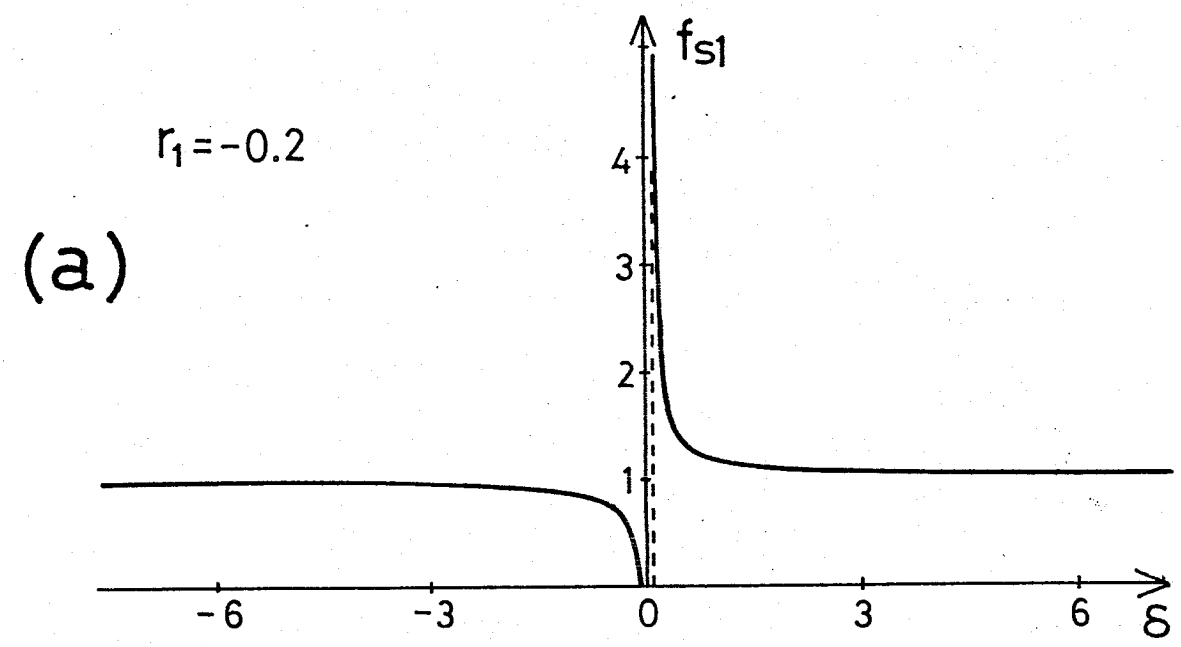

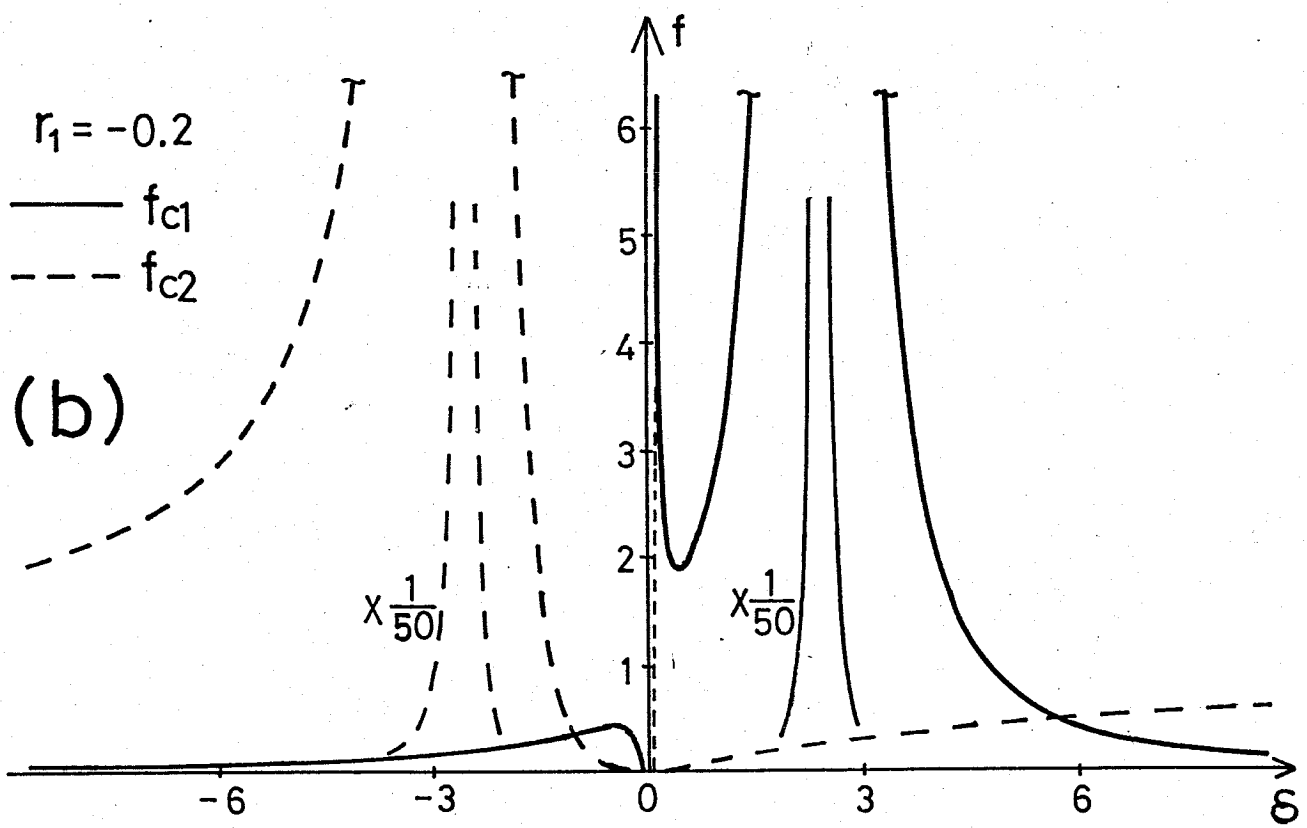

Fig. 5-9. Oscillator strengths of the surface excitons as functions of δ when $r_1=-0.2$ (δ and r_1 are given in units of λ): (a) f_{s1}, (b) f_{c1} and f_{c2}.

strong θ-dependence of the surface exciton oscillator strengths. Since the enhancement of the oscillator strengths due to the short-range interaction occurs only in the relatively narrow region of δ around δ=0, the sum $f_{c1}+f_{c2}$ exceeds f_{s1} for most values of δ. Therefore we can expect that the surface excitons are more easy to be excited by the oblique incident p-polarized radiation than by the normal incident one in most cases.

§6 Discussion

6-1 Analysis of the 'Surface Polariton' Mode

In §5-1 we have pointed out the existence of the 'anomalous' surface localized mode, which we have called 'surface polariton'. Here the term 'anomalous' means that this mode belongs to the type [I] surface modes, which is in contrast to the usual surface excitons being the type [II] modes. In this subsection, first we study the behavior of this mode in real space in some detail and then discuss the relation of this mode to the surface polariton of the usual sense.

For simplicity, we consider the case where r_1 is not so large that the energy of the 'surface polariton' is located within the bulk band gap ($r_1/\lambda<3/4$)*). The Hamiltonian in the real space representation is given in eq. (3.18). As we have shown in the arguments about the DOS, the surface potential

---

*) On (100) surfaces of cubic lattice structure r_1/λ is at most nearly unity (see Table 3-1) and the relations (3.16). When r_1/λ exceeds unity, the bulk T- and L-bands overlap each other in our model. We do not know the exact value of r_1 on other surfaces such as (111) and (110) surfaces. The work by Heller and Marcus[44] may be of some help, who calculated the three dimensional dipole sum with the wave vector in <111>, <110>, and <100> directions in fcc crystal using Evald's method extended by Born and Bradburn.[48] According to their result, there are no cases where the T- and L-bands overlap. We had better think of r_1 as the parameter into which the next (third, and so on) nearest layer short-range interactions are renormalized. Therefore it seems reasonable to assume that r_1/λ is less than unity. The condition $r_1/\lambda<3/4$ is a bit tighter than this condition.

has littel influence on this mode, so we may omit $\delta\vec{a}_1^{\dagger}\cdot\vec{a}_1$ from the Hamiltonian. Also the K-linear terms in the intralayer interaction may be neglected since they play no significant roles. The Heisenberg equation of motion for $\vec{a}_\ell$ yields the eigenvalue equation;

$$\begin{pmatrix}\varepsilon_b-r_0-\varepsilon, & 0\\ 0, & \varepsilon_b+2r_0-\varepsilon\end{pmatrix}\vec{a}_\ell+\begin{pmatrix}-r_{1/2}, & 0\\ 0, & r_1\end{pmatrix}(\vec{a}_{\ell-1}+\vec{a}_{\ell+1})$$

$$+3\lambda K\Big\{\sum_{m=1}^{\ell-1}e^{-K|\ell-m|}V_1\,\vec{a}_m+\sum_{m=\ell+1}^{\infty}e^{-K|\ell-m|}V_2\,\vec{a}_m\Big\}=0$$

$$(\ell\neq 1)\quad , \tag{6.1}$$

$$\begin{pmatrix}\varepsilon_b-r_0-\varepsilon, & 0\\ 0, & \varepsilon_b+2r_0-\varepsilon\end{pmatrix}\vec{a}_1+\begin{pmatrix}-r_{1/2}, & 0\\ 0 & r_1\end{pmatrix}\vec{a}_2$$

$$+3\lambda K\sum_{m=2}^{\infty}e^{-K(m-1)}V_2\,\vec{a}_m=0\qquad(\ell=1)\quad , \tag{6.2}$$

where we have considered the limit $N\to\infty$. We assume that the ℓ-dependence of $\vec{a}_\ell$ is represented by the sum of two terms; one is extended rather deep into the bulk (slow decay in space) and has the form $\vec{u}e^{-\bar{K}\ell}$ where $\bar{K}$ is positive and of the order of K, and the other is some function $\vec{a}_\ell'$ which swiftly damps in space:

$$\vec{a}_\ell=\vec{u}\,e^{-\bar{K}\ell}+\vec{a}_\ell' \quad . \tag{6.3}$$

We call the first term the slowly damping part and the second

one the swiftly damping part. We note that

$$K \sum_{m=1}^{\infty} e^{-K|\ell-m|} \vec{a}'_m = O(K) \ . \tag{6.4}$$

This means that the swiftly damping part produces only a weak long-range field on any layer, which can be neglected. We consider a sufficiently deep layer ℓ such that $\vec{a}'_\ell$ has a negligible amplitude. For such ℓ eq. (6.1) approximately becomes

$$\begin{pmatrix} \varepsilon_b - 2\lambda - \varepsilon, & 0 \\ 0, & \varepsilon_b + 4\lambda - \varepsilon \end{pmatrix} \vec{\vec{u}} + 3\lambda K \left\{ \frac{e^{(\bar{K}-K)\ell} - 1}{e^{\bar{K}-K} - 1} V_1 \right.$$

$$\left. + \frac{1}{e^{\bar{K}+K} - 1} V_2 \right\} \vec{\vec{u}} = 0 \ , \tag{6.5}$$

where we have used the sum rule $r_0 + r_1 = 2\lambda$. In order for this equation to hold for any (large) ℓ, we must have

$$V_1 \vec{\vec{u}} = \begin{pmatrix} 1, & i \\ i, & -1 \end{pmatrix} \vec{\vec{u}} = 0 \ , \tag{6.6}$$

which has the solution

$$\vec{\vec{u}} = \begin{pmatrix} 1, \\ i \end{pmatrix} \ , \tag{6.7}$$

If we substitute this into the vector equation (6.5), we obtain two equations that should be satisfied at the same time. This condition determines both ε and $\bar{K}$ as

$$\varepsilon = \varepsilon_b + \lambda \ , \tag{6.8}$$

$$e^{\bar{K}} = (1+2K)\, e^{-K} , \quad \therefore \bar{K} \simeq K . \tag{6.9}$$

We notice that the energy of this mode is determined solely by the slowly damping part. Now for sufficiently small ℓ such that the swiftly damping part has a significant amplitude, eqs. (5.1) and (5.2) can be rewritten approxiamtely as

$$\begin{pmatrix} \varepsilon_b - r_0 - \varepsilon, & 0 \\ 0, & \varepsilon_b + 2r_0 - \varepsilon \end{pmatrix} \vec{a}'_\ell + \begin{pmatrix} -r_1/2, & 0 \\ 0, & r_1 \end{pmatrix} (\vec{a}'_{\ell-1} + \vec{a}'_{\ell+1}) = 0 \quad (\ell \neq 1) , \tag{6.10}$$

$$\begin{pmatrix} \varepsilon_b - r_0 - \varepsilon, & 0 \\ 0, & \varepsilon_b + 2r_0 - \varepsilon \end{pmatrix} \vec{a}'_1 + \begin{pmatrix} -r_1/2, & 0 \\ 0, & r_1 \end{pmatrix} \vec{a}'_2 = \begin{pmatrix} -r_1/2, & 0 \\ 0, & r_1 \end{pmatrix} \vec{\bar{u}}$$

$$(\ell = 1) , \tag{6.11}$$

We assume that the ℓ-dependence of $\vec{a}'_\ell$ is represented by

$$\vec{a}'_\ell = \begin{pmatrix} u'_x \exp[(-\kappa_1 + i\pi)\ell], \\ u'_z \exp[(-\kappa_2 + i\pi)\ell] \end{pmatrix} , \qquad (\kappa_1, \kappa_2 > 0) \tag{6.12}$$

Substitution of this expression into eq. (6.10) determines κ_1 and κ_2. A straightforward calculation yields

$$\begin{aligned} \kappa_1 &= \cosh^{-1}\{(3\lambda - r_1)/r_1\} , \\ \kappa_2 &= \cosh^{-1}\{(3\lambda - 2r_1)/2r_1\} , \end{aligned} \tag{6.13}$$

where the positive branch of $\cosh^{-1}$ should be taken in order for κ_1 and κ_2 to be positive. As far as the condition $r_1/\lambda < 3/4$ holds, κ_1 and κ_2 are finite, which is consistent with the assumption that $\vec{a}'_\ell$ is swifty damping. Finally substitution of the expression (6.12) into eq. (6.11) determines u'_x and u'_z.

We get

$$u_x' = \frac{r_1}{r_1 \exp(-2\kappa_1) - 2(3\lambda - r_1)\exp(-\kappa_1)},$$
$$u_z' = \frac{ir_1}{r_1 \exp(-2\kappa_2) - (3\lambda - 2r_1)\exp(-\kappa_2)}. \qquad (6.14)$$

The swiftly damping part $\vec{a}_\ell'$ is related to the short-range interaction. In fact, if r_1 vanishes, κ_1 and κ_2 in eq. (5.13) become infinite and as a result $\vec{a}_\ell'$ vanishes for any ℓ. Since the amplitudes $\vec{\vec{u}}$ and (u_x', u_z') of the slowly and the swiftly damping parts are of the same order with respect to K, we can say that the main body of the 'surface polariton' wave function is composed of the slowly damping part. The normalization of its wave function as well as its energy are determined soley by this part (in the lowest order with respect to K).

It is interesting to note the property of $\vec{\vec{u}}$. In general, $V_1\vec{\vec{u}}$ describes the macroscopic electric field which the dipole moment $\vec{\vec{u}}$ distributed on a layer on the surface side produces at a layer on the bulk side (see the Hamiltonian (3.18)). On the contrary, $V_2\vec{\vec{u}}$ describes the field at a surface side layer produced by $\vec{\vec{u}}$ on the bulk side layer. Therefore the meaning of eq. (6.6) is that in the 'surface polariton' mode the motion of the dipole moment on one layer is so determined that it produces no macroscopic field at any layers deeper than that layer. This makes possible for this mode to localize near the surface.

We note that when $r_1/\lambda>3/4$ (but $r_1/\lambda<1$; see the footnote on page 103) the argument of $\cosh^{-1}$ for κ_2 in eq. (6.13) becomes less than unity. In this case κ_2 becomes pure imaginary ($=ik_2$) and the z-component of $\vec{a}'_\ell$ is no more a decaying but propagating function. As far as $|k_2|>>K$ holds, however, the estimate given in eq. (6.4) is still true and also the separation of $\vec{a}_\ell$ into $\vec{u}e^{-\bar{K}\ell}$ and $\vec{a}'_\ell$ so as for $\vec{u}$ to satisfy eq. (6.5) is possible. So the argument given above suffers no significant modifications except for the propagating property of $\vec{a}'_\ell$. In this case the mode in cosideration becomes a surface resonance state.

Now let us find the connection between the mode in consideration and the surface polariton in the usual sense. Since the short-range interaction plays no role in determining the energy of the 'surface polariton', we assume $r_1=0$ in the following argument, although this is not an inevitable assumption. We consider the dielectric function $\chi(\omega)$ of the bulk (i.e. with the periodic boundary condition being imposed) crystal in our model. This is given by

$$\chi(\omega) = 1 + \frac{6\lambda}{\varepsilon_b - 2\lambda - \hbar\omega} \quad . \tag{6.15}$$

This expression can be obtained from the first principle calculation in which the linear response theory is applied to the system with the Hamiltonian H_b of the bulk crystal.*)

---

*) In so doing, the treatment of the long-range interaction in H_b should require some care.[49] Probably the easiest way to obtain eq. (6.15) is to start with the atomic polarizability $|M|^2/(\varepsilon_b-\hbar\omega)$ and then to relate it to $\chi(\omega)$ with the Lorentz-Lorenz local field correction being taken into account.

Here we satisfy ourselves only to note that $\chi(\omega)$ in eq.(6.15) gives correctly the T-mode energy $(\varepsilon_b - 2\lambda)$ and the L-mode one $(\varepsilon_b + 4\lambda)$ from the familiar formulae $\chi(\omega)=\infty$ and $\chi(\omega)=0$, respectively. It is well-known that the dispersion relation $\omega(K_{//})$ of the surface polariton is obtained from

$$(\frac{cK_{//}}{\omega})^2 = \frac{\chi(\omega)}{1+\chi(\omega)} \quad , \tag{6.16}$$

where c is the light velocity. If we are to neglect the retardation effects (polariton effects), we are allowed to put $c=\infty$ and eq. (6.16) becomes

$$1 + \chi(\omega) = 0 \quad . \tag{6.17}$$

using the expression (6.15) for $\chi(\omega)$, we get the solution of this equation as

$$\hbar\omega = \varepsilon_b + \lambda \quad . \tag{6.18}$$

This is exactly the energy of the 'surface polariton' in our model. Thus we have found that the 'surface polariton' as we have called is the usual surface polariton, but without the retardation effects. This is to be expected, since we have no transverse electromagnetic fields (i.e. photons) in our Hamiltonian.

6-2 Applications of the Model

Although our model seems too naïve to be applied to real

solids, we now try to interpret the experimental data, especially those obtained on GaAs(110) surface on the basis of our results. In §2-4 we have mentioned the observation of Lapeyre and Anderson that the surface core excitons on GaAs(110) surface show the giant anisotropy in the CIS measurement (see Fig. 2-2). Because of the high surface sensitivity of the CIS technique and probably because of its nature that only those core excitations which are easy to decay into valence excitation continuum can be detected in the CIS's, there can be seen no structures due to the bulk core excitations in their CIS's. On the other hand, the bulk core excitations are more easily observed in reflection spectra. Fig. 6-1 shows the second derivative of the reflection spectrum on the GaAs(110) surface measured by Skibowski and Sprüssel.[50] The four structures at higher energies were identified as due to the bulk core excitons associated with transitions from Ga 3d to L and X points in the conduction band. The lower two structures correspond in energy to the surface core excitons observed in the CIS's.

We have three parameters in our model; the surface potential δ, the L-T splitting Δ_{LT} ($=6\lambda$), and the short-range interaction parameter r_1. In order to apply our theory to the GaAs core excitons with such rather complicated structures, we must make some avaraging procedures. As the average energy separation between the two surface excitons and the four bulk excitons we may roughly take the value of 0.5 eV, which we use as the value

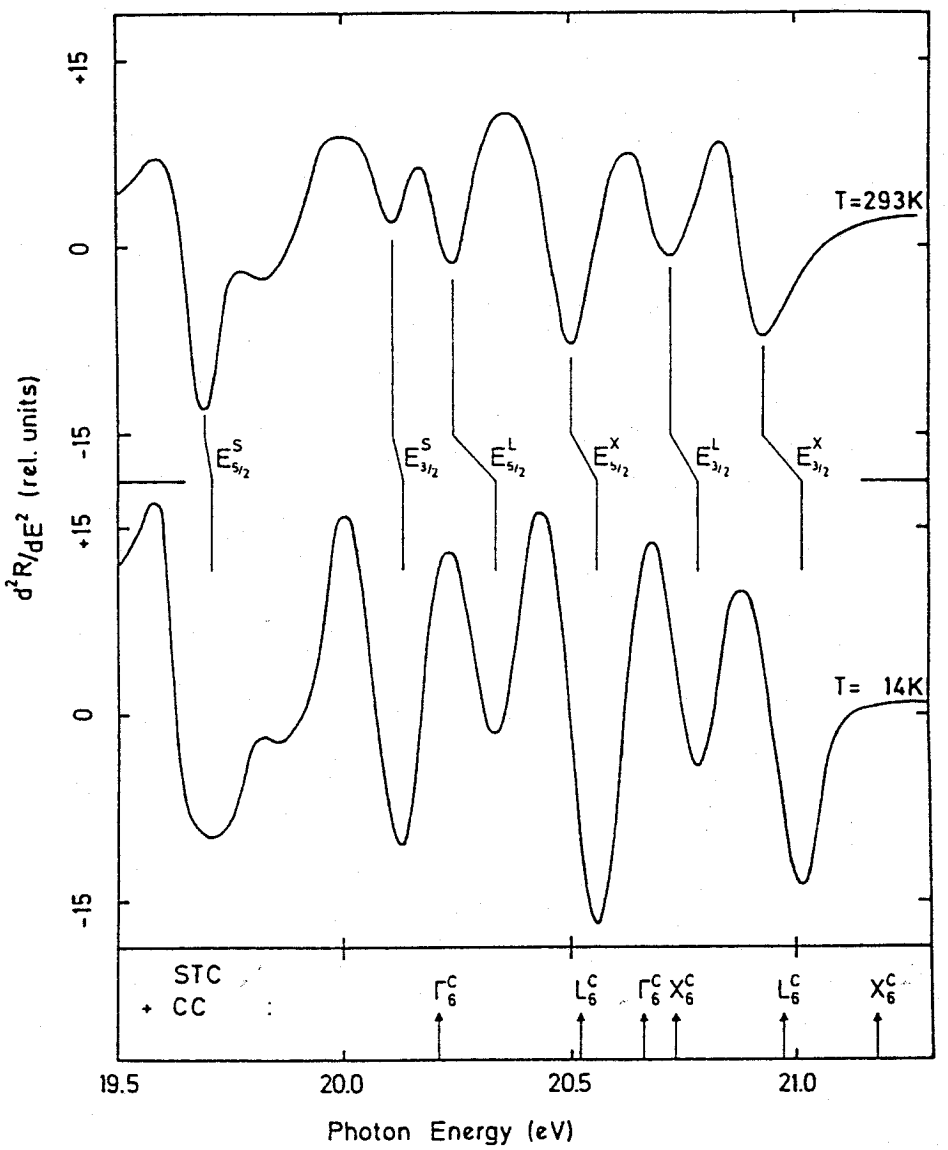

Fig. 6-1. Second derivative of the GaAs reflection spectrum assciated with Ga3d excitation for two different temperatures. The four minimums at higher photon energies have been assigned as due to transitions to the X and the L points in the conduction bands, and the two (or tree) minimums as due to the surface core exciton (after Skibowski and Sprüssel[50]).

of $-\delta$. Estimation of Δ_{LT} is difficult. In the case of excitons located within the fundamental band gap, the width of the reflection spectrum gives a good measure for Δ_{LT}. The average width of the structures shown in Fig. 6-1 is roughly estimated to be 0.2 eV, although it is quite dangerous to expect that the width of the structure of the second derivative spectrum gives a measure of Δ_{LT}. If we assume the transitions in consideration to be purely atomic, we can make a crude estimate of the dipole-moment M associated with transitions from five 3d orbitals to three 4p ones with the aid of the Slater orbitals.[51] Then Δ_{LT} is obtained from the formula $\Delta_{LT}=4\pi M^2/\Omega$ where Ω is the volume of the unit cell. In this way we made the estimate that $\Delta_{LT}\sim 0.3$ eV, which is not so far from the previous one. Therefore we may adopt 0.3 eV as the value of Δ_{LT}. The value of r_1/λ on fcc(110) surface is around 0.2.[44] If we calculate the polarization ratio of the oscillator strength $(f_{c1}+f_{c2})/f_{s1}$ from the formulae (5.58)$\sim$(5.60) using these values, the result is very near to its asymptotic (i.e. $|\delta|\to\infty$) value 1. That is, we cannot expect such a large anisotropy of the surface exciton transitions as observed in the CIS's.

The situation is not so simple, though. The reflection spectrum shown in Fig. 6-1 is for the near normal incidence case. As we have mentioned in §2-4, the energy positions of the surface exciton peaks in the CIS's are highly sensitive to the polarization of the incident radiation. Their shifts amount

to 0.5 eV which is about twice as large as the full width at half maximum of the peaks. The Fano effect alone may be difficult to explain this large polarization dependence of the peak positions. Another possibility to explain this phenomenon is the crystal field splitting of the surface excitons. Since the symmetry of the (110) surface of a zincblende crystal is very low (Cs with only one mirror plane),[52] more or less such splitting must take place. If the peak shift of 0.5 eV is attributed to the crystal field splitting, the energy of the surface exciton excited by p-polarized radiation can come very near or even above some of the bulk exciton energies. In terms of the parameters in our model, $|\delta|$ may be smaller than Δ_{LT}, which results in a large anisotropy of the oscillator strengths as can be seen in Figs. 5-7∿5-9. In other words, it is possible to relate the observed large polarization dependence of the CIS peak intensities to that of the CIS peak shifts on the basis of our model. We point out that the observed fact that the peak intensities for p-polarized radiation are larger than those for s-polarized one is at least not contradictory to the results of our simple model, although a quantitative or even a further qualitative argument is beyond the scope of our model. A quantitative argument will require us to take account of

i) the effect of interactions between the surface core excitons and the valence excitation continuum (Fano effect),

ii) the effect of the surface atomic geometry including relaxation on the anisotropy of valence excitations which are the final

states in the CIS, as well as on that of the surface core excitons,

iii) the difference in character of the wave functions between the surface core excitons and the bulk ones, if the interaction between them is effective (see the footnote on page 24),

and so on. In addition, the main drawback of our simple model is that the retardation effects are not taken into account in it. This point will be discussed in the following subsection. Till now, however, we have no theory concerning how effectively the retardation effects work in the energy region of the core excitation.

Our model predicts the large polarization dependence of the surface exciton oscillator strengths depending on the parameter values. It suggests which experimental geometry is favorable to observe surface excitons in optical measurements as well as the usefulness of polarization-resolved technique to study the detailed nature of surface excitons. Our model also tells us that in some cases two surface exciton levels associated with one bulk exciton level can be observed by oblique incident p-polarized radiation. Perhaps the systems to which our model can be applied rather directly are the surface excitons in rare gas solids, since the Frenkel model gives a relatively good description for both the bulk and the surface excitons in these solids.

6-3 Limitations and Extensions of the Model

As we have already noted, the retardation (or polariton) effects are not taken into account in our model. Neglect of these effects are allowed for large values of $K_{//}$ such that $K_{//} >> \omega/c$ holds. However, since ω/c for the optical frequency region is usually quite small compared with the dimension of the Brillouin zone, there may still exist the region in the $(\omega, K_{//})$-plane where the neglect of the retardation effects and the use of the $K_{//}$-expansion as we have made are justified at the same time. In such a region our results for the DOS is valid. The effects on the results of the absorption spectrum might be severer. We have shown that the 'surface polariton' in our terminology corresponds to the surface polariton in the usual sence but without the retardation effects. This means that the surface polariton is a composite particle of the photon and the 'surface polariton'. As is well-known, the dispersion curve of the surface polariton can exist only in the larger $K_{//}$ side of the dispersion line $\omega = cK_{//}$ of the light and thus cannot be excited directly by the vacuum radiation, which contradicts to our result that the 'surface polariton' has a large absorption intensity proportional to $1/K$. However, it does not necessarily contradicts to the fact that the 'surface polariton' has a large oscillator strength proportional to $1/K$. We have shown that the oscillator strength is a measure of the spatial extension of the wave function. The 'surface polariton' as a constituent

of the surface polariton can, in fact, have such a large spatial extension. The above mentioned fact that the usual*) absorption measurement cannot detect the 'surface polariton' only means that the retardation effects prevent the 'surface polariton' from coupling with the vacuum radiation. However, we have no a priori reason to think that the retardation effects inhibit the surface excitons from coupling with the vacuum radiation. Therefore we can expect that the results on the oscillator strengths of the surface excitons on which we have made the rather detailed discussion do not suffer significant modifications even if we take the retardation effects into consideration.

However, it is in itself an interesting question to ask how the retardation affects the system containing the surface excitons. It may be in the reflection spectrum that the retardation effects show themselves most explicitly, because the reflection spectrum is directly related to the structure of the dispersion curves of polaritons. As we know, much theoretical and experimental attention has been attracted by the so-called 'ABC' problem in recent polariton physics. If we rephrase the previous question along this line, it may be 'how the additional boundary conditions are influenced by the existence of the surface excitons?'. Since our model is simple enough, to answer it on the basis of our model will provide a deeper physical insight about the 'ABC'. Here we want to point out that the resolvent which we have used in the calculations is essentially the polarizability tensor in the k-representation.

---

*) See the second footnote on page 3.

Its Fourier transform into the real space representation gives the non-local inhomogeneous polarizability, which is known to be useful in solving for the 'ABC's'.[53] Therefore our formalism will give a good starting point to answer that question.

Finally we want to give some comments about the possible variations of the model:

(i) Among the surface-induced anisotropies we have considered only the surface geometrical anisotropy. The surface crystal-field anisotropy may be easily incorporated into the model by replacing the surface potential δ by a tensor quantity.

(ii) The absorption spectrum is usually taken on a thin crystal. When the crystal thickness is of the order of or less than the wave length of the incident light, the interference term in the long-range interaction between the two surfaces of the slab, which we have omitted, should be retained.

(iii) As we have already mentioned, the wave functions of the surface excitons on semiconductor surfaces have usually different characters from those of the bulk excitons. One simple way to represent this effect is to make the magnitude of the dipole moment on the surface layer to be different from those on the bulk layers.

(iv) The spatial dispersion effect (the wave vector dependence of the exciton energies) caused by the dipole-dipole interaction alone is usually too small to affect the reflection spectrum.[20] In real solids, however, the overlaps of the

one-electron wave functions on near neighbor atomic sites are usually more important origins of the short-range interactions than those arising from the dipole-dipole couplings. We can represent this effect by enlarging the value of the short-range interaction parameter r_1 and at the same time disregarding the sum rule $r_0+r_1=2\lambda$.

(v) The bulk and surface excitons in real solids are frequently composed of multiplets, so the extension of the model along this direction is required in such cases.

Some or all of these modifications will be more or less inevitable when we want to apply the model to real solids and to make a quantitative analysis even in the cases where the Frenkel's model gives a good description of the excitons.

§7 Summary

How the interplay between the dipole - dipole interactions and the surface geometrical anisotopy influences the optical properties of the surface Frenkel excitons has been investigated with the use of the simple model. The dipole-dipole interactions, expressed in the layerwise form, consist of the intralayer terms, the interlayer short-range ones, and the interlayer long-range ones which are represented by the parameters r_0, r_1 and λ, respectively. Internal consistency of the model requires the sum rule: $r_0+r_1=2\lambda$. Together with the surface potential δ, our model is characterized by three independent parameters. Dyson's equation for the resolvent Green's function has been solved. The detailed analyses have been made with the aid of the $K_{//}$-expansion. How the exchanges of the DOS and the oscillator strengths between the surface localized states and the bulk band states as well as their rearrangement within the bulk bands occur through the presence of the surface has been clarified for various values of the parameters. Our lowest order solution in the $K_{//}$-expansion suggests that the existences and the energy positions of the surface excitons are insensitive to the presence of the long-range interaction, while their oscillator strengths are highly sensitive to it. The particular feature to be noted is the enhancement of the oscillator strengths. That is, depending on the values of the parameters, the surface

excitons show giant oscillator strengths, the origin of which can be attributed either to the short-range interactions or to the long-range ones. In addition, this phenomenon especially of the latter origin is strongly dependent on the polarization of the excitation radiation. On the basis of these results, a possible explanation has been given to the recently observed giant anisotropy of the CIS structures due to the GaAs surface core excitons. Besides the usual surface excitons, our model predicts the 'anomalous' surface localized mode, which has been identified as the surface polariton mode without retardation corrections.

Appendix A: Integral Approximation of the Intralayer Dipole-Dipole Interactions*)

We evaluate the following two-dimensional integrals in power series of k:

$$I = \iint_{r>r_0} d\vec{r}\, \frac{\exp(-i\vec{k}\cdot\vec{r})}{r^5} \begin{pmatrix} -2x^2+y^2, & -3xy, & 0 \\ -3xy, & x^2-2y^2, & 0 \\ 0, & 0, & x^2+y^2 \end{pmatrix} , \tag{A-1}$$

where $\vec{r}=(x,y,0)$ and $\vec{k}=(k,0,0)$. Since the integral containing xy as a factor of its integrand vanishes by symmetry, we only need to know the following two integrals;

$$I_{xx} = \iint_{r>r_0} d\vec{r}\, \frac{\exp(-i\vec{k}\cdot\vec{r})}{r^5}\, x^2 , \tag{A-2}$$

$$I_{yy} = \iint_{r>r_0} d\vec{r}\, \frac{\exp(-i\vec{k}\cdot\vec{r})}{r^5}\, y^2 . \tag{A-3}$$

Using the polar coordinates (r,θ), we rewrite I_{xx} as

$$I_{xx} = \int_{r_0}^{\infty} \frac{dr}{r^2} \int_0^{2\pi} d\theta\, e^{-ikr\cos\theta} \cos^2\theta . \tag{A-4}$$

Integration with respect to θ yields

$$I_{xx} = \pi k \int_{r_0}^{\infty} dr\, \frac{J_0(kr)-J_2(kr)}{r^2} , \tag{A-5}$$

---

*) A part of the results in this appendix is also found in ref. 54).

where J_0 and J_2 are the 0-th and the 2nd order Bessel functions, respectively. As to the first term in (A-5), integration by parts yields

$$\int_{r_0}^{\infty} dr \frac{J_0(kr)}{r^2} = \frac{J_0(kr_0)}{kr_0} - \int_{kr_0}^{\infty} dx \frac{J_1(x)}{x} \quad , \tag{A-6}$$

where we have used the formula $dJ_0(x)/dx=J_1(x)$ (J_1 is the 1st order Bessel function). Expanding the first term of eq. (A-6) with respect to kr_0, and retaining up to first order in kr_0, we have

$$\frac{J_0(kr_0)}{kr_0} \simeq \frac{1}{kr_0} + \frac{kr_0}{4} \ . \tag{A-7}$$

The second term of eq. (A-6) is rewritten as

$$\int_{kr_0}^{\infty} dx \frac{J_1(x)}{x} = \int_{0}^{\infty} dx \frac{J_1(x)}{x} - \int_{0}^{kr_0} dx \frac{J_1(x)}{x} \ . \tag{A-8}$$

The first term of this equation can be evaluated analytically as

$$\int_{0}^{\infty} dx \frac{J_1(x)}{x} = \frac{\Gamma(1/2)}{2\Gamma(3/2)} = 1 \quad , \tag{A-9}$$

where Γ is the gamma function. As for the second term of eq. (A-8), first we expand the integrand with respect to x, and then integrate it over x. Thus we obtain

$$\int_0^{kr_0} dx \, \frac{J_1(x)}{x} \simeq \frac{kr_0}{2} \quad , \tag{A-10}$$

From eqs. (A-6)∿(A-10), we have

$$\int_{r_0}^{\infty} dr \, \frac{J_0(kr)}{r^2} \simeq \frac{1}{kr_0} - 1 + \frac{kr_0}{4} \, . \tag{A-11}$$

Next we evaluate the second term in eq. (A-5), which can be rewritten as

$$\int_{r_0}^{\infty} dr \, \frac{J_2(kr)}{r^2} = \int_0^{\infty} dr \, \frac{J_2(kr)}{r^2} - \int_0^{r_0} dr \, \frac{J_2(kr)}{r^2} \quad . \tag{A-12}$$

Similar procedure to that of getting eq. (A-11) yields

$$\int_{r_0}^{\infty} dr \, \frac{J_2(kr)}{r^2} \simeq \frac{1}{3} - \frac{kr_0}{8} \, . \tag{A-13}$$

From eqs. (A-5), (A-11), and (A-13), we obtain

$$I_{xx} \simeq \pi k \left(\frac{1}{kr_0} - \frac{4}{3} + \frac{3}{8} \, kr_0 \right) \, . \tag{A-14}$$

similarly, we can also evaluate that

$$I_{yy} \simeq k \left(\frac{1}{kr_0} + \frac{2}{3} + \frac{kr_0}{8} \right) \, . \tag{A-15}$$

Using eqs. (A-14) and (A-15), we arrive at the final result;

$$I \cong \pi k \begin{pmatrix} -\frac{1}{kr_0} + 2 - \frac{5}{8} kr_0, & 0, & 0 \\ 0, & -\frac{1}{kr_0} + \frac{kr_0}{8}, & 0 \\ 0, & 0, & \frac{2}{kr_0} - 2 - \frac{kr_0}{2} \end{pmatrix}, \qquad \text{(A-16)}$$

which is correct up to first order in kr_0. If we retain the terms up to linear in k (note the factor k in the front), this becomes equivalent to eq. (3.7) in the text.

Appendix B: Approximate Expression of $\alpha(k)$

We prove the following approximate formula for $\alpha(k)=\frac{1}{e^{K+ik}-1}$:

$$\alpha(k) = \frac{1}{K+ik}\frac{k}{2}\cot\frac{k}{2} - \frac{1}{2} + O(K) , \qquad (B\text{-}1)$$

where $O(K)$ means a collection of terms that are of the order of or higher order than K and, at the same time, analytic with respect to k in the domain $|k|\leq\pi$. We make use of the Laurent expansion

$$\frac{1}{e^{z}-1} = \frac{1}{z} - \frac{1}{2} + f(z) , \qquad (B\text{-}2)$$

where $f(z)$ is a power series of z starting from a term linear in z (expansion coefficients of $f(z)$ are expressed by Bernoulli numbers, although the detailed form of $f(z)$ does not matter in the following argument). The radius of convergence of the expansion (B-2) is 2π. Using eq. (B-2), we have

$$\begin{aligned}\alpha(k) &= \frac{1}{K+ik} - \frac{1}{2} + f(K+ik) \\ &= \frac{1}{K+ik} - \frac{1}{2} + f(ik) + O(K) .\end{aligned} \qquad (B\text{-}3)$$

We rewrite $f(ik)$ in this equation as

$$f(ik) = \frac{K}{K+ik} f(ik) + \frac{ik}{K+ik} f(ik) . \qquad (B\text{-}4)$$

The first term in the above equation is rewritten to give

$$\frac{K}{K+ik} f(ik) = \frac{K}{K+ik} (f(K+ik) + O(K)) . \qquad (B-5)$$

Since $f(z)/z$ is analytic in the region $|z|<2\pi$, we can make the estimate, from eq. (B-5), such that

$$\frac{K}{K+ik} f(ik) = O(K) . \qquad (B-6)$$

From eqs. (B-4) and (B-6), we obtain

$$f(ik) = \frac{ik}{K+ik} f(ik) + O(K) . \qquad (B-7)$$

By applying the formula (B-2) to the function $f(ik)$ in the right hand side of this equation, we get

$$f(ik) = \frac{ik}{K+ik} \left(\frac{1}{e^{ik}-1} - \frac{1}{ik} + \frac{1}{2}\right) + O(K) . \qquad (B-8)$$

Substituting eq. (B-8) into eq. (B-3), we have

$$\alpha(k) = \frac{ik}{K+ik} \left(\frac{1}{e^{ik}-1} + \frac{1}{2}\right) - \frac{1}{2} + O(K) . \qquad (B-9)$$

A straightforward manipulation of this equation yields the desired result (B-1).

Appendix C: Bulk Eigenmodes

In this appendix, we solve the eigenvalue problem (3.28) which appeared in the text, with the special attention paid to the order with respect to K. The solution is correct up to the first order in K. First we prove the following theorem:

Theorem

Let f(k) be a function of k that is analytic near k=0 and does not contain K. Then, within the region where f(k) is analytic,

(i) if f(k) is an even function of k, we can make the estimate such that

$$\cos^2\theta\ f(k) = \cos^2\theta\ f(0) + O(K^2) ,$$

(ii) otherwise, we have

$$\cos^2\theta\ f(k) = \cos^2\theta\ f(0) + O(K) ,$$

where θ is defined in the text.

It is easy to prove this theorem. In the case of (i), f(k) can be expanded as

$$f(k) = f(0) + \sum_{n=1}^{\infty} c_n\, k^{2n} .$$

Therefore, we have

$$\cos^2\theta\ f(k) = \cos^2\theta\ f(0) + \frac{K^2}{K^2+k^2} \sum_{n=1}^{\infty} c_n k^{2n}$$

$$= \cos^2\theta\, f(0) + K^2 \sin^2\theta \sum_{n=0}^{\infty} c_{n-1} k^{2n}$$

Since $\sum_{n=0}^{\infty} c_{n-1} k^{2n}$ is also analytic in the region where f(k) is analytic, we obtain the densired result, at once. The proof for the case (ii) can be similarly made.

Now we examine the eigenvalue equation (3.28). With the aid of the power series expansion of $\frac{k}{2}\cot\frac{k}{2}$ (see eq. (3.29) in the text), as well as the above theorem, eq. (3.28) can be rewritten as

$$\left\{\begin{pmatrix} \varepsilon_b - r_0 - r_1 \cos k - \varepsilon, & 0 \\ 0, & \varepsilon_b + 2r_0 + 2r_1 \cos k - \varepsilon \end{pmatrix} + 6\lambda \cos\theta \begin{pmatrix} \cos\theta, & \sin\theta \\ \sin\theta, & -\cos\theta \end{pmatrix} + \begin{pmatrix} O(K^2), & O(K) \\ O(K), & O(K^2) \end{pmatrix}\right\} \vec{u} = 0 \qquad \text{(C-1)}$$

If we are to evaluate the eigenvalues up to first order in K, the diagonal terms of order K^2 and the off-diagonal terms of order K are unrelevant, and we can neglect the third term in the curly bracket of eq. (C-1). In order for non-trivial solutions to exist, the determinant of the matrix should vanish. After some manipulations we get

$$E^2 - E^2(k) + 4\lambda \cos^2\theta\, E(k) - 4\lambda^2 \cos^2\theta = 0 , \qquad \text{(C-2)}$$

where we have defined E(k) and E as

$$E(k) = (r_0 + r_1 \cos k)/2 , \qquad \text{(C-3)}$$

and

$$E = (\varepsilon - \varepsilon_b - E(k))/3 , \qquad \text{(C-4)}$$

respectively. If we apply the above theorem to the third term in eq. (C-2), with keeping the sum rule (see eq. (3.26) in the text) in mind, we can show that the last two terms cancel each other (up to first order in K). Finally we obtain

$$E = \pm E(k) + O(K^2) \ . \qquad (C\text{-}5)$$

Now we seek for the eigenvector corresponding to the eigenvalue E(k). From the original eigenvalue equation (3.28), we see that $\vec{u}$ must satisfy

$$[-E(k) + \lambda \cos^2\theta \ \frac{k}{2} \cot\frac{k}{2}, \ -\lambda \cos\theta \sin\theta \ \frac{k}{2} \cot\frac{k}{2}] \ \vec{u} = 0 \ . \qquad (C\text{-}6)$$

Using the theorem as well as the sum rule (3.26), we can show that

$$\begin{aligned} E(k) &= E(k)(\sin^2\theta + \cos^2\theta) \\ &= E(k) \sin^2\theta + \lambda \cos^2\theta + O(K^2) \ , \end{aligned} \qquad (C\text{-}7)$$

and also that

$$\lambda \cos^2\theta \ \frac{k}{2} \cot\frac{k}{2} = \lambda \cos^2\theta + O(K^2) \ . \qquad (C\text{-}8)$$

Substitution of eqs. (C-7) and (C-8) into eq. (C-6) yields

$$(-E(k) \sin\theta \ , \ \lambda \cos\theta \ \frac{k}{2} \cot\frac{k}{2}) \ \vec{u} = 0 \ , \qquad (C\text{-}9)$$

which is valid up to first order in K. This equation is solved to give

$$\vec{u} = \begin{pmatrix} \dfrac{r_0+r_1}{r_0+r_1\cos k} \ \dfrac{k}{2} \cot\dfrac{k}{2} \cos\theta, \\ \\ \sin\theta \end{pmatrix} \ , \qquad (C\text{-}10)$$

We point out that $\vec{u}$ is normalized correctly up to the order of K;

$$|\vec{u}| = 1 + O(K^2) \ , \tag{C-11}$$

this can be proved with the help of the theorem, again. The eigenvector corresponding to the eigenvalue $-E(k)$ can be similarly obtained.

If we use the original energy parameter ε, our results are summarized as follows; the energy eigenvalues and the eigenvectors of the bulk excitons are given by

$$\begin{cases} \varepsilon_t(k) = \varepsilon_b - r_0 - r_1 \cos k + O(K^2) \\ \vec{u}_t(k) = \begin{pmatrix} -\sin\theta \ , \\ \dfrac{r_0 + r_1}{r_0 + r_1 \cos k} \dfrac{k}{2} \cot\dfrac{k}{2} \cos\theta \end{pmatrix} + O(K^2) \end{cases} \tag{C-12}$$

and

$$\begin{cases} \varepsilon_\ell(k) = \varepsilon_b + 2r_0 + 2r_1 \cos k + O(K^2) \\ \vec{u}_\ell(k) = \begin{pmatrix} \dfrac{r_0 + r_1}{r_0 + r_1 \cos k} \dfrac{k}{2} \cot\dfrac{k}{2} \cos\theta, \\ \sin\theta \end{pmatrix} + O(K^2) \ . \end{cases} \tag{C-13}$$

In the text we have adopted the function $\cos\theta$ in place of the rather complicated function $\dfrac{r_0+r_1}{r_0+r_1\cos k} \dfrac{k}{2} \cot\dfrac{k}{2} \cos\theta$ in $\vec{u}_t(k)$ and and $\vec{u}_\ell(k)$. We note that the corrections due to this replacement are of the order of K. This can be easily proved in the same way as the proof of the theorem mentioned above.

Appendix D: Evaluations of the Integrals

In this appendix, we express the integrals appearing in the matrix [I] in the text in terms of the following integrals, the result of which will be correct up to the order required for each integral in the $K_{//}$-expansion:

$$I = \begin{pmatrix} I^t, & 0 \\ 0, & I^\ell \end{pmatrix} = \frac{1}{2\pi} \int dk \; G_0(k) \; , \tag{D-1}$$

$$J = \begin{pmatrix} J^t, & 0 \\ 0, & J^\ell \end{pmatrix} = \frac{1}{2\pi} \int dk \; e^{ik} \; G_0(k) \; , \tag{D-2}$$

$$\tilde{I} = \begin{pmatrix} \tilde{I}^t, & 0 \\ 0, & \tilde{I}^\ell \end{pmatrix} = \frac{K}{2\pi} \int dk \; |\alpha(k)|^2 \; G_0(k) \; , \tag{D-3}$$

where the range of integration is from $-\pi$ to π in all cases. These six integrals can be evaluated easily with the aid of the residue theorem. It is convenient to use the two energy parameters x and y with the corresponding complex energies v and w, as well as the complex square root function ${}^c\sqrt{}$ which are defined in eqs. (5.10), (5.11) and (5.13) respectively. The explicit expressions for I^t, J^t, and $\tilde{I}^t$ are as follows;

$$I^t = \frac{1}{{}^c\sqrt{v^2 - r_1^2}} \; , \tag{D-4}$$

$$J^t = (1 - vI^t)/r_1 \; , \tag{D-5}$$

$$\tilde{I}^t = \frac{K\, e^{-K}}{2(v+r_1 \cosh K)} \left(\frac{1}{\sinh K} + r_1 I^t\right)$$

$$= \frac{e^{-K}}{2(v+r_1)} (1+K\, r_1\, I^t) + O(K^2) \ . \qquad \text{(D-6)}$$

In the last line of eq. (D-6) we have expanded coshK and sinhK in terms of K. We may of course expand e^{-K}, too, but we use it as it stands for a later calculational convenience. The expressions for I^ℓ, J^ℓ, and $\tilde{I}^\ell$ can be obtained by simply replacing r_1 and v in the above expressions with $-2r_1$ and w, respectively.

There are twenty-one independent integrals in the matrix [I]. Here we examine only some of them. The others can be examined similarly. Typical integrals appearing in the matrix [I] are

(a) $Icc = \frac{1}{2\pi} \int dk\ G_0(k) \cos^2\theta$,

(b) $I_{sc} = \frac{1}{2\pi} \int dk\ G_0(k) \sin^2\theta$,

(c) $I_{\gamma\beta} = \frac{1}{2\pi} \int dk\ G_0(k)\ \gamma^*(k)\ \beta(k)$,

(d) $I_{c\beta} = \frac{1}{2\pi} \int dk\ G_0(k) \cos\theta\ \beta(k)$,

(e) $I_{s\beta} = \frac{1}{2\pi} \int dk\ G_0(k) \sin\theta\ \beta(k)$,

where $\beta(k)=\alpha(k)e^{i\theta}$ and $\gamma(k)=\alpha(-k)e^{-i\theta}e^{K-ik}$ are the first two elements of the vector [f(k)] defined in the text. In the following we examine these integrals.

For (a): Since $\cos^2\theta$ has significant values only in the small

region of k around k=0 the width of which is roughly K, we immediately obtain

$$I_{cc} = O(K) \ . \tag{D-7}$$

For (b): Using the above estimate, we get

$$\begin{aligned} I_{ss} &= \frac{1}{2\pi} \int dk \ G^0(k) \ (1-\cos^2\theta) \\ &= I + O(K) \ . \end{aligned} \tag{D-8}$$

For (c): We can approximate $\gamma^*(k)$ as

$$\begin{aligned} \gamma^*(k) &= e^{i\theta} \ \frac{e^{K+ik}}{e^{K+ik}-1} \\ &= e^{i\theta} \ (\alpha(k)+1) \\ &= \frac{\cos\theta}{K} \ \frac{k}{2} \cot\frac{k}{2} + \frac{e^{i\theta}}{2} + O(K) \\ &= e^{-i\theta} \ \alpha(-k) + \cos\theta \ \alpha(k) \ e^{i\theta} + O(K) \ . \end{aligned} \tag{D-9}$$

In the third and the fourth lines we have mada use of the estimate (4.29) in the text. Thus we have

$$\gamma^*(k) \ \beta(k) = |\alpha(k)|^2 + \cos\theta \ \alpha(k) \ e^{i\theta} + \alpha(k) \ e^{i\theta} \times O(K) \ . \tag{D-10}$$

We introduce a notation $\hat{O}(K)$ which means that it is a function of k and that when integrated over k it becomes of the order of K. It is easy to show that $\alpha(k)e^{i\theta} = \hat{O}(K^0)$. Therefore the third term in the last line in eq. (D-10) is written as $\hat{O}(K)$. Concerning the second term, we can rewrite it as

$$\cos\theta\ \alpha(k)\ e^{i\theta} = \frac{\cos^2\theta}{K} + \hat{O}(K)$$
$$= K|\alpha(k)|^2 + \hat{O}(K)\ . \qquad \text{(D-11)}$$

Therefore eq. (D-10) is rewritten as

$$\gamma^*(k)\ \beta(k) = (1+K)|\alpha(k)|^2 + \hat{O}(K)$$
$$= e^K\ |\alpha(k)|^2 + \hat{O}(K)\ .$$

Finally we get

$$I_{\gamma\beta} = \frac{e^K}{K}\ \hat{I} + O(K)\ . \qquad \text{(D-12)}$$

For (d): Using eq. (D-11), we immediately obtain

$$I_{c\beta} = \hat{I} + O(K)\ . \qquad \text{(D-13)}$$

For (e): First we rewrite the integrand as

$$\sin\theta\ \beta(k) = \sin\theta\ \left(\frac{\cos\theta}{K}\ \frac{k}{2}\ \cot\frac{k}{2} - \frac{\cos\theta}{2} - i\ \frac{\sin\theta}{2}\right) + O(K)$$

Since $G_0(k)$ is the odd function of k, the first and the second terms in the bracket do not contribute to the integral. Hence

$$I_{s\beta} = -\frac{i}{2}\ I_{ss} + O(K)$$
$$= -\frac{I}{2} + O(K)\ . \qquad \text{(D-14)}$$

Appendix E: The Wave Functions of the Surface Excitons

The wave functions of the surface excitons are obtained by directly solving the Schrödinger equation. We can do this in the real space representation in the same manner as in §6-1 for the 'surface polaritons' assuming that the ℓ-dependence of the wave functions is of the form given in eq. (5.68). Instead, in the following, we briefly sketch the outline of solution in the k-space.

The Schrödinger equation in the k-representation reads

$$\begin{pmatrix} \varepsilon_t(k)-\varepsilon, & 0 \\ 0, & \varepsilon_\ell(k)-\varepsilon \end{pmatrix} \vec{\psi}(k) + \frac{1}{N} \sum_{k'} V_{kk'} \vec{\psi}(k') = 0 \ , \qquad \text{(E-1)}$$

where $V_{kk'}$ is given in eq. (4.18) in the text and

$$\vec{\psi}(k) = \begin{pmatrix} <0| & b_t(k) & |\psi> \\ <0| & b_\ell(k) & |\psi> \end{pmatrix} . \qquad \text{(E-2)}$$

is the surface exciton wave function. Since $V_{kk'}$ is of the separable form, there arise no difficulties in principle. The method to solve eq. (E-1) is similar to, but simpler than that to solve Dyson's equation. We introduce a six-dimensional column vector $[\psi]$ with each element $\vec{\psi}_i$ being a two-dimensional vector defined by

$$\vec{\psi}_i = \frac{1}{N} \sum_k f_i(k) \vec{\psi}(k) \ , \qquad (i=1\sim6) \qquad \text{(E-3)}$$

where $f_i(k)$ is the i-th element of the vector $[f(k)]$ given in

eq. (4.16) in the text. If we are to seek for a truely localized mode, we may assume that its energy ε is located out of the bulk band $\varepsilon_t(k)$ and $\varepsilon_\ell(k)$. Then eq. (E-1) can be rewritten as

$$\vec{\psi}(k) = G_0(k)\ {}^t[f^*(k)][M][\psi] \ . \qquad (E\text{-}4)$$

We multiply the both sides by $f_i(k)$ and then sum over k. The result in the matrix representation is

$$[\psi] = [I][M][\psi] \ . \qquad (E\text{-}5)$$

This equation determines both ε and $[\psi]$ at the same time. Substitution of the solution $[\psi]$ into eq. (E-4) yields the wave function. The $K_{//}$-expansion is possible and we assume at the outset that

$$\begin{aligned} &\vec{\psi}_1,\ \vec{\psi}_2,\ \vec{\psi}_3,\ \vec{\psi}_4 = O(K^0) \ , \\ &\vec{\psi}_5,\ \vec{\psi}_6 = O(K^1) \ . \end{aligned} \qquad (E\text{-}6)$$

These assumptions can be ascertained self-consistently after we solve the problem. The energy eigenvalues have been given in the text. We only show the final result of the wave functions in the lowest order approximations in the $K_{//}$-expansion;

$$\vec{\psi}(k) = \sqrt{\frac{4\delta^2 - r_1^2}{4\delta^2 N}}\ \left(\frac{r_1}{2} + \delta e^{-ik}\right)\ G_0(k;\varepsilon)\ \times$$

$$\times\left\{ \frac{-3\lambda}{\varepsilon - \varepsilon_b - \lambda} \begin{bmatrix} i \\ 1 \end{bmatrix} \cos\theta + \begin{bmatrix} \sin\theta \\ \cos\theta \end{bmatrix} \right\} \cdots \text{'x-pol.'} \ ,$$

$$\vec{\psi}(k) = \sqrt{\frac{\delta^2 - r_1^2}{\delta^2 N}}\,(\delta\, e^{-ik_- r_1})\, G_0(k;\varepsilon) \times \tag{E-7}$$

$$\times\left\{ \frac{-3\lambda}{\varepsilon-\varepsilon_b-\lambda} \begin{pmatrix} 1 \\ -i \end{pmatrix} \cos\theta + \begin{pmatrix} -\cos\theta \\ \sin\theta \end{pmatrix} \right\} \cdots \text{'z-pol.'} \ ,$$

with the understanding that ε is the energy eigenvalue of each mode. In deriving the above results we have made use of the estimates (5.43). Since $\cos\theta$ is nearly zero for most values of k except for very small values ($|k| \lesssim K$), we can say that the 'x-pol.' ('z-pol.') surface exciton is mainly composed of the bulk T(L)-excitons.

Finally we point out that instead of the assumption (E-6) the other one such that

$$\begin{aligned} &\vec{\psi}_1,\ \vec{\psi}_2,\ = O(K^0) \ , \\ &\vec{\psi}_3,\ \vec{\psi}_4,\ \vec{\psi}_5,\ \vec{\psi}_6 = O(K^1) \ , \end{aligned} \tag{E-8}$$

leads to the solution of the 'surface polariton'. It also can be ascertained that this assumption is consistent with the final solution.

Appendix F: Explicit Expressions of the Absorption Spectrum

The final results for the four components $\bar{I}_s(\varepsilon)$, $\bar{I}_c(\varepsilon)$, $\Delta I_s(\varepsilon)$ and $\Delta I_c(\varepsilon)$ of the absorption spectrum are as follows:

$$\bar{I}_s(\varepsilon) = \delta(x+r_1) + \frac{\sqrt{r_1^2-x^2}}{\pi(x+r_1)^2}\,\theta(r_1^2-x^2)\ , \tag{F-1}$$

$$\begin{aligned}\bar{I}_c(\varepsilon) = {} & \Big[\frac{2}{K}+1+9\lambda^2\left\{\frac{\lambda_1}{(\lambda_1^2-r_1^2)^{3/2}}-\frac{1}{(\lambda_1+r_1)^2}\right\} \\ & + \frac{\lambda_2}{\sqrt{\lambda_2^2-4r_1^2}}\Big]\,\delta(\varepsilon-\varepsilon_b-\lambda) \\ & + \Big[-\frac{2}{K}+\frac{9\lambda^2}{(\lambda_1+r_1)^2}\Big]\,\delta(x+r_1) \\ & + \frac{9\lambda^2(r_1-x)}{\pi(r_1+x)(x-\lambda_1)^2\sqrt{r_1^2-x^2}}\,\theta(r_1^2-x^2) \\ & + \frac{\sqrt{4r_1^2-y^2}}{\pi(y-\lambda_2)^2}\,\theta(4r_1^2-y^2)\ , \qquad (|\lambda_2|>|2r_1|)\end{aligned} \tag{F-2}$$

$$\begin{aligned}\Delta I_s(\varepsilon) = {} & \frac{2\delta-r_1}{2\delta+r_1}\,\delta(x-x_0)-\frac{r_1+2\delta}{2(r_1+x_0)}\,\delta(x-r_1) \\ & - \frac{\sqrt{r_1^2-x^2}}{2\pi(x-x_0)(x+r_1)}\,\theta(r_1^2-x^2)\ , \qquad (|\delta|>|r_1/2|)\end{aligned} \tag{F-3}$$

$$
\begin{aligned}
\Delta I_c(\varepsilon) = & \frac{9\lambda^2(2\delta-r_1)}{(\lambda_1-x_0)^2(2\delta+r_1)}\ \delta(x-x_0) \\
& + \frac{(\delta-r_1)^2(\delta^2-r_1^2)}{\delta^2(\lambda_2-y_0)^2}\ \delta(y-y_0) \\
& + \frac{9\lambda^2}{2(x_0+r_1)}\left\{\frac{x_0-2\delta}{(\lambda_1-x_0)^2} + \frac{2\delta+r_1}{(\lambda_1+r_1)^2}\right. \\
& \left. + \frac{-x_0\lambda_1+r_1^2}{(\lambda_1-x_0)^2\sqrt{\lambda_1^2-r_1^2}} - \frac{r_1}{(\lambda_1+r_1)\sqrt{\lambda_1^2-r_1^2}}\right\}\delta(x-\lambda_1) \\
& + \left\{-\frac{1}{2} - \frac{(\delta-r_1)^2(\delta^2-r_1^2)}{2\delta^2(x_0-\lambda_2)^2} - \frac{\lambda_2}{2\sqrt{\lambda_2^2-4r_1^2}}\right. \\
& \left. + \frac{(2r_1-x_0)(-x_0\lambda_1+4r_1^2)}{2(\lambda_2-x_0)^2\sqrt{\lambda_2^2-4r_1^2}}\right\}\delta(y-\lambda_2) \\
& - \frac{9\lambda^2\sqrt{r_1^2-x^2}}{2\pi(x-\lambda_1)^2(x+r_1)(x-x_0)}\ \theta(r_1^2-x^2) \\
& - \frac{(y-2r_1)\sqrt{4r_1^2-y^2}}{2\pi(y-\lambda_2)^2(y-y_0)}\ \theta(4r_1^2-y^2)\ . \qquad \begin{pmatrix} |\delta|>|r_1| \\ |\lambda_2|>|2r_1| \end{pmatrix}
\end{aligned}
\tag{F-4}
$$

Here we have defined λ_1 and λ_2 as

$$
\begin{aligned}
\lambda_1 &= \lambda + r_0\ , \\
\lambda_2 &= \lambda - 2r_0\ .
\end{aligned}
\tag{F-5}
$$

Note that λ_1 (λ_2) is the energy of the 'surface polariton' measured from the center of the T(L)-band. The above expressions hold when $|\delta|>|r_1|$ and $|\lambda_2|>|2r_1|$. When $|\delta|<|r_1|$, the term containing $\delta(y-y_0)$ should be removed from the expression (F-4), and when $|\delta|<|r_1/2|$, also the terms containing $\delta(x-x_0)$ should be removed in the expressions (F-3) and (F-4). On the other hand, if $|\lambda_2|<|2r_1|$ the terms containing $\sqrt{\lambda_2^2-4r_1^2}$ as a factor should be omitted in the expressions (F-2) and (F-4).

References

1) For example, G. D. Mahan: "Elementary Excitations in Solids, Molecules, and Atoms; Part B" ed. J. T. Devreese, A. B. Kunz, and T. C. Collins (Plenum, London and New York, 1974) p. 93.

2) A. Otto: "Polaritons" ed. E. Burstein and F. De. Martini (Pergamon, New York, 1974) p. 117.

3) K. Cho (ed.): "Excitons" (Springer-Verlag, Berlin, 1979) and references therein.

4) V. Saile, M. Skibowski, W. Steimann, P. Gürtler, E. E. Koch, and A. Kozenikov: Phys. Rev. Letters 37 (1976) 305.

5) R. S. Knox: "Theory of Excitons" Solid State Physics, ed. F. Seitz and D. Turnball, Suppl. 5 (Academic Press, New York, 1963).

6) R. Del Sole and E. Tosatti: Solid State commun. 22 (1977) 307.

7) M. F. Deigen and M. D. Glinchuk: Soviet Physics-Solid State 5 (1964) 2377.

8) C. S. Ting, M. J. Frankel, and J. L. Birman: Solid State Commun. 17 (1975) 1285.

9) S. Sakoda: J. Phys. Soc. Japan 40 (1976) 152.

10) I. Balslev: Phys. Status solidi (b) 88 (1978) 155.

11) A. D'Andrea and R. Del Sole: Solid State Commun. 30 (1979) 145.

12) M. R. Philpott and J. M. Turlet: J. chem. Phys. 64 (1976) 3852.

13) V. E. Henrich, G. Dresselhaus, and H. J. Zeiger: Phys. Rev. Letters 36 (1976) 158.

14) G. J. Lapeyre and J. Anderson: Phys. Rev. Letters 35 (1975) 117.

15) J. M. Turlet and M. R. Philpott: J. chem. Phys. 62 (1975) 2777.

16) J. Hoshen and R. Kopelman: J. chem. Phys. 61 (1974) 330.

17) P. E. Schipper: Molecular Phys. 29 (1975) 501.

18) H. Ueba and S. Ichimura: J. Phys. Soc. Japan 41 (1976) 1974.

19) C. W. Deutche and C. A. Mead: Phys. Rev. 138 (1965) A63.

20) G. D. Mahan and G. Obermair: Phys. Rev. 183 (1969) 834.

21) J. E. Sipe and J. van Kranendonk: Canad. J. Phys. 53 (1975) 2095.

22) See ref. 15)

23) R. M. Hochstrasser and P. N. Prasad: J. chem. Phys. 56 (1972) 2814.

24) E. Glockner and H. C. Wolf: Z. Naturforsch. A24 (1969) 943.

25) J. M. Turlet and M. R. Philpott: J. chem. Phys. 62 (1975) 4260.

26) N. I. Ostapenko, M. P. Chernomorets and M. T. Shpak: Phys. Status solidi (b) 72 (1975) K117.

27) G. F. Koster and J. C. Slater: Phys. Rev. 95 (1954) 1167; 96 (1954) 1208.

28) H. Ueba: J. Phys. Soc. Japan 43 (1977) 353.

29) S. Ino: Japan J. Appl. Phys. 19 (1980) 1277, and references therein.

30) G. Margaritondo and J. E. Rowe: Phys. Letters 59 A (1977) 464.

31) M. Altarelli, G. Bachelet, and R. Del Sole: J. Vac. Sci. Technol. 16 (1979) 1370.

32) L. J. Sham and T. M. Rice: Phys. Rev. 144 (1966) 708.

33) For example, V. V. Nemoshkalenko and V. G. Aleshin: "Electron Spectroscopy of Crystals" (Plenum, New York and London, 1979) chap. 1.

34) D. J. Chadi: Phys. Rev. B18 (1978) 1800.

35) E. J. Mele and J. D. Joannopoulos: Phys. Rev. B17 (1978) 1816.

36) J. R. Chelikowsky and M. L. Cohen: Phys. Rev. B20 (1979) 4150.

37) A. Zunger: Phys. Rev. B22 (1980) 959.

38) D. E. Eastman and J. L. Freeouf: Phys. Rev. Letters 33 (1974) 1601.

39) Y. Onodera and Y. Toyozawa: J. Phys. Soc. Japan 22 (1967) 833.

40) U. Fano: Phys. Rev. 124 (1961) 1866.

41) P. Zurcher, G. J. Lapeyre, R. Avci, and J. Anderson: J. Vac. Sci. Technol. 18 (1981) 778.

42) C. A. Swartz, W. A. Goddard III, and T. C. McGill: J. Vac. Sci. Technol. 19 (1981) 360.

43) M. S. Daw, D. L. Smith, and T. C. McGill: J. Vac. Sci. Technol. 19 (1981) 388.

44) W. R. Heller and A. Marcus: Phys. Rev. 84 (1951) 809.

45) M. R. Philpott: Phys. Rev. B14 (1976) 3471.

46) V. Saile: private communication.

47) E. I. Rashba and G. E. Gurgenishvili: Soviet Physics--Solid State 4 (1962) 759.

48) M. Born and M. Bradburn: Proc. Cambridge Phil. Soc. 39 (1943) 104.

49) K. Ehara and K. Cho: Solid State Commun. 44 (1982) 453.

50) M. Skibowski and G. Sprüssel: Proc. 14th Int. Conf. Physics of Semiconductors, ed. B. L. H. Wilson (Institute of Physics, London, 1978) p. 1359.

51) J. C. Slater: Phys. Rev. 36 (1930) 57.

52) W. Ranke and K. Jakobi: Progr. Surf. Sci. 10 (1981) 1.

53) A. D'Andrea and R. Del Sole: Phys. Rev. B25 (1982) 3714, and references therein.

54) K. Miyamoto: Master thesis (Faculty of Engineering Science, Osaka University, 1981).